Fall 2014

Adipogenic and myogenic stem cells in brown fat: A study of progenitors and regenerative capacity

Xin Yang
Purdue University

Graduate School Form 30
(Revised 08/14)

PURDUE UNIVERSITY
GRADUATE SCHOOL
Thesis/Dissertation Acceptance

This is to certify that the thesis/dissertation prepared

By Xin Yang

Entitled
Adipogenic and myogenic stem cells in brown fat: a study of progenitors and regenerative capacity

For the degree of Master of Science

Is approved by the final examining committee:

Dr. Shihuan Kuang

Dr. Kolapo Ajuwon

Dr. Wayne W. Campbell

To the best of my knowledge and as understood by the student in the Thesis/Dissertation Agreement, Publication Delay, and Certification/Disclaimer (Graduate School Form 32), this thesis/dissertation adheres to the provisions of Purdue University's "Policy on Integrity in Research" and the use of copyrighted material.

Dr. Shihuan Kuang

Approved by Major Professor(s): _____

_____

Approved by: Todd Applegate 10/10/2014

Head of the Department Graduate Program Date

ADIPOGENIC AND MYOGENIC STEM CELLS IN BROWN FAT: A STUDY OF PROGENITORS AND REGENERATIVE CAPACITY

A Thesis

Submitted to the Faculty

of

Purdue University

by

Xin Yang

In Partial Fulfillment of the

Requirements for the Degree

of

Master of Science

December 2014

Purdue University

West Lafayette, Indiana

To my family

ACKNOWLEDGEMENTS

I would like to take this opportunity to thank everyone who has helped me complete my M. S. study.

Firstly, I would like to thank my major advisor Dr. Kuang for support and advisory. It is Dr. Kuang's interest in innovative ideas and new technologies that made the development of my projects possible. Dr. Kuang has greatly helped me to learn, write and teach with his patience and expertise. Dr. Kuang's many lifetime advices such as thinking actively and critically, maintaining hardworking and thriftiness, and reaching out and being supportive to others, will always light up my path in the future.

At the same time, I would like to thank my committee members Dr. Ajuwon and Dr. Campell, and my teacher Dr. Bidwell for academic and lifetime guidance. Dr. Calve from the biomedical engineering department is particularly appreciated for her continuous contribution to the SeeDB method and 3D reconstruction.

Secondly, I would like to thank all of the lab mates for help and suggestions. Thank you Dr. Liu (Weiyi), Dr. Shan, Dr. Liu (zuojun), Dr. Yue, Dr. Nie, Dr. Shi, Dr. Jiang, Dr. Wang, Sandra, Xinyuan, Pengpeng (Zhang), Chris, Tim, and Pengpeng (Bi) (in no particular order). I will never forget how many times we had each other's back, taught each other things, and work together crazily till late at night. Special thanks go to

Pengpeng Bi for kindly providing Myod$^{Cre/+}$/Rosa$^{LSLiDTR/+}$/Rosa$^{LSLtdTomato/+}$ mice and Dr. Shan for indulging my endless questions and curiosities.

I would also like to personally thank Christie, Brittany, Amber, Kayla, Jing, Qian, Xiaoyu, Ziao, Shardul, Chenhua, and Yi for being my friends and sharing part of the life with me during the past years. Thank you for supporting me as the “mad scientist”. Thank you for correcting my English, and thank you for checking upon me when I needed courage to try new ideas. I could never have done all of these without my dearest friends.

Last but not least, I want to specially express my gratefulness to my family. I want to thank Helen for always being there like my guardian angel. I want to thank my dad for insisting a scientific training for me which benefits me tremendously. I want to thank my mom for caring and teaching me how to balance work and life. I truly appreciate you for being supportive all the way.

Thank you all for helping me and you will all be remembered!

TABLE OF CONTENTS

Page

Page

LIST OF TABLES

LIST OF FIGURES

Figure Page

Figure Page

LIST OF ABBREVIATIONS

BAT	Brown adipose tissue
aP2	Adipocyte binding protein 2
AdipoQ	Adiponectin
ADSC	Adipose derived mesenchymal stem cells
AP	Adipose progenitor
ASC	Adipose stem cells
Adrs	Adrenergic receptors
AA	Amino acids
AMPK	AMP-activate protein kinase
BMSC	Bone marrow derived mesenchymal stem cell
BMP	Bone morphogenetic protein
CTX	Cardiotoxin
C/Ebp	CCAAT-enhancer-binding protein
DT	Diphtheria toxin
ddH2O	Distilled water
DMEM	Dulbecco's Moified Eagle Medium
E17.5	Embryonic day 17.5

ESC	Embryonic stem cells
eYFP	Enhanced yellow florescent protein
EDL	Extensor digitorum longus muscle
FBS	Fetal bovine serum
FACS	Fluorescence activated cell sorting
FFA	Free Fatty Acid
gWAT	Gonadal white adipose tissue
HSC	Hematopoietic stem cells
H&E	Hematoxylin and Eosin
HFD	High fat diet
H2B-eGFP	Histone 2B-enhanced green fluorescent protein
iPSC	Induced pluripotent stem cell
iWAT	Inguinal white adipose tissue
isBAT	Interscapular brown adipose tissue
IMAT	Intramuscular fat
IMLC	Intramuscular lipids content
LCFA	Long-chain fatty acids
MSC	Mesenchymal stem cells
MAPK	Mitogen activated protein kinase
NE	Norepinephrine
O.C. T.	Optimal cutting temperature compound
Pparg	Peroxisome proliferator-activated receptor gamma

Pgc-1α	Peroxisome proliferator-activated receptor gamma, coactivator 1 alpha
Pparγ	Peroxisome proliferator-activated receptor γ
Pdgfra	Platelet-derived growth factor receptor alpha
PFA	Poly formaldehyde
P/S	Polypeniciliin/strepomycine
MRI	Postmortem magnetic resonance imaging
P1	Postnatal day 1
PKA	Protein kinase A
SeeDB	See deep brain tissue clarification
SOL	Soleus muscle
Shh	Sonic hedgehog
Sca1	Stem cell antigen1
SVF	Stromal vascular fraction
SNS	Sympathetic nervous system
TA	Tibialis anterior muscle
Ucp1	Uncoupling protein1
VE-cad	Vascular endothelial cadherin
WAT	White adipose tissue
WT	Wild type

ABSTRACT

Yang, Xin. M.S., Purdue University, December 2014. Adipogenic and Myogenic Stem Cells in Brown Fat: a Study of Progenitors and Regenerative Capacity. Major Professor: Shihuan Kuang.

Brown adipose tissue (BAT) utilizes stored lipids to generate heat, therefore reducing body fat content and favoring a leaner body composition. Recent identification of metabolically active BAT in adult humans has sparked broad interests in understanding the developmental origin and postnatal homeostasis of BAT. However, the stem cell population that gives rise to BAT during development and maintains BAT mass at postnatal stage has not been characterized. In addition, whether adult BAT has the capacity to regenerate after injury or to proliferate in response to cold is flargely unknown. Furthermore, although BAT and skeletal muscle are known to share a common *Myf5* lineage origin, it is unknown if postnatal BAT contains bipotent adipomyogenic stem cells, or subpopulations of unipotent adipogenic and myogenic progenitors. The overall aim of this thesis is to fill in these gaps in knowledge. Using $Pdgfra^{GFP/+}$ reporter mice to mark the platelet-derived growth factor receptor alpha (*Pdgfra*) expressing progenitors that give rise to BAT, I show that *Pdgfra* lineage progenitors contribute to only 3% of cells in the classical intrascapular BAT (isBAT). In contrast, adipogenic progenitors isolated from isBAT and grown in culture are

predominantly *Pdgfra*$^{+}$. Likewise, GFP^{+}/Sca1+ cells isolated from white adipose tissue (WAT) and intramuscular fat (IMAT) are highly adipogenic in culture. Although genetic ablation of brown adipocytes results in compensatory regrowth of BAT, the *Pdgfra*$^{+}$ cells rarely proliferate and contribute to the adipogenesis. Cold stimulation also fails to induce proliferation of the *Pdgfra*$^{+}$ cells *in vivo*. Interestingly, BAT contains a population of unipotent *Pdgfra*$^{-}$ myogenic progenitors. The myogenic progenitors are located in a small flat muscle that penetrates the BAT. Surgical excision or genetic ablation of the skeletal muscle from BAT eliminates its myogenic gene expression signature, which has been thought to be a feature of brown adipocytes. In conclusion, results from this study demonstrate that embryonic and postnatal BAT progenitors are distinct in *Pdgfra* lineage origin. Adult BAT contains populations of unipotent adipogenic and myogenic stem cells. The results further suggest that skeletal muscle contamination significantly contributes to the previously reported myogenic gene expression in the BAT. This study is the first to systemically characterize stem cells in classical isBAT, and provides critical understanding of the cellular basis of postnatal BAT homeostasis.

CHAPTER 1. LITERATURE REVIEW

1.1 Adipogenic and myogenic stem cells

Stem cells are unspecialized cells that can differentiate into terminal cell types, yet retain self-renewal ability through mitotic division. The adult human body consists of mostly specialized cells (except exogenous microbial) such as muscle cells or myocytes, blood cells, and epithelial cells. Unlike specialized cells that hardly divide or cycle, a stem cell has the ability to divide more often and give rise to specialized cells or stem cells that can further divide.

1.2 Types of stem cells

Stem cells can be classified in many ways. The most recognized parameters are time of origin and type of commitment. Regardless of the basis of classifications, it is widely accepted that stem cells exhibit hierarchy in their potency (or the ability to differentiate into various terminal cell types). Stem cells that are able to form an entire embryo and its supportive placenta are totipotent. Stem cells that form an embryo are considered pluripotent. Stem cells that form multiple lineages of cells are regarded as multipotent. Stem cells that are only committed to one mature cell type are referred as unipotent (Chopra, Hans, & Shetty, 2013).

1.2.1 Embryonic and adult stem cells

Stem cells exist in the inner cell mass of developing embryos (termed embryonic stem cells) and mature adult tissues (termed somatic or adult stem cells). In embryos, embryonic stem cells (ESCs) are detrimental for individual growth and development. The inner cell mass specifies into 3 germ layers, and thereby differentiates into various tissues to form a complete individual. In adult tissues, stem cells remain as a pool of cells that are ready to repair tissue wears and tears at all times. For instance, deep wound healing requires the activation of various types of stem cells to perform immune response, muscle repair, angiogenesis, and fibrosis in scaring (King & Newmark, 2012).

The term "induced pluripotent stem cells" or iPSCs refers to the artificially generated stem cells by cellular induction cues involving gene transfer or chemical exposure (Csobonyeiova, Polak, Koller, & Danisovic, 2014). Yamanaka, the researcher who established the iPSCs, was awarded the Nobel Prize in 2012 (Takahashi & Yamanaka, 2006) because of the promising application of iPSCs to tissue regeneration and drug screening. Merging interests in iPSCs have been mainly focused on either developing simpler induction cues or deriving iPSCs from distinct somatic cell populations.

1.2.2 Stem cells from different tissues/organs

According to committed cell types, stem cells are classified into many types including: adipose stem cells (ASCs), satellite cells (or skeletal muscle stem cells), hematopoietic stem cells (HSCs), mesenchymal stem cells (MSCs), epithelial stem cells,

mammary stem cells, germ line stem cells, neural stem cells, liver and pancreatic stem cells, cardiac stem cells and so on (Lanza et al., 2005).

1.3 Adipogenic stem cells

Adipogenic stem cells are the stem cells that possess the potential to form fat cells or adipocytes. When adipogenic stem cells are committed to adipose lineage (sometimes with the ability to differentiate into other lineages as well), they are referred as adipose progenitors (APs) (Billon & Dani, 2012) or preadipocytes (E. D. Rosen & MacDougald, 2006; Q. Q. Tang & Lane, 2012). Despite the clear understanding of the adipocyte differentiation process and transcriptional cascades controlling adipocyte maturation (Berry, Jeffery, & Rodeheffer, 2014; Son, Ka, Kim, & Kim, 2014; Q. Q. Tang & Lane, 2012), little is known about ASC origin. Extensive studies have been conducted to isolate, characterize and developmentally trace ASCs (Berry, Jeffery, & Rodeheffer, 2014).

1.3.1 Isolation of ASCs and APs

Isolation of APs from mice has been performed for years. In 2008, Tang and et al. found that *Pparg* (*Peroxisome proliferator-activated receptor gamma*) expressing cells (marked by GFP expression) are high in preadipocyte gene expressions, like *Pref1* (*Preadipocyte factor 1*), and low in mature adipocyte gene expressions, like *AdipoQ* (*Adiponectin*) (Park, Halperin, & Tontonoz, 2008). These APs can actively form mature adipocytes in nude mice and reside in a vasculature niche, which has been suggested by

anatomical analysis previously (W. Tang et al., 2008). Another independent group used Fluorescence Activated Cell Sorting (FACS) to isolate various cellular subpopulations from lipoatrophic A-Zip mouse stromal vascular fraction (SVF) and identified a pool of APs in the SVF of adipose tissues. These APs with cell surface markers lin^- /$CD34^+$ /$CD29^+$ /$Sca1^+$ /$CD24^+$ differentiated into mature adipocytes in culture and formed fat depots after transplantation, meaning these cells are adipogenic *in vitro* and *in vivo* (Rodeheffer, Birsoy, & Friedman, 2008). Although few studies were conducted on cell surface marker characteristics for APs from different types/depots of fat, the isolation and culture of mouse APs have progressed.

In humans, isolation of ASCs and APs has also been practiced for a decade. A population of bone marrow derived MSCs (BMSCs) were initially found to be adipogenic *in vitro* (Sekiya, Larson, Vuoristo, Cui, & Prockop, 2004). However, with the population of liposuction technique, ASCs are now efficiently isolated from lipoasperates (Zuk et al., 2001) and applied for clinical use (Kim & Heo, 2014; West et al., 2014) especially in plastic surgery(Salibian, Widgerow, Abrouk, & Evans, 2013) and tissue regeneration(Konno et al., 2013; Naaijkens et al., 2014). Stromal cells that are believed to contain APs can be derived from adipose tissues from distinct anatomical locations like legs, arms and buttocks in humans, and have the ability to differentiate into not only adipocytes but also osteocytes, chondrocytes and more (Sachs et al., 2012). Distinguishing fibroblasts in the stromal cells from APs by molecular markers is difficult, since they are similar in molecular signatures. They are both positive for CD29, CD73, and CD105 and negative for CD14, CD31 and CD45 (Sachs et al., 2012). Although

fibroblasts share similar morphology in culture with APs, they do not differentiate into any adipocytes, chondrocytes or osteocytes (Sengenes, Lolmede, Zakaroff-Girard, Busse, & Bouloumie, 2005). Therefore, APs can be efficiently isolated from the SVF of mice and humans and can differentiate into adipocytes and multiple other cell lineages depending on the environmental cues provided.

1.3.2 Characteristics of ASCs

ASCs are present throughout the lifespan of mice and humans. ASCs can be derived from embryonic fibroblasts or adult adipose tissues (Dani & Billon, 2012). During individual development, ASCs from the mesoderm proliferate and differentiate to form fat depots. A subpopulation of ASCs originates from neural crest which is ectodermal (Billon et al., 2007). In adults, since mature adipocytes do not divide, the expansion of adiposity depends on the increase in size of mature fat cells (hypertrophy) and number of newly formed adipoctyes from a reserved pool of APs (hyperplasia) (Hauner, Wabitsch, Zwiauer, Widhalm, & Pfeiffer, 1989; Hirsch & Batchelor, 1976; Spalding et al., 2008). Whether the adipose plasticity is mediated by hypertrophy or hyperplasia can be depot dependent. Early studies in mice showed that in obesity, abdominal fat depots generally exhibit hyperplasia, whereas subcutaneous fat mainly expand by hypertrophy (Johnson & Hirsch, 1972). These together suggested that an active pool of APs is reserved in adult mice and humans. These APs can quickly respond to mechanical, chemical or signaling cues for local adipose remodeling.

ASCs have limited ability to proliferate and differentiate. The limited lifespan of ASCs is thought to be connected to the lack of telomerase expression in human adipose derived stem cells (ADSCs) (Katz, Tholpady, Tholpady, Shang, & Ogle, 2005). However, current conclusion is ambiguous. This notion was supported by independent studies suggesting that human adipose derived from mesenchymal stem cells show no detectable telomerase activity (Zimmermann et al., 2003). The ASC culture from human subcutaneous fat also lacked telomerase and show telomere erosion with serial passaging (Sachs et al., 2012). In contrast, several studies detected telomerase activity (Izadpanah et al., 2008) and the hTERT (Peng et al., 2008), which is the catalytic component of telomerase in human ASCs. In addition, force expression of exogenous hTERT in human ASCs elevated telomerase activity (S. K. Kang et al., 2004). Although disagreement occurred among studies, the primary culture of ASCs or APs normally show replicative senescence, affecting proliferation and differentiation ability of high passage ASCs and APs (Dani & Billon, 2012; Di Battista et al., 2014).

1.3.3 ASCs, MSCs and other adipogenic cells

Because of the resemblance of ASCs to the multipotent MSCs in cell structure and differentiation potential (G. Lin et al., 2008), studies usually do not distinguish between ASCs with ADSCs. A current view regards ASCs as a subpopulation of MSCs (Locke, Windsor, & Dunbar, 2009; Q. Q. Tang & Lane, 2012). When compared to bone BMSCs, ASCs are generally more committed to the adipose lineage, although they still possess a profound ability to differentiate into other cell lineages like skeletal muscle

cells, osteocytes, chondrocytes, fibroblastic cells in tendons and so on (Konno et al., 2013), just like BMSCs (Peng et al., 2008). In clinical application, ADSCs based therapy has advantages over BMSCs because of its greater abundance, easier accessibility and almost equivalent regeneration ability.

Unlike ASCs and MSCs, other cell types are rarely adipogenic. Satellite cells, which are adult muscle stem cells, are rational candidates since they undergo adipogenic differentiation *in vitro* under glucose treatment (Aguiari et al., 2008). The adipogenic potential of satellite cells is also partially supported by the fact that adult muscle cells incorporate and utilize cellular lipids content (IMLC) (Dube et al., 2008). More directly, a study suggested that cultured satellite cells on myofibers spontaneously differentiate into osteocytes and adipocytes, but after attachment to culture dishes, they are only myogenic unless supplied with adipogenic induction cues or BMPs (bone morphogenetic proteins) (Asakura, Komaki, & Rudnicki, 2001). However, more recent studies in human and mouse myoblasts showed that satellite cells do not form adipocytes. Lineage tracing experiment showed that skeletal muscle derived adipogenic cells are negative for skeletal muscle stem cell marker *Myod* (Starkey, Yamamoto, Yamamoto, & Goldhamer, 2011). Human satellite cells purified by a double immune-magnetic purification based on surface maker $CD56^{+}$/$Desmin^{+}$ do not form adipocytes even under adipogenic differentiation environment (Agley, Rowlerson, Velloso, Lazarus, & Harridge, 2013). These studies suggested that the adipogenic population in muscle derived stem cells is likely the attached MSCs or other cell types. Other potential adipogenic stem cells remain under evaluated. Many believe vasculature cells like

prericytes and hematopoitic lineage cells are adipogenic, but this view greatly overlaps with the ongoing debate about ASC origin, making a converged conclusion difficult.

1.4 Myogenic stem cells

Myogenic stem cells are the progenitor cells that give rise to mature muscles. Satellite cells are a common type of committed stem cells that form skeletal muscles. This cell type was discovered in the early 1960s and proved to be involved in muscle growth and repair (Mauro, 1961). Since myofiber number is set at birth (Rowe & Goldspink, 1969a, 1969b), postnatal muscle growth mostly relies on muscle hypertrophy. This requires the integration of differentiated satellite cells into the existing myofibers. In addition, muscle damage activates dormant satellite cells to proliferate, differentiate and fuse into muscles to repair damage. Therefore, satellite cells are essential for understanding muscle regeneration and are important for clinical application to treat muscle diseases such as muscular dystrophy.

1.4.1 Isolation and culture of satellite cells

Techniques to isolate and culture satellite cells in mice are currently mature. Myoblast (satellite cell *in vitro*) culture and single myofiber culture are the two common approaches. Satellite cells are attached underneath the basal lamina but above the plasma membrane of myofibers (Mauro, 1961). The isolation of satellite cells usually involves enzymatic digestion to dissociate satellite cells from their residential niche. In myoblast culture, extensive pre-plating and differential centrifugation have been

commonly used for enriching myoblasts from other cell types and debris from enzymatic digestion. The cultured myoblasts are then seeded on a collagen or matrigel coated culture dish to best mimic the extracellular matrixes. The myofiber culture also involves enzymatic digestion, but further requires mechanical dissociation of fibers. The process must be gentle to avoid dissociation of satellite cells from the myofiber. The dissociated fibers are then placed in culture medium waiting for satellite cells to proliferate and form myoblast clusters. Isolation of satellite cells with the attached myofiber is believed to better preserve the nascent satellite cell environment.

More emphasis has been put on the human satellite cell isolation (Bareja et al., 2014). In humans, with the advance in FACS techniques, isolation of muscle cells usually combines with FACS purification based on cell surface marker like $CD34^{-}/CD56^{+}$ (Bareja et al., 2014). Notably, the $CD34^{+}/CD56^{+}$ population is also myogenic, but is not considered satellite cells because of the adipogenic property (Pisani, Clement, et al., 2010; Pisani, Dechesne, et al., 2010). The isolated mouse myoblasts appear to be round and bright in culture, whereas human myoblasts are usually elongated and fibroblast-like.

1.4.2 Satellite cells and other myogenic cells

Although satellite cells are the main source of myogenic cells, other cell types may also contribute to muscle lineage. One example is BMSCs (Ferrari et al., 1998). In wild type (WT) or dystrophic mouse regenerating muscles, satellite cell numbers greatly exceed the number of residential satellite cells, suggesting muscle repair may involve

other cells. Indeed, genetically marked BMSCs were incorporated into regenerating muscles *in vivo* (Ferrari et al., 1998). The chemokines that induced this process are unknown. Apart from BMSCs, studies suggest that neural stem cells, hematopoitic lineage cells, and vessel-associated cells possess a certain degree of myogenic ability (Tedesco, Dellavalle, Diaz-Manera, Messina, & Cossu, 2010).

The accuracy of the localization and physiological relevance of the non-satellite cells or myogenic cells remains disputable. The localization of myogenic cells to the satellite cell niche does not necessarily indicate direct contribution to mature muscle since whether the cells go through fusion, a necessary step of myogenesis (Hindi, Tajrishi, & Kumar, 2013), is not clear; not to mention a possible inaccurate detection of whether the cells are in satellite cell niches or not (Relaix & Zammit, 2012). Because the sensitivity of detecting labeled cells reaches a single cell level, the incorporated non-satellite cell population in muscles may not have physiological significance. Isolated and cultured cell transplantation may not be representative for studying muscle regeneration because cell properties are commonly modified in processing, or may be altered with molecular approaches such as virus infection (Relaix & Zammit, 2012).

1.5 Adult stem cell mediated regeneration

Wild animals, especially lower vertebrates, exhibit the amazing ability to regenerate tissues (Gurley & Alvarado, 2008). The typical example is a salamander (D. A. Berg, Kirkham, Wang, Frisen, & Simon, 2011; McCusker & Gardiner, 2014; Morrison, Loof, He, & Simon, 2006; Sandoval-Guzman et al., 2014; Voss, Kump, Walker, & Voss,

2013). Salamanders have the ability to regenerate a complete limb after injury. Many cases require the formation of blastemal, a mass of undifferentiated progenitor cells covered by epithelium. A study has shown that the salamander limb muscle repair also largely depends on satellite cells (Morrison et al., 2006). Neuron, bone and blood vessels are also regenerated fully in function and morphology. Frogs, toads, planarians and zebra-fishes are other samples of animals that can spontaneously regenerate.

On the contrary, the human tissue regeneration ability is limited. Dynamic tissues such as muscle, adipose and epidermis undergo the most regeneration or remodeling compared to other tissues. Spontaneous regeneration commonly relies on the local progenitor cells such as satellite cells and MSCs. However, many important organs such as the heart, liver, and pancreas have little to no regenerative ability, although reserved pools of stem cells have been identified in these mature tissues.

The current clinical approaches for organ regeneration are either transplantation or biomaterial facilitated cell therapy. Autologous (self) transplantation is almost impossible with traditional donor-to-host organ transplant, but can be performed with stem cell based transplantation with the hope to eliminate the risk of immune rejection. Stem cell transplantation therapies have been clinically applied for treating diseases such as leukemia (Andersson et al., 2009), blindness (Rama et al., 2010), muscle dystrophy (Alexeev et al., 2014; Meregalli et al., 2013; Nishiyama & Takeda, 2012) and coronary syndromes (R. C. Huang, 2012). Adult stem cells are now a promising cure for many types of injuries and diseases.

Using adult stem cells in regenerative medicine is advantageous (West et al., 2014). Adult stem cells can be isolated relatively easily and in large quantities compared to stem cells acquired by other methods. Harvesting ESCs raises ethical concerns which can be avoid by using adult stem cells. It is also not clear whether the highly proliferative ESCs will result in cancer. On the other hand, the reprogramming process of iPSCs usually involves artificial modification, which introduces viruses, chemicals or bio-molecules, and can potentially cause problems when transplanted into humans. The adult stem cells, however, can be applied after a simple *in vitro* expansion. The disadvantage of using adult stem cells is mainly due to the limited expandability and unmanageable differentiation *in vivo* (West et al., 2014).

ASCs have been greatly employed in regenerative medicine. The minimum discomfort for isolation and large availability makes ASCs ideal for clinical usage. Fat grafting involving local ADSCs is commonly used in soft tissue augmentation especially in plastic surgeries. This method, which is named cell-assisted lipotransfer, significantly improves tissue survival and is widely applied in clinics worldwide (Salibian et al., 2013). Many of the other ADSC applications include bone and cartilage repair (Di Battista et al., 2014), treatment of neural disorders (Chan et al., 2014), healing of acute myocardial infarction (Naaijkens et al., 2014) and more (Konno et al., 2013; Ong & Sugii, 2013). Importantly, ASCs *in vivo* facilitate regeneration not only because they serve as a cell replacement source, but also exert paracrine effects promoting local tissue repair (Ong & Sugii, 2013). In fact, an ASC tissue bank has been set up in the United Kingdom (West

et al., 2014) and efforts have been made to create an international ASC tissue bank for global application.

Satellite cell therapy is mainly applicable to muscular dysfunctions like atrophy, dystrophy and injury. Of the many approaches used to combat muscle dystrophy, current studies of satellite cell transplantation has attracted much attention (Bareja & Billin, 2013). The current challenge is to purify satellite cells for transplantation instead of transplanting myoblasts. Myoblast transfer was studied in earlier years, but quickly proved to be problematic mainly due to the limited proliferation and immune rejection of the transplanted allogeneic cells. Another problem is that myoblast transplantation has low incorporation efficiency, but the direct transplantation of even a single satellite cell can give rise to mature myofibers (Sacco, Doyonnas, Kraft, Vitorovic, & Blau, 2008). Transplanting a single myofiber is also more efficient than myoblast transfer, and previous research has shown that transplanting few satellite cells associated with one single myofiber can result in more than 100 new fibers (Collins et al., 2005).

1.6 Adipose tissues

Adipose tissues are generally loose connective tissues characterized by the fat cells or adipocytes they contain. Adipocytes are parenchymal cells enlarged with cellular lipid content, which can be stained by lipid dyes such as Oil-Red-O. It was previously believed that adipose tissue is a single unorganized organ. This view was quickly disrupted by the understanding of fat types and dynamics.

1.6.1 Obesity and fat

The epidemic of obesity has spread. Obesity is defined as a body mass index (BMI) greater or equal to 30. Over 30% of adults and as many as 25% of children in the United States are diagnosed with obesity (Barness, Opitz, & Gilbert-Barness, 2007). The rise of obesity is parallel with many metabolic complications such as diabetes and cardiovascular diseases. Extensive studies on obesity have been performed in both animals and humans, however, since the causative factors are numerous, effective methods to prevent and treat obesity are lacking (Barness et al., 2007).

Obesity is closely associated with adipose tissue. The accumulation of FFA induces rapid expansion of adipose tissues either though hypertrophy or hyperplasia or combined approach depending on specific depots (Evan D. Rosen & Spiegelman, 2014). The accumulation of adipose tissue is a common indicator of positive energy balance, meaning a greater energy intake than the expenditure. Energy storage is crucial for animal survival when food supply is low. However, it also creates an obese phenotype in modern society due to over-nutrition and lack of exercise. The accumulation and redistribution of fat to the abdomen compartment is representative of the first-stage obesity phenotypes. Once gained, the adipocyte number is difficult to lose. Weight loss programs are effective in reducing adiposity in the aspect of reducing adipocyte volume but not overall number. This partially explains the rapid rebound of adiposity after weight loss programs.

1.6.2 Types of adipose tissues and their characteristics

To date, three types of adipose tissues have been identified. They are white adipose tissue (WAT), brown adipose tissue (BAT) and beige adipose tissue. The following chapter will discuss the main characteristics and developmental origin of these different types of adipose tissues.

1.6.2.1 White adipose*

White adipose tissue, as its name suggests, is white in appearance because of its composition of white adipocytes. White adipocytes are characterized by a spherical shape, a large single lipid droplet that takes up to 90% of the total cell volume, and few mitochondria (Cinti, 2012). White adipocytes constitute the bulky WAT located under the skin (subcutaneous fat), in the muscle (intramuscular fat or “marbling” fat), and in the abdominal cavity attached to the visceral mass (visceral fat).The white adipocytes appear in white color due to the high lipid content. They store excess food intake in the form of triglycerides which can be utilized to generate energy under energy deficit conditions. Recent studies have revealed a vasculature or peri-vasculature origin or localization of white adipocytes, and identified several molecular markers of white adipocyte precursor cells (for example Zfp423, VE-Cad, PDGFRβ, and PDGFRα) (Berry & Rodeheffer, 2013; Gupta et al., 2012; W. Tang et al., 2008; Tran et al., 2012).

1.6.2.2 Brown adipose*

Brown adipocytes contain multilocular lipid droplets and numerous mitochondria. They were found in BAT that mainly located in the interscapular regions

---

The * sections are adopted from a review: Yang X, Bi P, Kuang S. 2014. Fighting obesity: When muscle meets fat. *Adipocyte*.

of rodents and human infants (Lidell et al., 2013). Unlike white adipocytes, brown adipocytes break down lipids to produce heat, thus reducing adiposity. The thermogenesis of brown adipocytes is mediated by uncoupling protein 1 (UCP1) that is uniquely located in their inner mitochondria membrane. Of note, uncoupling activity of UCP1 is under control by sympathetic innervation (Cannon & Nedergaard, 2004) as well as other factors like free fatty acids from lipolysis (Fedorenko, Lishko, & Kirichok, 2012). The thermogenic "energy-leaking" feature of brown adipocytes has made BAT an appealing therapeutic target for treatmenting obesity.

Although brown and white adipocytes share multiple morphological and functional similarities, their developmental origins are surprisingly different. The classic brown fat, but not white fat, shares a developmental origin with skeletal muscles. Lineage tracing studies demonstrate that muscle and brown fat are from a population of mesodermal progenitors that express classic myogenic marker genes *Myf5*, *Pax7* and *Pax3* (Lepper & Fan, 2010; Liu, Liu, Lai, & Kuang, 2012; Seale et al., 2008). Furthermore, brown adipocytes and muscle cells share a similar mitochondrial proteomic signature (Forner et al., 2009) and both contribute to thermogenesis (Rolfe & Brand, 1996; Schonfeld & Wojtczak, 2012). In fact, brown fat precursors express a variety of myogenic genes before differentiation (Timmons et al., 2007). The progressive loss of myogenic signature gene expression during brown fat maturation urges a deeper understanding of factors diverging brown adipose from muscle development.

Particularlly, PRDM16 (PRD1-BF-1-RIZ1 homologous domain-containing protein-16) has been shown to be a bidirectional switch that determines BAT versus muscle fate

(Seale et al., 2008). Loss of PRDM16 in brown preadipocytes leads to a phenotypic switch to muscle cells, while ectopic expression of PRDM16 in myoblasts switches them back to brown adipocytes (Seale et al., 2008). More recently, it was reported that miR-133 acts as an upstream regulator of PRDM16 to control skeletal muscle versus BAT fate choice in muscle stem cells (satellite cells) (Yin et al., 2013). Although BAT-specific deletion of PRDM16 does not affect embryonic BAT development, it promotes white fat-specific gene expression in BAT in young mice and attenuates thermogenesis in old mice (M. J. Harms et al., 2014). These lines of evidence suggest that BAT originates differently from WAT, but shares developmental similarities with skeletal muscles.

1.6.2.3 Beige adipose*

It has long been known that when rodents are exposed to cold stress or β-adrenergic stimulating drugs, certain depots of WAT undergo a "browning" process, giving rise to brown adipocyte-like cells (called beige or brite adipocytes) with multilocular lipid droplets, UCP1 expression and thermogenic activity (Shabalina et al., 2013). However, whether adult humans have a similar capacity to form inducible BAT (iBAT) has been unclear. Recently, advanced imaging analysis using positron emission tomography (PET) revealed that in cold climates, active "brown-like" adipocytes form along the cervical-supraclavicular area in human adults (Cypess et al., 2009; Nedergaard, Bengtsson, & Cannon, 2007; Saito et al., 2009; van Marken Lichtenbelt et al., 2009). These cells retain radioactive fluorodeoxyglucose, suggesting that they actively uptake and utilize glucose. Different from classic WAT and BAT, iBAT is characterized by the

---

The * section is adopted from a review: Yang X, Bi P, Kuang S. 2014. Fighting obesity: When muscle meets fat. *Adipocyte*.

presence of beige adipocytes (Wu et al., 2012). Beige cells specifically express several marker genes (for example, Tnfrnfs9, Tmem26 and Tbx1 in mice and HOXC8, HOXC9 and CITED1 in humans) that are not expressed by white or brown adipocytes. By contrast, brown adipocytes uniquely express several maker genes (for example, Eva1, Hspb7 and Pdk4 in mouse and EPSTI1, LHX8 and ZIC1 in human) that are not expressed by beige or white cells (Bartelt & Heeren, 2014). Notably, genetic analysis of human iBAT suggests it contains both brown and beige adipocytes (Jespersen et al., 2013; Nedergaard & Cannon, 2013).

Beige adipocytes can be differentiated *de novo* from precursors or transdifferentiate from mature white adipocytes. Beige cell precursors are believed to be enriched in Pax3- cell lineage (Liu et al., 2013). A study using Adiponectin-Cre combined with Tert inducible lacZ mice (named Adipo-chaser mice) shows that in response to cold stimulation, preadipocytes in subcutaneous fat undergo *de novo* differentiation to form beige cells, while abdominal beige fat cells accumulate through proliferation (Wang, Tao, Gupta, & Scherer, 2013). Another group, using EdU labeling, combined with β3-adrenergic receptor stimulation reports approximately 7.5 times more mitotic index in epididymal WAT than inguinal WAT. UCP1 co-localizes with a fraction of the proliferating cells (Y. H. Lee, Petkova, Mottillo, & Granneman, 2012). Together, these studies suggest the existence of beige preadipocytes.

It is worth mentioning that an independent study identified a population of beige precursors within skeletal muscle that respond to BMP7 stimulation (Schulz et al., 2011). On the other hand, interconversion of white and beige adipocytes has also been

observed. Even before the characterization of beige cells, researchers discovered that white adipose precursors do not increase in response to cold acclimation, and iBAT formation is predominantly due to β3-adrenergic receptor-dependent transdifferentiation of white adipocytes (Barbatelli et al., 2010). Indeed, murine perivascular *Pdgfra*$^{+}$ cells differentiate into beige adipocytes upon β-adrenergic receptor stimulation, but become white adipocytes in response to high fat diet (HFD) feeding (Rosenwald, Perdikari, Rulicke, & Wolfrum, 2013). Based on these studies, cold can induce *de novo* formation of beige adipocytes from a population of beige precursor cells.

These beige adipocytes are plastic: they can become white adipocytes upon warm adaption and switch back to beige adipocytes after additional cold stimulation. Beige cell formation is regulated by many factors. Among these, inhibition of Prdm16 blocks the function of beige adipose and induces redistribution of subcutaneous white fat to unfavorable visceral fat, resulting in obesity and metabolic disorders (Cohen et al., 2014). In contrast, inhibition of Notch signaling dramatically promotes "browning" of white adipocyte through activating Prdm16 and Pparg. Importantly, the Notch inhibitor dibenzazepine (DBZ) effectively reduces adiposity and improves glucose metabolism in ob/ob mice (Bi et al., 2014). Further understanding of mechanisms underlying beige cell development and adipose "browning" will have huge impact in the treatment of obesity.

1.6.3 Adipose depots*

Adipose depots at different anatomical locations not only differ in the relative composition of brown, beige and white adipocytes (Cinti, 2005), but are also

---

The * section is adopted from a review: Yang X, Bi P, Kuang S. 2014. Fighting obesity: When muscle meets fat. *Adipocyte*.

heterogeneous in developmental origins (Chau et al., 2014; Sanchez-Gurmaches & Guertin, 2014a, 2014b; Wan & Longaker, 2014). Classic brown adipose depots include interscapular BAT (isBAT), subscapular BAT (sBAT), cervical BAT (cBAT), peri-aortic BAT (paBAT) and renal BAT (rBAT), whereas white adipose depots include anterior subcutaneous WAT (asWAT), inguinal WAT (inWAT), retroperitoneal WAT (rWAT), gonadal WAT (gWAT), mesenteric WAT (mWAT), and intramuscular fat (IMAT) (Addison, Marcus, Lastayo, & Ryan, 2014; Cinti, 2005; Gesta, Tseng, & Kahn, 2007; Sanchez-Gurmaches & Guertin, 2014a, 2014b). The white adipose depots can also be broadly divided into subcutaneous WAT (asWAT and inWAT) and visceral WAT (sWAT, rWAT and gWAT). IMAT is the WAT in muscle and is different from the intramyocellular triglycerides, which refer to cellular lipid droplets within muscle cells.

Developmentally, visceral WAT develops from the lateral plate mesoderm Wnt+ cells whereas no subcutaneous or BAT were found to come from the Wnt+ population (Chau et al., 2014). A recent *in vivo* lineage tracing experiment employing the Myf5-Cre, Myod-Cre, Pax3-Cre mice models combined with mTmG dual reporter mice shows that while isBAT depot contains 99% *Myf5* lineage adipocytes, cBAT had only ~60% *Myf5* lineage adipocytes. *Myf5* lineage cells also contribute to 25% and 50% to asWAT and rWAT progenitors, respectively. Pax3 lineage tracing shows similar results, but interestingly, shows gender differences in various depots especially in rBAT and gWAT(Sanchez-Gurmaches & Guertin, 2014b). These experiments together suggest that depot-specific origin of adipose tissues is a combined result of genetic, breeds, age, gender and even seasons.

1.6.4 Adipogenesis

In vitro adipogenesis involves (1) the specification of stem cells to ASCs (2) further determination of ASCs into adipoblast, which are committed but not differentiated APs, (3) accumulation of cellular lipid droplets in adipoblast to form the preadipocytes, and (4) maturation of preadipocytes into functional adipocytes. Growth arrest and a sudden clonal expansion are frequently observed in step (2) in ASC primary cultures and in adipogenic cell lines like 3T3-L1.

In vivo, adipogenesis generally starts from late gestation and varies among species. Adipocytes are detectable around embryonic 16.5-17.5 days in rodents. Early experiments showed that [(3)H]thymidine labeled epididymal adipocytes cease formation around 50 days (Greenwood & Hirsch, 1974). This suggested that adipogenesis begins late and ends early in rodents. In humans, adipose formation starts as early as in mid gestation and continues to grow after birth until sexual maturity. Many argue that later fat maturation mainly relies on increased cellularity because the total adipocyte number is set and remains homeostatic if not interrupted by abnormal nutrition conditions. It is also indicated that adipocyte turnover rate is much faster in rodents than humans (Evan D. Rosen & Spiegelman, 2014).

Angiogenesis commonly accompanies adipogenesis. The adipose formation in many species starts from “primitive organs” which are essentially local blood vessel networks. This is supported by the notion that blood vessel associated cells such as

mural cells, pericytes and hematopoietic cells are thought to form adipocytes, or seem to take part in adiposgenesis (Evan D. Rosen & Spiegelman, 2014).

Progresses have been made in understanding molecular player in adipogenic cell fate determination (Q. Q. Tang & Lane, 2012). Emerging evidence suggested that BMP signaling, especially BMP2 and 4, promotes the commitment of ASCs into APs (H. Huang et al., 2009). Sonic hedgehog (Shh) signaling inhibits adipogenic lineage commitment since mesenchymal cell lines that are successfully differentiated into adipocytes by recombinant BMP2 treatment cannot form adipocytes after Shh treatment (Spinella-Jaegle et al., 2001; Zehentner, Leser, & Burtscher, 2000). Wnt signaling, however, seemed to have dual effects. It is necessary for early specification of APs (Bowers & Lane, 2008) but inhibitory for terminal adipogenic differentiation (S. Kang et al., 2007). More studies are needed in understanding ASC early determination.

Molecular signatures for adipocyte terminal differentiation have been well established because most commercial cell lines studied in adipose biology are readily determined for adipogenic differentiation (E. D. Rosen & MacDougald, 2006). Peroxisome proliferator-activated receptor γ (PPARγ) and CCAAT-enhancer-binding proteins (C/EBPs) are top promoters of adipocyte terminal differentiation. Ppars belong to the nuclear receptor family which functions through heterodimerizion with retinoidX receptor. Pparγ is the master regulator of adipogenesis and has been proven to be both necessary and sufficient for fat formation. C/EBPα and γ acts at least partially with Pparγ securing terminal differentiation through two rounds of positive feedback loop. Other enhancers include Krüppel-like factors, early growth response protein-2, Liver X

receptor, sterol response element-binding protein-1c and more. Recently, numerous microRNAs were also shown to be involved in regulating adipogenic commitment and differentiation (Son et al., 2014).

1.6.5 Adipose functions

The functions of adipose tissue are numerous. Fundamentally, body fat serves as an energy preserving pool. Energy surplus is stored in the form of free fatty acids (FFA) in adipose tissues, which can be mobilized and converted into large quantities of ATP when food is scarce. Adipose tissues are also endocrine organs secreting hormonal factors named adipokines including important ones like leptin and adiponectin (Ouchi, Parker, Lugus, & Walsh, 2011). Leptin mainly suppresses food intake and promotes energy expenditure through the central nervous system. Adiponectin, on the contrary, increases fat deposition but reduces insulin resistance and benefits a numbers of organs like the heart, liver, and pancreas (Raschke & Eckel, 2013). Last but not least, adipose tissues are space fillers, heat insulators and mechanical cushions. In artic animals, thick deposition of fat are found under the skin to reduce heat emission and creating a streamline body figure for swimming(Evan D. Rosen & Spiegelman, 2014). In vertebrates, adipose protects internal organs such as the kidneys and heart, and also the eyes and heels from daily contact damage (Pond, 1992).

1.7 Brown adipose tissues

BAT is a kind of adipose that has currently attracted public attention because of its energy dissipating feature against obesity, in parallel with the surprising discovery of

browning in WAT. However, studies after 2007 mainly focus on inducible BAT (iBAT) rather than classic BAT. Here we discuss the classic BAT focusing on its histology, function mechanism and progenitor population.

1.7.1 Brown adipose morphology

1.7.1.1 Histology analysis

Different depots of classic BAT (isBAT, sBAT, cBAT, paBAT and rBAT) share similar histological appearance although identified in distinct anatomical locations in mammals (Cinti, 2005). When examined by the human eyes, BAT is “brown” or dark in color due to high levels of vascularization and compact cell density (Cinti, 2005). They are usually lobulated (especially in isBAT), and frequently surrounded by white adipose tissue and/or skeletal muscle. The isBAT, in particular, is located above muscles of the back and covered with a sheath of white adipocytes on the dorsal area. Under a light microscope (LS), BAT is composed of densely packed mulilocculated brown adipocytes and many cells in the interstitial space such as fibroblasts, preadipocytes, blood cells and vasculature cells. Brown adipocytes located closer to the vasculature are usually smaller which suggests a delayed formation of these cells and a potential progenitor pool near the vasculature.

1.7.1.2 Development

The existence of BAT is species dependent. From an evolutionary stand point, brown adipose tissue is found in eutherian (placental) mammals and

“protoendothermic’’ mammals. Protoedothermic animals can adjust body temperature to the environment during critical times such as when they are caring for their young (Evan D. Rosen & Spiegelman, 2014). Humans and rodents both possess classic BAT as discussed previously. Importantly, BAT is also abundantly found in livestock such as lambs, calves and reindeer (Smith & Carstens, 2005; Soppela, Sormunen, Saarela, Huttunen, & Nieminen, 1992). Different from rodents, who have most BAT in the interscapular region, the parirenal-abdominal space is the most abundant site for livestock BAT. Postnatal BAT in livestock is believed to be quickly lost through apoptosis, but important for progeny body temperature maintenance when they are young (Smith & Carstens, 2005). Pigs, however, do not have BAT since the gene encoding UCP1 is truncated by several mutations. Therefore pigs only rely on shivering thermogenesis with the absence of BAT (F. Berg, Gustafson, & Andersson, 2006).

In mice, BAT appears around embryonic day 15.5 (Schulz & Tseng, 2013). The late appearance of BAT is thought to relate to the fact that altriacial animals like rodents have short gestation period and do not rely on BAT mediated non-shivering thermogenesis but instead cuddle for warmth after birth (Symonds, 2013). The judgment of BAT appearance in rodents currently depends on general histological pictures from embryonic mouse. The embryonic BAT cannot be co-stained with UCP1 to confirm brown adipose function since UCP1 expression rises at least around or after birth during BAT maturation (Evan D. Rosen & Spiegelman, 2014). This leads to possible inaccuracy to define embryonic BAT. The difference between strains may also occur but has not been discussed either.

In humans and other precocial mammals (like sheep and cattle), BAT development starts during mid gestation, but is believe to mature during late gestation since the non-shivering thermogenesis peaks in newborns for maintaining body temperature (Symonds, 2013). Brown adipose tissue in lamb and rabbit newborn is typically 2-4% body weight (Alexander & Bell, 1975; Hull & Segall, 1965).

1.7.1.3 Dynamic

Brown adipose tissue has an alternative name called “hibernating gland”. It is critical for maintaining body temperature in hibernating species such as ground squirrels and bears, and commonly undergoes dramatic morphology changes during such time. In ground squirrels, BAT weight and volume increase during the hibernating season and drops rapidly after (Milner, Wang, & Trayhurn, 1989). Lipid catabolism, ketogenesis and gluconeogenesis activity is decreased while fatty acid synthesis is reduced in BAT (Williams et al., 2011). This indicates the BAT is activated and the stored lipid contents are utilized during hibernation.

Rodents do not have seasonal changes in BAT but maintain classic isBAT throughout their lives. On the contrary, human and lamb BAT can be found abundantly in neonates but lost in infancy. A recent study using postmortem magnetic resonance imaging (MRI) test confirmed that bona fide brown fat co-exists with beige fat in supraclavicular area in human infants (Lidell, Betz, & Enerback, 2014). The brown to beige proportion increases as it grows deeper down (Nedergaard & Cannon, 2013). The amount of BAT in infants averaged around 3.6 ± 2.4ml (Lidell et al., 2013) and as little as

60g of BAT utilizes up to 20% daily heat production (Ouellet et al., 2012). Although classic BAT is not found in adults, whether they undergo cell death or trans-differentiation into other fat types remains unknown. The post natal loss of sheep BAT is replaced by white (Clarke, Buss, Juniper, Lomax, & Symonds, 1997) or beige (Pope, Budge, & Symonds, 2014) adipose, accompanied by the loss of BAT function (Symonds, Andrews, & Johnson, 1989). A decline of serum cortisol and thyroid hormones indicate the BAT recruitment and maintenance is thyroid dependent (Schermer, Bird, Lomax, Shepherd, & Symonds, 1996).

BAT distribution is not only different in species, but also varies by breed and the birth season even in the same species. For example, purebred Brahman calves have on average 109 ± 10 g of BAT, whereas newborn Angus calves have as much as 208 ± 14 g of BAT. Newborn Fall Angus calves have significantly less BAT weight (99 ± 11 g) than the spring calves (208 ± 14 g) ($p<0.05$), but higher cell density and mitochondria areas (Martin et al., 1999). This suggests that BAT dynamic varies by breeds and environmental factors.

BAT is affected by sex in rats, but whether this is true in human remains unknown. In rats, females have significantly greater BAT weight/body weight to males, increased protein content and more mature mitochondria subtypes(Justo et al., 2005). Due to the limitation in technology and sample availability, sex effects of human classic BAT have not been examined. However, studies have shown that iBAT amount and activity is up-regulated by puberty and the up-regulation is more significant in boys

(Gilsanz et al., 2012). In adults, aging reduces iBAT abundancy and the iBAT activity is higher in aged females than males (Pfannenberg et al., 2010).

1.7.2 Functions

The dominant function of BAT is non-shivering thermogenesis. Apart from thermogenesis, BAT seems to take part in glyceride clearance and glucose disposal through CD36 activity, and secrete different patterns of adipokines such as IL-6 (Townsend & Tseng, 2012). BAT function can be detected by PET scan combined with FDG ingestion (Evans, Tulloss, & Hall, 2007) or partially reflected by respiratory index (more oxygen consumption is correlated to more thermogenesis) and mitochondria activity in BAT.

The main mediator of this function is UCP1. On BAT mitochondria membrane, UCP1 protein is specifically expressed, mediating a proton leak to convert energy from oxidation to heat instead of producing ATPs. This protein is activated by long-chain fatty acids (LCFAs) to serve as a LCFA anion/proton symporter (Fedorenko et al., 2012). Direct patch-clamp showed that LCFA shuttling mediates proton translocation; once it binds, the LCFA anion remains attached to UCP1 after activation.

1.7.3 Activation

It is important to understand that BAT and beige adipocytes are not activated at basal level. The abundance of BAT tissue does not necessary relate to a better metabolic phenotype or less obesity. BAT activation requires cold exposure or diet induction. The

activation is indicated by up-regulation of Ucp1 protein and thermogenic genes such as *Ucp1*, *Prdm16*, *Cidea* and so on.

BAT thermogenesis is under the control of the sympathetic nervous system (SNS). Hormonal regulators like melatonin and dietary induction like high fat diet (HFD) stimulate SNS, and thereby activate BAT. Upon activation, catecholamine neurotransmitter, norepinephrine (NE), is released by the SNS and binds with the G-protein coupled adrenergic receptors (Adrs) in BAT (α1–α3 or β1–β3 Adr). The dominant form β3Adr in mice (β1Adr in human) induces Cyclic adenosine monophosphate (cAMP) downstream to activate protein kinase A (PKA), PKA then phosphorylates Hormone-sensitive lipase and perilipin A to release FFA, stimulating UCP1 action through the LCFA anion binding. Some report that beside the SNS, macrophages also secrete catecholamine to stimulate BAT action (Nguyen et al., 2011). And beside NE, epinephrine may also affect *Ucp1* (Sharara-Chami, Joachim, Mulcahey, Ebert, & Majzoub, 2010). Interestingly, without the effect of the SNS, brown adipocytes can be directly activated through cold stimulus.

The thyroid hormone has synergistic effect with the SNS in BAT activation. T3 form (or T4 converted T3 form) thyroid hormone binds with the β thyroid receptor on BAT and induces Ucp1 gene expression (Ribeiro et al., 2010). This is also supported by the fact that hypothyroid animal survival rates decrease when challenged with low temperature (Townsend & Tseng, 2012).

1.7.4 Progenitors

The embryonic expansion of brown fat in rodents is believed to be associated with multiplication of BAT progenitors from mesenchyme. The Ki67 expression which indicates mitotic division is widely detected in embryonic mouse BAT. Lineage tracing experiments showed that Zfp423 and VE-cad marks brown adipose progenitors *in vitro* and *in vivo*, suggesting that BAT progenitors originate from the vasculature. These markers also mark WAT progenitors which may lead to the difficulty of distinguishing BAT progenitors from WAT progenitors. The distinction of BAT progenitors from WAT progenitors remains elusive.

Adult BAT expansion in rodents is believed to be mediated partially by progenitor hyperplasia. Early studies employing radioactive thymidine have shown that in cold acclimation, the number of proliferating cells increases ~60-70 times and peaks after 48 hours in cold (L. Bukowiecki, Collet, Follea, Guay, & Jahjah, 1982; L. J. Bukowiecki, Geloen, & Collet, 1986). The proliferating cells are not mature adipocytes, but vasculature cells, preadipocytes or interstitial cells. Another study used chronic β Adrenergic receptor stimulating drug such as CL316,243, BRL 26830A, and leI 07114 have found significant increase in BAT DNA content, Ucp1 protein abundance and insulin sensitive glucose transporter amount (Thiazolidinediones (TZDs)Nagase et al., 1994). These lines of evidence infer that BAT progenitors can be activated with the substantial activation of brown adipocyte function.

Pdgfra lineage cells are a distinct population of MSCs that gives rise to WAT and beige adipocytes. In 2010, Akiyoshi Uezumi and colleagues identified *Pdgfra* cells in skeletal muscle as IMAT ASCs. $CD31^{-}/CD45^{-}/Pdgfra^{+}$ cells proliferate actively in culture and form functional adipocytes (Uezumi, Fukada, Yamamoto, Takeda, & Tsuchida, 2010). The same group confirmed in 2014 that $Pdgfra^{+}$ marks human muscular ASCs. The human $Pdgfra^{+}$ progenitors are highly adipogenic as well (Uezumi et al., 2014). Importantly, one study showed that subcutaneous WAT adipocytes completely originate from *Pdgfra* line+ cells using mTmG dual labeling mouse line combined with $Pdgfra^{Cre}$ recombinant (Berry & Rodeheffer, 2013). More interestingly, the $Pdgfra^{+}$ population gives rise to both white and beige adipocytes and forms fat pads *in vivo* (Y. H. Lee et al., 2012). These lines of evidence suggest the importance of $Pdgfra^{+}$ cells in adipocyte progenitors. Whether *Pdgfra* marks the BAT progenitors has not been examined.

Molecular control of BAT progenitor fate determination is unknown. But the transcriptional cascade regulating differentiation involves similar components with WAT, which involves Pparγ and C/Ebps. After differentiation, genes determining BAT thermogenesis come into play (Townsend & Tseng, 2012). For example, Peroxisome proliferator-activated receptor gamma, coactivator 1 alpha (Pgc-1α) is the master regulator of brown adipose mitochondrial biosynthesis as well as in many other cell types such as skeletal muscles. Pgc-1α is not required by BAT development possibly due to compensatory effect of Pgc-1β (J. Lin et al., 2004). Sympathetic stimulation activates p38 mitogen activated protein kinase (MAPK) to further activate Pgc-1α. Pgc-1α then binds to transcriptional controllers such as Pparγ, α, thyroid receptor, completing the

nerve-to-transcription control of BAT function. Pgc-1α inhibitory transcriptional factors such as the retinoblastoma family members and nuclear co-repressor Rip140 (or Nrip1) repress BAT Ucp1 expression. These indicated that Pgc-1α is potent regulator of BAT function but not development (M. Harms & Seale, 2013). Prdm16 also promotes brown adipocyte differentiation through activation of Pgc-1α. The forkhead family transcription factor forkhead box C2 induces UCP1 mediated through activation of Protein kinase A. Some microRNAs such as miR-193b-365 clusters are specifically required by BAT differentiation.

1.7.5 Brown fat as a therapeutic target in obesity and comorbidities

In the context of obesity, BAT has been extensively studied as a therapeutic target. Mouse models with BAT depletion either through genetic ablation or surgical removal had increases in WAT amount (Hamann, Flier, & Lowell, 1996; Rothwell & Stock, 1989). In contrast, transplantation of even 100mg BAT increases insulin sensitivity and glucose tolerance (Stanford et al., 2013). To what degree that BAT affects human metabolism is still elusive, but BAT mediated thermogenesis holds a promising future in the treatment of obesity.

Currently, no anti-obesity drug has been developed to target BAT function. The current approach for dietary supplement of obesity treatment relies on appetite control and inhibition of lipase. Previously, 2,4-Dinitrophenol (DNP) , a brown fat stimulator, was used as a weight loss drug for body builders (Grundlingh, Dargan, El-Zanfaly, & Wood, 2011). DNP activates mitochondrial UCP1, therefore redirecting the energy from

ATP synthesis to thermogenesis and raising the basal body metabolic rate. Consumption in humans has dramatic weight loss effects as much as 1.5kg/week, which targets fat but does not affect muscle bulk. The rapidly built up heat causes body overheating, and in some cases results in severe fever and mortality. Although DNP was applied for clinical use in 1933, it was quickly banned by the Federal Food, Drug and Cosmetic Act of 1938 and labeled “extremely dangerous and not fit for human consumption”. DNP usage in UK was banned in 2003. However, the drug is still widely available on the internet and in other places of the world. Despite the fact that DNP usage was a dangerous attempt in treating obesity, it reflects that a controllable UCP activation may be a treatment for obesity. Therefore, studies on BAT are important to date.

1.8 Skeletal muscle and its interactions with brown adipose

1.8.1 Skeletal muscle structure and functions

Skeletal muscle comprises approximately 50% of body mass (Zierath & Hawley, 2004). Histologically, skeletal muscle is composed of cylindrical multi-nucleated myofibers (and satellite cells), vasculature structures, nerve branches, fat and connective tissues (Kuang & Rudnicki, 2008). Myofibers are made up of tubular myofibrils lining up with repetitive contractile units called sarcomeres. Sarcomeres are the source of skeletal muscle striations.

Generally, skeletal muscles are divided into fast and slow types based on the contraction speed (slow vs. fast) and fatigability. Slow muscle is characterized by more

oxidative metabolism (Bassel-Duby & Olson, 2006), higher myoglobin content, higher mitochondria number (Schiaffino, 2010; Westerblad, Bruton, & Katz, 2010), greater fat content, denser capillary distribution (Bassel-Duby & Olson, 2006) and lower susceptibility to fatigue (Bottinelli & Reggiani, 2000) than fast muscle. More current classification groups muscles into Type I, IIA, IIX, IIB based on the myosin heavy chain (MHC) content, with Type I being the slowest, type IIA being the slow, type IIX being the fast and type IIB being the fastest (Schiaffino, 2010; Westerblad et al., 2010). Each muscle usually consists of several fiber types, while myofiber contains one type of MHC (Greising, Gransee, Mantilla, & Sieck, 2012). Many factors such as innervation(Buller, Eccles, & Eccles, 1960), gene regulations(Rasbach et al., 2010), age, and hormone secretion affect muscle type and alteration can lead to fiber type change(Pette & Staron, 2000) from fast to slow and from slow to fast (Schiaffino, Sandri, & Murgia, 2007).

Skeletal muscle has three major functions: Movement conduct, energy metabolism, and support and protection. Skeletal muscle is the motor organ mediating body movements. Upon chemical (neural transmitter acetylcholine) and physical (electrical stimulus) stimulation, calcium influx is induced in muscle cell cytoplasm. The cytoplasmic reticulum calcium signaling promotes the movements of myofilaments, resulting in muscle contraction. Skeletal muscle affects body temperature and energy metabolism. Skeletal muscle as a large organ actively metabolizes glucose, lipids and protein for an energy source or structural materials. Like BAT, skeletal muscle expresses Ucp and takes part in non-shivering thermogenesis when body temperature is low (van den Berg, van Marken Lichtenbelt, Willems van Dijk, & Schrauwen, 2011). Apart from

the first two functions, skeletal muscle tension is essential in protecting and supporting body postures and internal organs.

1.8.2 Skeletal muscle development

Embryonic mygenesis starts from the formation of the paraxial mesoderm. Body skeletal muscles develop from the hypaxial and epexial dermomyotome, which are the two parts of somite that arise from paraxial mesoderm (Bailey, Holowacz, & Lassar, 2001; Bentzinger, Wang, & Rudnicki, 2012). Head muscles originate differently from other parts of the mesoderm (Bentzinger et al., 2012). To generate a mature muscle, thin and tubular primary myofibers are formed by proliferation and fusion of *Myf5* and MyoD expressing stem cells, followed by secondary fusion of myogenic cells to enhance the volume and force of the muscle (Buckingham et al., 2003).

1.8.3 Satellite cells

Satellite cells represent ~2%-7% myofiber associated cell population (Relaix & Marcelle, 2009). They are presented in late embryonic myogenesis and normally remained mitotically quiescent in their myofiber niche throughout the life of an individual (Relaix, Rocancourt, Mansouri, & Buckingham, 2005). In response to muscle growth or injury, satellite cells and many other cell types within muscle are activated and prompted to multiply (Ceafalan, Popescu, & Hinescu, 2014). The activated satellite cells relocate into the center of the tubular myofiber instead of staying on the edge when they are inactive. The centered satellite cells then undergo a differentiation process and generate new muscles. The mechanism or signaling underlining satellite cell

activation is under examination. Many factors have been identified in satellite cell activation including hepatocyte growth factors (HGFs), fibroblast growth factors (FGFs), cytokines and some myokines.

Activated satellite cells possess a profound ability to proliferate and self-renew (Relaix & Zammit, 2012). A single FACS isolated satellite cell gives rise to many more satellite cells in the regenerating animal. The self-renewal ability of satellite cells can be explained by their niche and signal transduction. Satellite cell niche regulates symmetrical and asymmetrical division (Kuang, Kuroda, Le Grand, & Rudnicki, 2007). When activated, satellite cells undergo planar division or baso-apical division in their niches. Basal-apical division is preferred to maintain satellite cell self-renewal ability since it stimulates asymmetrical division to form two daughter cells of different fates- one remains quiescent and one committed to myogenic differentiation. Planar division that favors symmetrically generation of two daughter cells committed to differentiation (*Pax7*$^{+}$/*Myf5*$^{+}$) are more frequently observed. Signal molecules like Notch induces Pax7 expression by repressing miR-1 and miR206, in turn promotes satellite cell self-renewal (Liu, Wen, et al., 2012). The regulation of satellite cell proliferation and self-renewal is under extensive examination.

1.8.4 Skeletal muscle metabolism*

Obesity results from an energy surplus (i. e. greater energy intake than expenditure). As the largest organ in the body, the skeletal muscle comprises ~40% of body mass (Neel, Lin, & Pessin, 2013) and serves as one of the major regulators of body

---

The * section is adopted from a review: Yang X, Bi P, Kuang S. 2014. Fighting obesity: When muscle meets fat. *Adipocyte*.

energy homeostasis. Even under severe obese conditions, skeletal muscles still account for ~25% of body mass and remain metabolically active to a certain extent. In order to satisfy the structural and functional needs for skeletal muscle, massive amounts of energy are utilized for muscle protein synthesis and motor function under both resting and exercise conditions. Skeletal muscles mainly utilize glucose as the energy source, but can also utilize free fatty acids (FFA) and amino acids (AA) as fuels or structural "building blocks". Thus, the skeletal muscle can affect not only glucose, but also fat and protein homeostasis in the body.

Skeletal muscles uptake ~75% of ingested carbohydrate from meals (Brault, Dohm, & Houmard, 2014). Postprandial plasma glucose is primarily taken up through glucose transporter 4 (GLUT4) facilitated infusion, and then subjected to glycolysis, oxidative phosphorylation, or glycogen synthesis depending on individual activity levels. The process of glucose uptake and catabolism during muscle activity contributes to a negative energy balance. Contraction and insulin stimulation are two main activators of muscle glucose uptake (Richter & Hargreaves, 2013).

Muscle contraction directly stimulates glucose uptake predominantly through activation of AMP-activate protein kinase (AMPK), which increases GLUT4 translocation to the muscle cell membrane (sarcolemma)(Friedrichsen, Mortensen, Pehmoller, Birk, & Wojtaszewski, 2013; JorgensenO'Neill, 2013). Briefly, muscle contraction increases the ratio of AMP/ATP, which is detected by energy sensor AMPK. The activated AMPK then phosphorylates TBC1 (Tre-2/USP6, BUB2, Cdc16) domain family member 4 and 1 (TBC1D

4 and TBC1D1), leading to the release of GLUT4 from cytoplasmic storage vesicles to the sarcolemma (JorgensenO'Neill, 2013). Differential phenotypes of mice lacking AMPK α, β, or γ subunit suggest that each subunit has a unique role in regulating muscle glucose uptake(Barnes et al., 2004; Dasgupta et al., 2012; Jorgensen et al., 2004; O'Neill et al., 2011; Steinberg et al., 2010). AMPK-independent mechanisms may also be involved in skeletal muscle glucose uptake. For example, the antioxidant N-acetyl-l-cysteine (NAC) and the nitric oxide synthase (NOS) inhibitor N(G)-monomethyl-l-arginine (l-NMMA) can attenuate contraction stimulated glucose uptake in both WT and muscle specific AMPKα2 knockout mice (Merry, Steinberg, Lynch, & McConell, 2010). As an energy "sensor" and regulatory molecule, AMPK also inhibits glycogen synthesis, promotes fatty acid oxidation, and enhances mitochondria oxidation in contracting muscle cells. AMPK also promotes exercise-mediated improvements in insulin sensitivity through mechanisms involving interleukin 6 (IL-6), adiponectin, IR, IRS, and mTOR (JorgensenO'Neill, 2013). Human studies indicate that AMPK mRNA and protein levels are down-regulated in obese subjects but elevated by exercise, suggesting the potential of AMPK mimetic as therapeutic agents to treat obesity and insulin resistance. In fact, metformin, an AMPK activating compound, has been used as the first-line drug in current clinical treatments of diabetes (Dunn & Peters, 1995; Hadley, Whaley, & Askins, 1998). The most updated meta-analyses also indicate that metformin also reduces colorectal, liver, pancreatic and stomach cancer risks in diabetic patients (Franciosi et al., 2013).

Insulin stimulates muscle glucose uptake and disposal through the IR-IRS-PI3K pathway. Insulin binding to the insulin receptor (IR) activates the intrinsic tyrosine kinase of IRβ-subunit, which phosphorylates insulin receptor substrate 1 (IRS-1). Phospho-IRS-1 docks class I phosphatidlyinositol-3-kinase (PI3K), which phosphorylates Akt and atypical protein kinase C zeta (aPKCζ), leading to GLUT4 translocation. Insulin resistance commonly associated with obesity and T2DM describes the condition of reduced cellular responsiveness to circulating insulin, resulting in the hyperinsulinemia, hyperglycinemia and hyperlipidemia. Insulin resistance dampers insulin signaling transduction without damaging the structures needed for glucose uptake, since insulin resistant human skeletal muscles exhibit normal GLUT4 translocation when stimulated by contraction or hypoxia (Azevedo, Carey, Pories, Morris, & Dohm, 1995; Dolan, Tapscott, Dorton, & Dohm, 1993). As ~80% of body insulin stimulated glucose uptake is mediated by the skeletal muscle (JorgensenO'Neill, 2013), skeletal muscle insulin resistance can be devastating, and can lead to a vicious circle of insulin resistance and metabolic disorders. Thus, exercise therapies and pharmaceutical compounds that improve muscle insulin sensitivity represent a promising direction to treat Type 2 diabetes and other metabolic syndromes.

In addition to glucose, skeletal muscle also utilizes fatty acids and proteins depending on availability of substrates. This adaptive process is known as “metabolic flexibility”. During fasting, fatty acid oxidation (FAO) accounts for up to 90% of muscle energy supply. Healthy human skeletal muscle actively catabolizes non-esterified fatty acid (NEFA) via hormone-sensitive lipoprotein lipase (LPL), whilst muscles of obese or

T2DM patients show nearly diminished NEFA uptake and deficiency in FAO (Blaak, 2004). The impaired FFA metabolism potentially causes ectopic lipid accumulation in skeletal muscle, liver, and heart; increasing the risk of insulin resistance and metabolic disorders. The impaired FFA metabolism may be associated with mitochondrial mass reduction or functional disruption, such as inhibition of carnitine palmitoyltransferase 1 (CPT-1) mediated lipid transport and ROS inactivation of mitochondrial membrane enzymes (Blaak, 2004; Wells, Noseworthy, Hamilton, Tarnopolski, & Tein, 2008).

The skeletal muscle is also highly active in protein metabolism since it requires rapid protein synthesis and degradation for maintaining muscle turnover. Proteins also serve as a source of energy for muscle contraction under extreme fasting conditions. Increased levels of plasma AA and decreased skeletal muscle protein synthesis were evident in obese animal models (Katsanos & Mandarino, 2011). Skeletal muscle protein metabolism is regulated by complex mechanisms. Mammalian target of rapamycin (mTOR), especially the mTOR complex 1 (mTORC1), is the most important regulator of skeletal muscle mass and protein synthesis in response to high plasma AA concentration. Activation of mTOR initiates canonical muscle protein synthesis pathways, and interestingly, partially decreases autophagic influx that facilitates protein degradation (Neel et al., 2013).

1.8.5 Muscle-fat crosstalk*

Skeletal muscle is not only a motor organ but also an endocrine organ releasing small secretive molecules known as myokines. Broadly speaking, “peptides or proteins that are produced, expressed and released by muscle fibers and exert a paracrine or

The * section is adopted from a review: Yang X, Bi P, Kuang S. 2014. Fighting obesity: When muscle meets fat. *Adipocyte*.

endocrine effect" are referred to as myokines (Eckardt, Gorgens, Raschke, & Eckel, 2014; Pal, Febbraio, & Whitham, 2014; L. Pedersen & Hojman, 2012; Raschke & Eckel, 2013). Myokines often alter body energy utilization, inflammatory status and adiposity, therefore affecting weight gain and fat composition. Common myokines include irisin, myostatin, interleukins (IL6, 7, 8, 15), Leukemia Inhibitory Factor (LIF), among others (B. K. Pedersen & Febbraio, 2012).

Irisin is the most recently identified and intensively investigated myokine due to its potential usage to target obesity. It is a short peptide cleaved from the extracellular domain of the Fndc5 (fibronectin domain-containing 5). Fndc5 mRNA is expressed abundantly in the heart, brain, rectum and skeletal muscle and moderately in the intracranial artery, tongue and optic nerve, with some disagreements among different studies (Ferrer-Martinez, Ruiz-Lozano, & Chien, 2002; Huh et al., 2012; Teufel, Malik, Mukhopadhyay, & Westphal, 2002). The expression pattern implies that irisin may exert functions on multiple tissues. One example is that exercising mice have elevated Fndc5 in their hippocampus, suggesting that Fndc5 positively regulates neural activities(Wrann et al., 2013). Another popular example is the original discovery demonstrating irisin as an "exercise hormone" secreted by skeletal muscle. Once secreted, irisin circulates through the bloodstream to fat tissues, where it promotes browning of white adipocytes (P. Bostrom et al., 2012). The irisin mediated "browning" of WAT depends on proliferator-activated receptor γ coactivator 1 alpha (PGC1-α) (Zhang et al., 2014). The "browning" can be synergistically enhanced by fibroblast growth factor21 (FGF21), a cold-induced myokine(Keipert et al., 2014; P. Lee et al., 2014; B. K. Pedersen, 2011).

Irisin also serves as a focal regulator of muscle cell metabolism through promoting mitochondria biogenesis and metabolic gene expression (Vaughan et al., 2014). Besides its hormonal function, Fndc5 may serve as a transmembrane signaling protein (Erickson, 2013). Contradicting results regarding association between plasma irisin levels and insulin sensitivity have been reported in human studies (Sanchis-Gomar, Alis, Pareja-Galeano, Romagnoli, & Perez-Quilis, 2014). For example, obesity and T2DM are reported to be negatively correlated with irisin/ FNDC5 secretion and mRNA expression (Kurdiova et al., 2014; Norheim et al., 2014). However, high levels of baseline plasma irisin are correlated with insulin resistance in obese patients, implying the possibility of "irisin resistance" (Crujeiras et al., 2013). In cell culture experiments, palmitate and glucose treatments that partially mimics diabetic and obese situations decrease muscle cell FNDC5 mRNA expression (Kurdiova et al., 2014). Other studies show that neither acute nor long term exercise significantly improves circulating irisin level or brown fat gene expression, despite elevated irisin/Fndc5 expression in muscle (Kurdiova et al., 2014; Norheim et al., 2014). Another independent study reports that the human FNCD5 gene start codon is mutated, and irisin treatment does not increase human brite cell formation *in vitro* (Raschke et al., 2013). Although the majority studies support that irisin/Fndc5 mediates the "crosstalk" of skeletal muscles to other tissues (P. A. Bostrom, Fernandez-Real, & Mantzoros, 2014; P. Lee et al., 2014), whether the effect of irisin can be translated to humans remains to be investigated.

Myostatin (Mstn), also called growth/differentiation factor 8 (GDF8), is another extensively studied and well-established myokine. Mstn belongs to the highly conserved

TGF-β family and its absence causes dramatic increases of muscle cell size (hypertrophy) in humans, mice, cattle and other mammals (Grobet et al., 1997; Kawada, Tachi, & Ishii, 2001; McPherron & Lee, 1997; Schuelke et al., 2004). Mstn also affects other tissues such as adipose and bone (Buehring & Binkley, 2013). Body weight gain and reduction of fat composition were induced in muscle-specific and whole body Mstn knockout, but not in adipose-specific Mstn knockout animals (Buehring & Binkley, 2013; Guo et al., 2009; McPherron & Lee, 2002). While adipose-specific Mstn deletion fails to induce "browning" of WAT, whole body deletion of Mstn robustly induces Fndc5 expression in skeletal muscle, which in turn promotes formation of beige fat cells (Shan, Liang, Bi, & Kuang, 2013). Although Mstn and one of its receptors – activin receptor IIB (ActRIIB) – are expressed by adipocytes, the expression level may be too low to provide physiological relevance (Allen et al., 2008; Allen, Hittel, & McPherron, 2011; Rebbapragada, Benchabane, Wrana, Celeste, & Attisano, 2003). Consistently, Mstn treatment has no effect on cultured adipocytes (Shan et al., 2013). Together these lines of evidence suggest that Mstn reduces body fat composition and induces "browning" of WAT likely through an indirect mechanism mediated by the skeletal muscle. In both human and rodents, Mstn is expressed at higher levels in obese individuals and lower levels in exercised subjects (Allen et al., 2011; Konopka et al., 2010; B. K. Pedersen & Febbraio, 2012; Roth et al., 2003). As Mstn seems to partially explain the beneficial effect of exercise, targeting Mstn signaling pathway using soluble ActRIIB decoy receptor ACE-031 is currently in clinical trial (Attie et al., 2013).

The IL family members (IL-4, 6, 7, 8, 15) are regarded as myokines for their versatile functions in regulating energy homeostasis, immune responses and cell movements (Guo et al., 2009). They are produced in muscle cells and infuse into bloodstream, though some are later found more abundantly produced by other cells (such as IL-8). Of these IL family myokines, IL-6 appears to have to most promising clinical value. IL6 production is low when cellular glucose import is high, but increases during exercise (Keller et al., 2001) or when skeletal muscle glycogen content is low (Keller et al., 2001). IL-6 also promotes muscle growth and regeneration (Serrano, Baeza-Raja, Perdiguero, Jardi, & Munoz-Canoves, 2008; Spangenburg & Booth, 2006) in addition to its function in improving muscle glucose metabolism (Carey et al., 2006). Recombinant IL-6 improves glucose metabolism, insulin sensitivity and helps to shift skeletal muscle energy source to fat in humans (B. K. Pedersen & Febbraio, 2012). However, IL-6 is also produced by adipocytes and has been shown to induce insulin resistance(Bastard et al., 2002; Rotter, Nagaev, & Smith, 2003; Tsigos et al., 1997) and inflammation in adipose tissues (Fontana, Eagon, Trujillo, Scherer, & Klein, 2007). Therefore, more systemic studies are needed since the long term elevation of IL-6 seems to have adverse influences (Golbidi & Laher, 2014). Other IL family members IL-7, 8 and 15 are all involved in immune responses that play key roles in adipose tissue function (B. K. Pedersen & Febbraio, 2012). Although they are not yet well characterized, they do seem to facilitate the maintenance of energy homeostasis or inflammation status. Notably, IL-15 mediates muscle-fat interaction by negatively regulating lipid metabolism (Quinn, 2008).

Other myokines and potential myokines include LIFs (B. K. Pedersen & Febbraio, 2012), FGF2 (B. K. Pedersen & Febbraio, 2012), brain-derived neurotrophic factor (Broholm et al., 2011; Raschke & Eckel, 2013; Zoladz & Pilc, 2010), follistatin (B. K. Pedersen & Febbraio, 2012), insulin-like growth factor 1 (Barton et al., 2012; Laviola, Natalicchio, & Giorgino, 2007; B. K. Pedersen & Febbraio, 2012), monocyte chemoattractant protein (Sell, Dietze-Schroeder, Kaiser, & Eckel, 2006; Yadav, Saini, & Arora, 2010), and myonectin (Lim et al., 2012; Seldin, Peterson, Byerly, Wei, & Wong, 2012). Myokines are secreted in different amounts and combinations depending on various physical activity levels. Some of the myokines are also produced in adipose tissue, therefore known as adipomyokines (Raschke & Eckel, 2013). The adipomyokines may be more involved in bidirectional muscle-fat cross talk.

Obesity and sarcopenia (age related loss of muscle) represent two typical situations in which fat mass and muscle mass are negatively correlated. Obesity is generally accompanied by increased fat and lean mass, but the fat mass increases at a larger scale, resulting in a smaller lean muscle to fat ratio. The overall increased body mass in obese individuals also leads to skeletal muscle overload, resulting in greater leg and trunk muscle strength but not handgrip or arm strength (Lafortuna, Maffiuletti, Agosti, & Sartorio, 2005). Sarcopenic obesity that affects 5-10% of the elderly is a type of obesity in which patients have normal body mass but little lean mass. Sarcopenic obesity is under the camouflage of normal body weight, therefore adding its difficulty to be discovered and treated (Sakuma & Yamaguchi, 2013). In addition to sarcopenic obesity, aging is naturally accompanied by sarcopenia and fat deposition (Brady, Straight,

& Evans, 2013; Schaap, Koster, & Visser, 2012; Yamada, Moriguch, Mitani, Aoyama, & Arai, 2014), together with redistribution of body fat from appendicular to stomach and ectopic sites such as liver and muscle (Addison et al., 2014).

Individuals who conduct exercise on a regular basis gain more muscle mass , have better muscle function, and lower risks of obesity and T2DM, depending on the type and duration of physical training. In contrast, physical inactivity is associated with decreased muscle mass, increased visceral adiposity, and increased macrophage infiltration, chronic systemic inflammation, insulin resistance, obesity, and T2DM (B. K. Pedersen & Febbraio, 2012). As discussed previously, skeletal muscle exercise increases energy expenditure, stimulates secretion of beneficial myokines, and increases insulin sensitivity. Muscle exercise also attenuates adipogenesis of mesenchymal stem cells through Akt-mediated mechanical signal responses (Menuki et al., 2008; Sen et al., 2011). An increase in skeletal muscle mass may directly lead to reduced body fat composition, manifested by the fact that body builders often find themselves stuck in an extremely lean condition (Bazzarre, Kleiner, & Litchford, 1990). Consistently, animals with enhanced muscle growth, such as Mstn knockout mice and Callipyge sheep, often have little body fat deposition (Koohmaraie, Shackelford, Wheeler, Lonergan, & Doumit, 1995; McPherron & Lee, 2002). However, moderate to high intensity exercise training increases intramyocellular triglycerides (Dube et al., 2008; Tarnopolsky et al., 2007; van Loon et al., 2004), a lipid store within muscle cells (Badin, Langin, & Moro, 2013). This phenomenon is referred to as “athlete's paradox”(Goodpaster, He, Watkins, & Kelley, 2001) and is likely associated with an increase in oxidative metabolism in exercised

muscle. The intramyocellular triacylglycerol droplets act as a FFA fuel source for muscle contraction (van Loon, 2004). Interestingly, diabetic individuals also have elevated levels intramyocellular triglycerides (Goodpaster et al., 2001; van Loon et al., 2004).

Body fat deposition in turn affects skeletal muscle function. It is widely accepted that inflammatory adipokines secreted by ectopic accumulation of fat leads to muscle insulin resistance (Kwon & Pessin, 2013; Romacho, Elsen, Rohrborn, & Eckel, 2014). It was also reported that FFA and exercise mimetics (such as AICAR) impact the secretion of myokines, especially the IL family members (Sanchez, Nozhenko, Palou, & Rodriguez, 2013). Importantly, fat deposition affects muscle homeostasis. Decreases of muscle mass were consistently reported in obese rodents and humans. In accordance, mice with ectopic fat accumulation exhibit impaired muscle regeneration possibly due to lipid toxicity, pro-inflammatory cytokines and compromised muscle stem cell or satellite cell function (Akhmedov & Berdeaux, 2013). However, adipocytes are nevertheless necessary for muscle regeneration, and in the absence of adipocytes skeletal muscles cannot regenerate after injury (Liu, Liu, et al., 2012). This observation suggests that adipocytes or their “crosstalk” to muscle cells may facilitate muscle recovery. Indeed, adiponenctin, an adipokine secreted by adipocytes, has recently been shown to improve skeletal muscle regeneration by promoting satellite cell proliferation and differentiation (Fiaschi, Magherini, Gamberi, Modesti, & Modesti, 2013).

1.9 Summary of literature review

The above review sections can be generally summarized in these aspects: (1) three types of adipose tissues have been identified in mammals- WAT, BAT and beige adipose tissues. They distribute at multiple locations in the body and display depot specificity. WAT is specialized in energy storage, organ protection and adipokine secretion, while BAT and beige adipose are important players in controlling energy homeostasis through thermogenesis. (2) Markers of adipocyte progenitors have been discovered. Zfp423 and VE-Cad marks WAT and BAT progenitors while Pdgfrα marks WAT and beige progenitors. Myogenic and adipogenic progenitors can be efficiently isolated and cultured *in vitro*, and are currently applied in the field of regenerative medicine. (3) BAT exhibits dramatic dynamics affected by age, species and environmental cues. BAT adipocyte differentiation is dependent on PPARs and CEBPs, and the activation is dependent on Adr mediated UCP1 function. (4) Skeletal muscles are closely associated with BAT in terms of lineage origin, functions and cellular interplay. They maintain body energy homeostasis through utilizing glucose, lipids and proteins. Skeletal muscle also cross-talk with fat tissues through secretion of myokines such as irisin.

However, several gaps of knowledge exist in the study of BAT. Little is known about the progenitor population in BAT. Whether the BAT stem cells are from *Pdgfra* lineage and are involved in maintaining BAT plasticity is also unknown. Furthermore, since a population of progenitors is identified in BAT SVF culture *in vitro*, it is speculated

that BAT may have the possibility to regenerate *in vivo*. The close relationship of BAT with skeletal muscle also triggers the assumption that skeletal muscle and satellite cells may associate with BAT structure and affect BAT function. This study aims to understand BAT plasticity and function from the perspective of adipogenic and myogenic progenitors in BAT. Mouse isBAT was chosen as it is the classical BAT depot in rodents, and a number of *in vivo* and *in vitro* assays were carried out to achieve this central aim.

References

Addison, O., Marcus, R. L., Lastayo, P. C., & Ryan, A. S. (2014). Intermuscular Fat: A Review of the Consequences and Causes. *Int J Endocrinol, 2014*, 309570. doi: 10.1155/2014/309570

Agley, C. C., Rowlerson, A. M., Velloso, C. P., Lazarus, N. R., & Harridge, S. D. (2013). Human skeletal muscle fibroblasts, but not myogenic cells, readily undergo adipogenic differentiation. *J Cell Sci, 126*(Pt 24), 5610-5625. doi: 10.1242/jcs.132563

Aguiari, P., Leo, S., Zavan, B., Vindigni, V., Rimessi, A., Bianchi, K., . . . Rizzuto, R. (2008). High glucose induces adipogenic differentiation of muscle-derived stem cells. *Proc Natl Acad Sci U S A, 105*(4), 1226-1231. doi: 10.1073/pnas.0711402105

Akhmedov, D., & Berdeaux, R. (2013). The effects of obesity on skeletal muscle regeneration. *Front Physiol, 4*, 371. doi: 10.3389/fphys.2013.00371

Alexander, G., & Bell, A. W. (1975). Quantity and calculated oxygen consumption during summit metabolism of brown adipose tissue in new-born lambs. *Biol Neonate, 26*(3-4), 214-220.

Alexeev, V., Arita, M., Donahue, A., Bonaldo, P., Chu, M. L., & Igoucheva, O. (2014). Human adipose-derived stem cell transplantation as a potential therapy for collagen VI-related congenital muscular dystrophy. *Stem Cell Res Ther, 5*(1), 21. doi: 10.1186/scrt411

Allen, D. L., Cleary, A. S., Speaker, K. J., Lindsay, S. F., Uyenishi, J., Reed, J. M., . . . Mehan, R. S. (2008). Myostatin, activin receptor IIb, and follistatin-like-3 gene expression are altered in adipose tissue and skeletal muscle of obese mice. *Am J Physiol Endocrinol Metab, 294*(5), E918-927. doi: 10.1152/ajpendo.00798.2007

Allen, D. L., Hittel, D. S., & McPherron, A. C. (2011). Expression and function of myostatin in obesity, diabetes, and exercise adaptation. *Med Sci Sports Exerc, 43*(10), 1828-1835. doi: 10.1249/MSS.0b013e3182178bb4

Andersson, B. S., de Lima, M., Thall, P. F., Madden, T., Russell, J. A., & Champlin, R. E. (2009). Reduced-toxicity conditioning therapy with allogeneic stem cell transplantation for acute leukemia. *Curr Opin Oncol, 21 Suppl 1*, S11-15. doi: 10.1097/01.cco.0000357469.83960.12

Asakura, A., Komaki, M., & Rudnicki, M. (2001). Muscle satellite cells are multipotential stem cells that exhibit myogenic, osteogenic, and adipogenic differentiation. *Differentiation, 68*(4-5), 245-253.

Attie, K. M., Borgstein, N. G., Yang, Y., Condon, C. H., Wilson, D. M., Pearsall, A. E., . . . Sherman, M. L. (2013). A single ascending-dose study of muscle regulator ACE-031 in healthy volunteers. *Muscle Nerve, 47*(3), 416-423. doi: 10.1002/mus.23539

Azevedo, J. L., Jr., Carey, J. O., Pories, W. J., Morris, P. G., & Dohm, G. L. (1995). Hypoxia stimulates glucose transport in insulin-resistant human skeletal muscle. *Diabetes, 44*(6), 695-698.

Badin, P. M., Langin, D., & Moro, C. (2013). Dynamics of skeletal muscle lipid pools. *Trends Endocrinol Metab, 24*(12), 607-615. doi: 10.1016/j.tem.2013.08.001

Bailey, P., Holowacz, T., & Lassar, A. B. (2001). The origin of skeletal muscle stem cells in the embryo and the adult. *Curr Opin Cell Biol, 13*(6), 679-689.

Barbatelli, G., Murano, I., Madsen, L., Hao, Q., Jimenez, M., Kristiansen, K., . . . Cinti, S. (2010). The emergence of cold-induced brown adipocytes in mouse white fat depots is determined predominantly by white to brown adipocyte transdifferentiation. *Am J Physiol Endocrinol Metab, 298*(6), E1244-1253. doi: 10.1152/ajpendo.00600.2009

Bareja, A., & Billin, A. N. (2013). Satellite cell therapy - from mice to men. *Skelet Muscle, 3*(1), 2. doi: 10.1186/2044-5040-3-2

Bareja, A., Holt, J. A., Luo, G., Chang, C., Lin, J., Hinken, A. C., . . . Billin, A. N. (2014). Human and mouse skeletal muscle stem cells: convergent and divergent mechanisms of myogenesis. *PLoS One, 9*(2), e90398. doi: 10.1371/journal.pone.0090398

Barnes, B. R., Marklund, S., Steiler, T. L., Walter, M., Hjalm, G., Amarger, V., . . . Andersson, L. (2004). The 5'-AMP-activated protein kinase gamma3 isoform has a key role in carbohydrate and lipid metabolism in glycolytic skeletal muscle. *J Biol Chem, 279*(37), 38441-38447. doi: 10.1074/jbc.M405533200

Barness, L. A., Opitz, J. M., & Gilbert-Barness, E. (2007). Obesity: genetic, molecular, and environmental aspects. *Am J Med Genet A, 143A*(24), 3016-3034. doi: 10.1002/ajmg.a.32035

Bartelt, A., & Heeren, J. (2014). Adipose tissue browning and metabolic health. *Nat Rev Endocrinol, 10*(1), 24-36. doi: 10.1038/nrendo.2013.204

Barton, E. R., Park, S., James, J. K., Makarewich, C. A., Philippou, A., Eletto, D., . . . Argon, Y. (2012). Deletion of muscle GRP94 impairs both muscle and body growth by inhibiting local IGF production. *FASEB J, 26*(9), 3691-3702. doi: 10.1096/fj.11-203026

Bassel-Duby, R., & Olson, E. N. (2006). Signaling pathways in skeletal muscle remodeling. *Annu Rev Biochem, 75*, 19-37. doi: 10.1146/annurev.biochem.75.103004.142622

Bastard, J. P., Maachi, M., Van Nhieu, J. T., Jardel, C., Bruckert, E., Grimaldi, A., . . . Hainque, B. (2002). Adipose tissue IL-6 content correlates with resistance to insulin activation of glucose uptake both in vivo and in vitro. *J Clin Endocrinol Metab, 87*(5), 2084-2089. doi: 10.1210/jcem.87.5.8450

Bazzarre, T. L., Kleiner, S. M., & Litchford, M. D. (1990). Nutrient intake, body fat, and lipid profiles of competitive male and female bodybuilders. *J Am Coll Nutr, 9*(2), 136-142.

Bentzinger, C. F., Wang, Y. X., & Rudnicki, M. A. (2012). Building muscle: molecular regulation of myogenesis. *Cold Spring Harb Perspect Biol, 4*(2). doi: 10.1101/cshperspect.a008342

Berg, D. A., Kirkham, M., Wang, H., Frisen, J., & Simon, A. (2011). Dopamine controls neurogenesis in the adult salamander midbrain in homeostasis and during regeneration of dopamine neurons. *Cell Stem Cell, 8*(4), 426-433. doi: 10.1016/j.stem.2011.02.001

Berg, F., Gustafson, U., & Andersson, L. (2006). The uncoupling protein 1 gene (UCP1) is disrupted in the pig lineage: a genetic explanation for poor thermoregulation in piglets. *PLoS Genet, 2*(8), e129. doi: 10.1371/journal.pgen.0020129

Berry, R., Jeffery, E., & Rodeheffer, M. S. (2014). Weighing in on adipocyte precursors. *Cell Metab, 19*(1), 8-20. doi: 10.1016/j.cmet.2013.10.003

Berry, R., & Rodeheffer, M. S. (2013). Characterization of the adipocyte cellular lineage in vivo. *Nat Cell Biol, 15*(3), 302-308. doi: 10.1038/ncb2696

Bi, P., Shan, T., Liu, W., Yue, F., Yang, X., Liang, X. R., . . . Kuang, S. (2014). Inhibition of Notch signaling promotes browning of white adipose tissue and ameliorates obesity. *Nat Med*. doi: 10.1038/nm.3615

Billon, N., & Dani, C. (2012). Developmental origins of the adipocyte lineage: new insights from genetics and genomics studies. *Stem Cell Rev, 8*(1), 55-66. doi: 10.1007/s12015-011-9242-x

Billon, N., Iannarelli, P., Monteiro, M. C., Glavieux-Pardanaud, C., Richardson, W. D., Kessaris, N., . . . Dupin, E. (2007). The generation of adipocytes by the neural crest. *Development, 134*(12), 2283-2292. doi: 10.1242/dev.002642

Blaak, E. E. (2004). Basic disturbances in skeletal muscle fatty acid metabolism in obesity and type 2 diabetes mellitus. *Proc Nutr Soc, 63*(2), 323-330. doi: 10.1079/PNS2004361

Bostrom, P. A., Fernandez-Real, J. M., & Mantzoros, C. (2014). Irisin in humans: recent advances and questions for future research. *Metabolism, 63*(2), 178-180. doi: 10.1016/j.metabol.2013.11.009

Bostrom, P., Wu, J., Jedrychowski, M. P., Korde, A., Ye, L., Lo, J. C., . . . Spiegelman, B. M. (2012). A PGC1-alpha-dependent myokine that drives brown-fat-like development of white fat and thermogenesis. *Nature, 481*(7382), 463-468. doi: 10.1038/nature10777

Bottinelli, R., & Reggiani, C. (2000). Human skeletal muscle fibres: molecular and functional diversity. *Prog Biophys Mol Biol, 73*(2-4), 195-262.

Bowers, R. R., & Lane, M. D. (2008). Wnt signaling and adipocyte lineage commitment. *Cell Cycle, 7*(9), 1191-1196.

Brady, A. O., Straight, C. R., & Evans, E. M. (2013). Body Composition, Muscle Capacity and Physical Function in Older Adults: An Integrated Conceptual Model. *J Aging Phys Act*.

Brault, Jeffrey J, Dohm, G Lynis, & Houmard, Joseph A. (2014). 22 Skeletal Muscle Metabolism and Obesity. *Handbook of Obesity: Epidemology, Etiology, and Physiopathology, 1*, 249.

Broholm, C., Laye, M. J., Brandt, C., Vadalasetty, R., Pilegaard, H., Pedersen, B. K., & Scheele, C. (2011). LIF is a contraction-induced myokine stimulating human myocyte proliferation. *J Appl Physiol (1985), 111*(1), 251-259. doi: 10.1152/japplphysiol.01399.2010

Buckingham, M., Bajard, L., Chang, T., Daubas, P., Hadchouel, J., Meilhac, S., . . . Relaix, F. (2003). The formation of skeletal muscle: from somite to limb. *J Anat, 202*(1), 59-68.

Buehring, B., & Binkley, N. (2013). Myostatin--the holy grail for muscle, bone, and fat? *Curr Osteoporos Rep, 11*(4), 407-414. doi: 10.1007/s11914-013-0160-5

Bukowiecki, L., Collet, A. J., Follea, N., Guay, G., & Jahjah, L. (1982). Brown adipose tissue hyperplasia: a fundamental mechanism of adaptation to cold and hyperphagia. *Am J Physiol, 242*(6), E353-359.

Bukowiecki, L. J., Geloen, A., & Collet, A. J. (1986). Proliferation and differentiation of brown adipocytes from interstitial cells during cold acclimation. *Am J Physiol, 250*(6 Pt 1), C880-887.

Buller, A. J., Eccles, J. C., & Eccles, R. M. (1960). Interactions between motoneurones and muscles in respect of the characteristic speeds of their responses. *J Physiol, 150*, 417-439.

Cannon, B., & Nedergaard, J. (2004). Brown adipose tissue: function and physiological significance. *Physiol Rev, 84*(1), 277-359. doi: 10.1152/physrev.00015.2003

Carey, A. L., Steinberg, G. R., Macaulay, S. L., Thomas, W. G., Holmes, A. G., Ramm, G., . . . Febbraio, M. A. (2006). Interleukin-6 increases insulin-stimulated glucose disposal in humans and glucose uptake and fatty acid oxidation in vitro via AMP-activated protein kinase. *Diabetes, 55*(10), 2688-2697. doi: 10.2337/db05-1404

Ceafalan, L. C., Popescu, B. O., & Hinescu, M. E. (2014). Cellular players in skeletal muscle regeneration. *Biomed Res Int, 2014*, 957014. doi: 10.1155/2014/957014

Chan, T. M., Chen, J. Y., Ho, L. I., Lin, H. P., Hsueh, K. W., Liu, D. D., . . . Harn, H. J. (2014). ADSC therapy in neurodegenerative disorders. *Cell Transplant, 23*(4-5), 549-557. doi: 10.3727/096368914X678445

Chau, Y. Y., Bandiera, R., Serrels, A., Martinez-Estrada, O. M., Qing, W., Lee, M., . . . Hastie, N. (2014). Visceral and subcutaneous fat have different origins and evidence supports a mesothelial source. *Nat Cell Biol*. doi: 10.1038/ncb2922

Chopra, H., Hans, M. K., & Shetty, S. (2013). Stem cells-the hidden treasure: A strategic review. *Dent Res J (Isfahan), 10*(4), 421-427.

Cinti, S. (2005). The adipose organ. *Prostaglandins Leukot Essent Fatty Acids, 73*(1), 9-15. doi: 10.1016/j.plefa.2005.04.010

Cinti, S. (2012). The adipose organ at a glance. *Dis Model Mech, 5*(5), 588-594. doi: 10.1242/dmm.009662

Clarke, L., Buss, D. S., Juniper, D. T., Lomax, M. A., & Symonds, M. E. (1997). Adipose tissue development during early postnatal life in ewe-reared lambs. *Exp Physiol, 82*(6), 1015-1027.

Cohen, P., Levy, J. D., Zhang, Y., Frontini, A., Kolodin, D. P., Svensson, K. J., . . . Spiegelman, B. M. (2014). Ablation of PRDM16 and beige adipose causes metabolic dysfunction and a subcutaneous to visceral fat switch. *Cell, 156*(1-2), 304-316. doi: 10.1016/j.cell.2013.12.021

Collins, C. A., Olsen, I., Zammit, P. S., Heslop, L., Petrie, A., Partridge, T. A., & Morgan, J. E. (2005). Stem cell function, self-renewal, and behavioral heterogeneity of cells from the adult muscle satellite cell niche. *Cell, 122*(2), 289-301. doi: 10.1016/j.cell.2005.05.010

Crujeiras, A. B., Zulet, M. A., Lopez-Legarrea, P., de la Iglesia, R., Pardo, M., Carreira, M. C., . . . Casanueva, F. F. (2013). Association between circulating irisin levels and the promotion of insulin resistance during the weight maintenance period after a dietary weight-lowering program in obese patients. *Metabolism*. doi: 10.1016/j.metabol.2013.12.007

Csobonyeiova, M., Polak, S., Koller, J., & Danisovic, L. (2014). Induced pluripotent stem cells and their implication for regenerative medicine. *Cell Tissue Bank*. doi: 10.1007/s10561-014-9462-9

Cypess, A. M., Lehman, S., Williams, G., Tal, I., Rodman, D., Goldfine, A. B., . . . Kahn, C. R. (2009). Identification and importance of brown adipose tissue in adult humans. *N Engl J Med, 360*(15), 1509-1517. doi: 10.1056/NEJMoa0810780

Dani, Christian, & Billon, Nathalie. (2012). Adipocyte precursors: Developmental origins, self-renewal, and plasticity *Adipose Tissue Biology* (pp. 1-16): Springer.

Dasgupta, B., Ju, J. S., Sasaki, Y., Liu, X., Jung, S. R., Higashida, K., . . . Milbrandt, J. (2012). The AMPK beta2 subunit is required for energy homeostasis during metabolic stress. *Mol Cell Biol, 32*(14), 2837-2848. doi: 10.1128/MCB.05853-11

Di Battista, J. A., Shebaby, W., Kizilay, O., Hamade, E., Abou Merhi, R., Mebarek, S., . . . Faour, W. H. (2014). Proliferation and differentiation of human adipose-derived mesenchymal stem cells (ASCs) into osteoblastic lineage are passage dependent. *Inflamm Res*. doi: 10.1007/s00011-014-0764-y

Dolan, P. L., Tapscott, E. B., Dorton, P. J., & Dohm, G. L. (1993). Contractile activity restores insulin responsiveness in skeletal muscle of obese Zucker rats. *Biochem J, 289 (Pt 2)*, 423-426.

Dube, J. J., Amati, F., Stefanovic-Racic, M., Toledo, F. G., Sauers, S. E., & Goodpaster, B. H. (2008). Exercise-induced alterations in intramyocellular lipids and insulin resistance: the athlete's paradox revisited. *Am J Physiol Endocrinol Metab, 294*(5), E882-888. doi: 10.1152/ajpendo.00769.2007

Dunn, C. J., & Peters, D. H. (1995). Metformin. A review of its pharmacological properties and therapeutic use in non-insulin-dependent diabetes mellitus. *Drugs, 49*(5), 721-749.

Eckardt, K., Gorgens, S. W., Raschke, S., & Eckel, J. (2014). Myokines in insulin resistance and type 2 diabetes. *Diabetologia, 57*(6), 1087-1099. doi: 10.1007/s00125-014-3224-x

Erickson, H. P. (2013). Irisin and FNDC5 in retrospect: An exercise hormone or a transmembrane receptor? *Adipocyte, 2*(4), 289-293. doi: 10.4161/adip.26082

Evans, K. D., Tulloss, T. A., & Hall, N. (2007). 18FDG uptake in brown fat: potential for false positives. *Radiol Technol, 78*(5), 361-366.

Fedorenko, A., Lishko, P. V., & Kirichok, Y. (2012). Mechanism of fatty-acid-dependent UCP1 uncoupling in brown fat mitochondria. *Cell, 151*(2), 400-413. doi: 10.1016/j.cell.2012.09.010

Ferrari, G., Cusella-De Angelis, G., Coletta, M., Paolucci, E., Stornaiuolo, A., Cossu, G., & Mavilio, F. (1998). Muscle regeneration by bone marrow-derived myogenic progenitors. *Science, 279*(5356), 1528-1530.

Ferrer-Martinez, A., Ruiz-Lozano, P., & Chien, K. R. (2002). Mouse PeP: a novel peroxisomal protein linked to myoblast differentiation and development. *Dev Dyn, 224*(2), 154-167. doi: 10.1002/dvdy.10099

Fiaschi, T., Magherini, F., Gamberi, T., Modesti, P. A., & Modesti, A. (2013). Adiponectin as a tissue regenerating hormone: more than a metabolic function. *Cell Mol Life Sci*. doi: 10.1007/s00018-013-1537-4

Fontana, L., Eagon, J. C., Trujillo, M. E., Scherer, P. E., & Klein, S. (2007). Visceral fat adipokine secretion is associated with systemic inflammation in obese humans. *Diabetes, 56*(4), 1010-1013. doi: 10.2337/db06-1656

Forner, F., Kumar, C., Luber, C. A., Fromme, T., Klingenspor, M., & Mann, M. (2009). Proteome differences between brown and white fat mitochondria reveal specialized metabolic functions. *Cell Metab, 10*(4), 324-335. doi: 10.1016/j.cmet.2009.08.014

Franciosi, M., Lucisano, G., Lapice, E., Strippoli, G. F., Pellegrini, F., & Nicolucci, A. (2013). Metformin therapy and risk of cancer in patients with type 2 diabetes: systematic review. *PLoS One, 8*(8), e71583. doi: 10.1371/journal.pone.0071583

Friedrichsen, M., Mortensen, B., Pehmoller, C., Birk, J. B., & Wojtaszewski, J. F. (2013). Exercise-induced AMPK activity in skeletal muscle: role in glucose uptake and insulin sensitivity. *Mol Cell Endocrinol, 366*(2), 204-214. doi: 10.1016/j.mce.2012.06.013

Gesta, S., Tseng, Y. H., & Kahn, C. R. (2007). Developmental origin of fat: tracking obesity to its source. *Cell, 131*(2), 242-256. doi: 10.1016/j.cell.2007.10.004

Gilsanz, V., Smith, M. L., Goodarzian, F., Kim, M., Wren, T. A., & Hu, H. H. (2012). Changes in brown adipose tissue in boys and girls during childhood and puberty. *J Pediatr, 160*(4), 604-609 e601. doi: 10.1016/j.jpeds.2011.09.035

Golbidi, S., & Laher, I. (2014). Exercise induced adipokine changes and the metabolic syndrome. *J Diabetes Res, 2014*, 726861. doi: 10.1155/2014/726861

Goodpaster, B. H., He, J., Watkins, S., & Kelley, D. E. (2001). Skeletal muscle lipid content and insulin resistance: evidence for a paradox in endurance-trained athletes. *J Clin Endocrinol Metab, 86*(12), 5755-5761. doi: 10.1210/jcem.86.12.8075

Greenwood, M. R., & Hirsch, J. (1974). Postnatal development of adipocyte cellularity in the normal rat. *J Lipid Res, 15*(5), 474-483.

Greising, S. M., Gransee, H. M., Mantilla, C. B., & Sieck, G. C. (2012). Systems biology of skeletal muscle: fiber type as an organizing principle. *Wiley Interdiscip Rev Syst Biol Med, 4*(5), 457-473. doi: 10.1002/wsbm.1184

Grobet, L., Martin, L. J., Poncelet, D., Pirottin, D., Brouwers, B., Riquet, J., . . . Georges, M. (1997). A deletion in the bovine myostatin gene causes the double-muscled phenotype in cattle. *Nat Genet, 17*(1), 71-74. doi: 10.1038/ng0997-71

Grundlingh, J., Dargan, P. I., El-Zanfaly, M., & Wood, D. M. (2011). 2,4-dinitrophenol (DNP): a weight loss agent with significant acute toxicity and risk of death. *J Med Toxicol, 7*(3), 205-212. doi: 10.1007/s13181-011-0162-6

Guo, T., Jou, W., Chanturiya, T., Portas, J., Gavrilova, O., & McPherron, A. C. (2009). Myostatin inhibition in muscle, but not adipose tissue, decreases fat mass and improves insulin sensitivity. *PLoS One, 4*(3), e4937. doi: 10.1371/journal.pone.0004937

Gupta, R. K., Mepani, R. J., Kleiner, S., Lo, J. C., Khandekar, M. J., Cohen, P., . . . Spiegelman, B. M. (2012). Zfp423 expression identifies committed preadipocytes and localizes to adipose endothelial and perivascular cells. *Cell Metab, 15*(2), 230-239. doi: 10.1016/j.cmet.2012.01.010

Gurley, Kyle A, & Alvarado, Alejandro Sánchez. (2008). Stem cells in animal models of regeneration.

Hadley, R. D., Whaley, J. W., & Askins, D. G., Jr. (1998). Treatment of type 2 diabetes: a review of metformin in clinical practice. *J S C Med Assoc, 94*(1), 12-15.

Hamann, A., Flier, J. S., & Lowell, B. B. (1996). Decreased brown fat markedly enhances susceptibility to diet-induced obesity, diabetes, and hyperlipidemia. *Endocrinology, 137*(1), 21-29. doi: 10.1210/endo.137.1.8536614

Harms, M. J., Ishibashi, J., Wang, W., Lim, H. W., Goyama, S., Sato, T., . . . Seale, P. (2014). Prdm16 is required for the maintenance of brown adipocyte identity and function in adult mice. *Cell Metab, 19*(4), 593-604. doi: 10.1016/j.cmet.2014.03.007

Harms, M., & Seale, P. (2013). Brown and beige fat: development, function and therapeutic potential. *Nat Med, 19*(10), 1252-1263. doi: 10.1038/nm.3361

Hauner, H., Wabitsch, M., Zwiauer, K., Widhalm, K., & Pfeiffer, E. F. (1989). Adipogenic activity in sera from obese children before and after weight reduction. *Am J Clin Nutr, 50*(1), 63-67.

Hindi, S. M., Tajrishi, M. M., & Kumar, A. (2013). Signaling mechanisms in mammalian myoblast fusion. *Sci Signal, 6*(272), re2. doi: 10.1126/scisignal.2003832

Hirsch, J., & Batchelor, B. (1976). Adipose tissue cellularity in human obesity. *Clin Endocrinol Metab, 5*(2), 299-311.

Huang, H., Song, T. J., Li, X., Hu, L., He, Q., Liu, M., . . . Tang, Q. Q. (2009). BMP signaling pathway is required for commitment of C3H10T1/2 pluripotent stem cells to the adipocyte lineage. *Proc Natl Acad Sci U S A, 106*(31), 12670-12675. doi: 10.1073/pnas.0906266106

Huang, R. C. (2012). [Stem cell therapy for the treatment of coronary heart disease: safety evaluation]. *Zhonghua Xin Xue Guan Bing Za Zhi, 40*(9), 721-722.

Huh, J. Y., Panagiotou, G., Mougios, V., Brinkoetter, M., Vamvini, M. T., Schneider, B. E., & Mantzoros, C. S. (2012). FNDC5 and irisin in humans: I. Predictors of circulating concentrations in serum and plasma and II. mRNA expression and circulating concentrations in response to weight loss and exercise. *Metabolism, 61*(12), 1725-1738. doi: 10.1016/j.metabol.2012.09.002

Hull, D., & Segall, M. M. (1965). Heat production in the new-born rabbit and the fat content of the brown adipose tissue. *J Physiol, 181*(3), 468-477.

Izadpanah, R., Kaushal, D., Kriedt, C., Tsien, F., Patel, B., Dufour, J., & Bunnell, B. A. (2008). Long-term in vitro expansion alters the biology of adult mesenchymal stem cells. *Cancer Res, 68*(11), 4229-4238. doi: 10.1158/0008-5472.CAN-07-5272

Jespersen, N. Z., Larsen, T. J., Peijs, L., Daugaard, S., Homoe, P., Loft, A., . . . Scheele, C. (2013). A classical brown adipose tissue mRNA signature partly overlaps with brite in the supraclavicular region of adult humans. *Cell Metab, 17*(5), 798-805. doi: 10.1016/j.cmet.2013.04.011

Johnson, P. R., & Hirsch, J. (1972). Cellularity of adipose depots in six strains of genetically obese mice. *J Lipid Res, 13*(1), 2-11.

Jorgensen, S. B., Viollet, B., Andreelli, F., Frosig, C., Birk, J. B., Schjerling, P., . . . Wojtaszewski, J. F. (2004). Knockout of the alpha2 but not alpha1 5'-AMP-activated protein kinase isoform abolishes 5-aminoimidazole-4-carboxamide-1-beta-4-ribofuranosidebut not contraction-induced glucose uptake in skeletal muscle. *J Biol Chem, 279*(2), 1070-1079. doi: 10.1074/jbc.M306205200

JorgensenO'Neill, H. M. (2013). AMPK and Exercise: Glucose Uptake and Insulin Sensitivity. *Diabetes Metab J, 37*(1), 1-21. doi: 10.4093/dmj.2013.37.1.1

Justo, R., Frontera, M., Pujol, E., Rodriguez-Cuenca, S., Llado, I., Garcia-Palmer, F. J., . . . Gianotti, M. (2005). Gender-related differences in morphology and thermogenic capacity of brown adipose tissue mitochondrial subpopulations. *Life Sci, 76*(10), 1147-1158. doi: 10.1016/j.lfs.2004.08.019

Kang, S., Bennett, C. N., Gerin, I., Rapp, L. A., Hankenson, K. D., & Macdougald, O. A. (2007). Wnt signaling stimulates osteoblastogenesis of mesenchymal precursors by suppressing CCAAT/enhancer-binding protein alpha and peroxisome proliferator-activated receptor gamma. *J Biol Chem, 282*(19), 14515-14524. doi: 10.1074/jbc.M700030200

Kang, S. K., Putnam, L., Dufour, J., Ylostalo, J., Jung, J. S., & Bunnell, B. A. (2004). Expression of telomerase extends the lifespan and enhances osteogenic differentiation of adipose tissue-derived stromal cells. *Stem Cells, 22*(7), 1356-1372. doi: 10.1634/stemcells.2004-0023

Katsanos, C. S., & Mandarino, L. J. (2011). Protein metabolism in human obesity: a shift in focus from whole-body to skeletal muscle. *Obesity (Silver Spring), 19*(3), 469-475. doi: 10.1038/oby.2010.290

Katz, A. J., Tholpady, A., Tholpady, S. S., Shang, H., & Ogle, R. C. (2005). Cell surface and transcriptional characterization of human adipose-derived adherent stromal (hADAS) cells. *Stem Cells, 23*(3), 412-423. doi: 10.1634/stemcells.2004-0021

Kawada, S., Tachi, C., & Ishii, N. (2001). Content and localization of myostatin in mouse skeletal muscles during aging, mechanical unloading and reloading. *J Muscle Res Cell Motil, 22*(8), 627-633.

Keipert, S., Ost, M., Johann, K., Imber, F., Jastroch, M., van Schothorst, E. M., . . . Klaus, S. (2014). Skeletal muscle mitochondrial uncoupling drives endocrine cross-talk through the induction of FGF21 as a myokine. *Am J Physiol Endocrinol Metab, 306*(5), E469-482. doi: 10.1152/ajpendo.00330.2013

Keller, C., Steensberg, A., Pilegaard, H., Osada, T., Saltin, B., Pedersen, B. K., & Neufer, P. D. (2001). Transcriptional activation of the IL-6 gene in human contracting skeletal muscle: influence of muscle glycogen content. *FASEB J, 15*(14), 2748-2750. doi: 10.1096/fj.01-0507fje

Kim, E. H., & Heo, C. Y. (2014). Current applications of adipose-derived stem cells and their future perspectives. *World J Stem Cells, 6*(1), 65-68. doi: 10.4252/wjsc.v6.i1.65

King, R. S., & Newmark, P. A. (2012). The cell biology of regeneration. *J Cell Biol, 196*(5), 553-562. doi: 10.1083/jcb.201105099

Konno, M., Hamabe, A., Hasegawa, S., Ogawa, H., Fukusumi, T., Nishikawa, S., . . . Ishii, H. (2013). Adipose-derived mesenchymal stem cells and regenerative medicine. *Dev Growth Differ, 55*(3), 309-318. doi: 10.1111/dgd.12049

Konopka, A. R., Douglass, M. D., Kaminsky, L. A., Jemiolo, B., Trappe, T. A., Trappe, S., & Harber, M. P. (2010). Molecular adaptations to aerobic exercise training in skeletal muscle of older women. *J Gerontol A Biol Sci Med Sci, 65*(11), 1201-1207. doi: 10.1093/gerona/glq109

Koohmaraie, M., Shackelford, S. D., Wheeler, T. L., Lonergan, S. M., & Doumit, M. E. (1995). A muscle hypertrophy condition in lamb (callipyge): characterization of effects on muscle growth and meat quality traits. *J Anim Sci, 73*(12), 3596-3607.

Kuang, S., Kuroda, K., Le Grand, F., & Rudnicki, M. A. (2007). Asymmetric self-renewal and commitment of satellite stem cells in muscle. *Cell, 129*(5), 999-1010. doi: 10.1016/j.cell.2007.03.044

Kuang, S., & Rudnicki, M. A. (2008). The emerging biology of satellite cells and their therapeutic potential. *Trends Mol Med, 14*(2), 82-91. doi: 10.1016/j.molmed.2007.12.004

Kurdiova, T., Balaz, M., Vician, M., Maderova, D., Vlcek, M., Valkovic, L., . . . Ukropcova, B. (2014). Are Skeletal Muscle & Adipose Tissue Fndc5 Gene Expression and Irisin Release Affected by Obesity, Diabetes and Exercise? In vivo & in vitro studies. *J Physiol*. doi: 10.1113/jphysiol.2013.264655

Kwon, H., & Pessin, J. E. (2013). Adipokines mediate inflammation and insulin resistance. *Front Endocrinol (Lausanne), 4*, 71. doi: 10.3389/fendo.2013.00071

Lafortuna, C. L., Maffiuletti, N. A., Agosti, F., & Sartorio, A. (2005). Gender variations of body composition, muscle strength and power output in morbid obesity. *Int J Obes (Lond), 29*(7), 833-841. doi: 10.1038/sj.ijo.0802955

Lanza, Robert, Gearhart, John, Hogan, Brigid, Melton, Douglas, Pedersen, Roger, Thomas, E Donnall, . . . West, Michael. (2005). *Essentials of stem cell biology*: Academic Press.

Laviola, L., Natalicchio, A., & Giorgino, F. (2007). The IGF-I signaling pathway. *Curr Pharm Des, 13*(7), 663-669.

Lee, P., Linderman, J. D., Smith, S., Brychta, R. J., Wang, J., Idelson, C., . . . Celi, F. S. (2014). Irisin and FGF21 Are Cold-Induced Endocrine Activators of Brown Fat Function in Humans. *Cell Metab, 19*(2), 302-309. doi: 10.1016/j.cmet.2013.12.017

Lee, Y. H., Petkova, A. P., Mottillo, E. P., & Granneman, J. G. (2012). In vivo identification of bipotential adipocyte progenitors recruited by beta3-adrenoceptor activation and high-fat feeding. *Cell Metab, 15*(4), 480-491. doi: 10.1016/j.cmet.2012.03.009

Lepper, C., & Fan, C. M. (2010). Inducible lineage tracing of Pax7-descendant cells reveals embryonic origin of adult satellite cells. *Genesis, 48*(7), 424-436. doi: 10.1002/dvg.20630

Lidell, M. E., Betz, M. J., Dahlqvist Leinhard, O., Heglind, M., Elander, L., Slawik, M., . . . Enerback, S. (2013). Evidence for two types of brown adipose tissue in humans. *Nat Med, 19*(5), 631-634. doi: 10.1038/nm.3017

Lidell, M. E., Betz, M. J., & Enerback, S. (2014). Two types of brown adipose tissue in humans. *Adipocyte, 3*(1), 63-66. doi: 10.4161/adip.26896

Lim, S., Choi, S. H., Koo, B. K., Kang, S. M., Yoon, J. W., Jang, H. C., . . . Park, K. S. (2012). Effects of aerobic exercise training on C1q tumor necrosis factor alpha-related protein isoform 5 (myonectin): association with insulin resistance and mitochondrial DNA density in women. *J Clin Endocrinol Metab, 97*(1), E88-93. doi: 10.1210/jc.2011-1743

Lin, G., Garcia, M., Ning, H., Banie, L., Guo, Y. L., Lue, T. F., & Lin, C. S. (2008). Defining stem and progenitor cells within adipose tissue. *Stem Cells Dev, 17*(6), 1053-1063. doi: 10.1089/scd.2008.0117

Lin, J., Wu, P. H., Tarr, P. T., Lindenberg, K. S., St-Pierre, J., Zhang, C. Y., . . . Spiegelman, B. M. (2004). Defects in adaptive energy metabolism with CNS-linked hyperactivity in PGC-1alpha null mice. *Cell, 119*(1), 121-135. doi: 10.1016/j.cell.2004.09.013

Liu, W., Liu, Y., Lai, X., & Kuang, S. (2012). Intramuscular adipose is derived from a non-Pax3 lineage and required for efficient regeneration of skeletal muscles. *Dev Biol, 361*(1), 27-38. doi: 10.1016/j.ydbio.2011.10.011

Liu, W., Shan, T., Yang, X., Liang, S., Zhang, P., Liu, Y., . . . Kuang, S. (2013). A heterogeneous lineage origin underlies the phenotypic and molecular differences of white and beige adipocytes. *J Cell Sci, 126*(Pt 16), 3527-3532. doi: 10.1242/jcs.124321

Liu, W., Wen, Y., Bi, P., Lai, X., Liu, X. S., Liu, X., & Kuang, S. (2012). Hypoxia promotes satellite cell self-renewal and enhances the efficiency of myoblast transplantation. *Development, 139*(16), 2857-2865. doi: 10.1242/dev.079665

Locke, M., Windsor, J., & Dunbar, P. R. (2009). Human adipose-derived stem cells: isolation, characterization and applications in surgery. *ANZ J Surg, 79*(4), 235-244. doi: 10.1111/j.1445-2197.2009.04852.x

Martin, G. S., Carstens, G. E., King, M. D., Eli, A. G., Mersmann, H. J., & Smith, S. B. (1999). Metabolism and morphology of brown adipose tissue from Brahman and Angus newborn calves. *J Anim Sci, 77*(2), 388-399.

Mauro, A. (1961). Satellite cell of skeletal muscle fibers. *J Biophys Biochem Cytol, 9*, 493-495.

McCusker, C. D., & Gardiner, D. M. (2014). Understanding positional cues in salamander limb regeneration: implications for optimizing cell-based regenerative therapies. *Dis Model Mech, 7*(6), 593-599. doi: 10.1242/dmm.013359

McPherron, A. C., & Lee, S. J. (1997). Double muscling in cattle due to mutations in the myostatin gene. *Proc Natl Acad Sci U S A, 94*(23), 12457-12461.

McPherron, A. C., & Lee, S. J. (2002). Suppression of body fat accumulation in myostatin-deficient mice. *J Clin Invest, 109*(5), 595-601. doi: 10.1172/JCI13562

Menuki, K., Mori, T., Sakai, A., Sakuma, M., Okimoto, N., Shimizu, Y., . . . Nakamura, T. (2008). Climbing exercise enhances osteoblast differentiation and inhibits adipogenic differentiation with high expression of PTH/PTHrP receptor in bone marrow cells. *Bone, 43*(3), 613-620. doi: 10.1016/j.bone.2008.04.022

Meregalli, M., Farini, A., Belicchi, M., Parolini, D., Cassinelli, L., Razini, P., . . . Torrente, Y. (2013). Perspectives of stem cell therapy in Duchenne muscular dystrophy. *FEBS J, 280*(17), 4251-4262. doi: 10.1111/febs.12083

Merry, T. L., Steinberg, G. R., Lynch, G. S., & McConell, G. K. (2010). Skeletal muscle glucose uptake during contraction is regulated by nitric oxide and ROS independently of AMPK. *Am J Physiol Endocrinol Metab, 298*(3), E577-585. doi: 10.1152/ajpendo.00239.2009

Milner, R. E., Wang, L. C., & Trayhurn, P. (1989). Brown fat thermogenesis during hibernation and arousal in Richardson's ground squirrel. *Am J Physiol, 256*(1 Pt 2), R42-48.

Morrison, J. I., Loof, S., He, P., & Simon, A. (2006). Salamander limb regeneration involves the activation of a multipotent skeletal muscle satellite cell population. *J Cell Biol, 172*(3), 433-440. doi: 10.1083/jcb.200509011

Naaijkens, B. A., van Dijk, A., Kamp, O., Krijnen, P. A., Niessen, H. W., & Juffermans, L. J. (2014). Therapeutic Application of Adipose Derived Stem Cells in Acute Myocardial Infarction: Lessons from Animal Models. *Stem Cell Rev*. doi: 10.1007/s12015-014-9502-7

Nedergaard, J., Bengtsson, T., & Cannon, B. (2007). Unexpected evidence for active brown adipose tissue in adult humans. *Am J Physiol Endocrinol Metab, 293*(2), E444-452. doi: 10.1152/ajpendo.00691.2006

Nedergaard, J., & Cannon, B. (2013). How brown is brown fat? It depends where you look. *Nat Med, 19*(5), 540-541. doi: 10.1038/nm.3187

Neel, B. A., Lin, Y., & Pessin, J. E. (2013). Skeletal muscle autophagy: a new metabolic regulator. *Trends Endocrinol Metab, 24*(12), 635-643. doi: 10.1016/j.tem.2013.09.004

Nguyen, K. D., Qiu, Y., Cui, X., Goh, Y. P., Mwangi, J., David, T., . . . Chawla, A. (2011). Alternatively activated macrophages produce catecholamines to sustain adaptive thermogenesis. *Nature, 480*(7375), 104-108. doi: 10.1038/nature10653

Nishiyama, T., & Takeda, S. (2012). [Induced pluripotent stem (iPS) cell-based cell therapy for muscular dystrophy: current progress and future prospects]. *Brain Nerve, 64*(1), 39-46.

Norheim, F., Langleite, T. M., Hjorth, M., Holen, T., Kielland, A., Stadheim, H. K., . . . Drevon, C. A. (2014). The effects of acute and chronic exercise on PGC-1alpha, irisin and browning of subcutaneous adipose tissue in humans. *FEBS J, 281*(3), 739-749. doi: 10.1111/febs.12619

O'Neill, H. M., Maarbjerg, S. J., Crane, J. D., Jeppesen, J., Jorgensen, S. B., Schertzer, J. D., . . . Steinberg, G. R. (2011). AMP-activated protein kinase (AMPK) beta1beta2 muscle null mice reveal an essential role for AMPK in maintaining mitochondrial content and glucose uptake during exercise. *Proc Natl Acad Sci U S A, 108*(38), 16092-16097. doi: 10.1073/pnas.1105062108

Ong, W. K., & Sugii, S. (2013). Adipose-derived stem cells: fatty potentials for therapy. *Int J Biochem Cell Biol, 45*(6), 1083-1086. doi: 10.1016/j.biocel.2013.02.013

Ouchi, N., Parker, J. L., Lugus, J. J., & Walsh, K. (2011). Adipokines in inflammation and metabolic disease. *Nat Rev Immunol, 11*(2), 85-97. doi: 10.1038/nri2921

Ouellet, V., Labbe, S. M., Blondin, D. P., Phoenix, S., Guerin, B., Haman, F., . . . Carpentier, A. C. (2012). Brown adipose tissue oxidative metabolism contributes to energy expenditure during acute cold exposure in humans. *J Clin Invest, 122*(2), 545-552. doi: 10.1172/JCI60433

Pal, M., Febbraio, M. A., & Whitham, M. (2014). From cytokine to myokine: the emerging role of interleukin-6 in metabolic regulation. *Immunol Cell Biol, 92*(4), 331-339. doi: 10.1038/icb.2014.16

Park, K. W., Halperin, D. S., & Tontonoz, P. (2008). Before they were fat: adipocyte progenitors. *Cell Metab, 8*(6), 454-457. doi: 10.1016/j.cmet.2008.11.001

Pedersen, B. K. (2011). Exercise-induced myokines and their role in chronic diseases. *Brain Behav Immun, 25*(5), 811-816. doi: 10.1016/j.bbi.2011.02.010

Pedersen, B. K., & Febbraio, M. A. (2012). Muscles, exercise and obesity: skeletal muscle as a secretory organ. *Nature Reviews Endocrinology, 8*(8), 457-465. doi: 10.1038/nrendo.2012.49

Pedersen, L., & Hojman, P. (2012). Muscle-to-organ cross talk mediated by myokines. *Adipocyte, 1*(3), 164-167. doi: 10.4161/adip.20344

Peng, L., Jia, Z., Yin, X., Zhang, X., Liu, Y., Chen, P., . . . Zhou, C. (2008). Comparative analysis of mesenchymal stem cells from bone marrow, cartilage, and adipose tissue. *Stem Cells Dev, 17*(4), 761-773. doi: 10.1089/scd.2007.0217

Pette, D., & Staron, R. S. (2000). Myosin isoforms, muscle fiber types, and transitions. *Microsc Res Tech, 50*(6), 500-509. doi: 10.1002/1097-0029(20000915)50:6<500::AID-JEMT7>3.0.CO;2-7

Pfannenberg, C., Werner, M. K., Ripkens, S., Stef, I., Deckert, A., Schmadl, M., . . . Stefan, N. (2010). Impact of age on the relationships of brown adipose tissue with sex and adiposity in humans. *Diabetes, 59*(7), 1789-1793. doi: 10.2337/db10-0004

Pisani, D. F., Clement, N., Loubat, A., Plaisant, M., Sacconi, S., Kurzenne, J. Y., . . . Dechesne, C. A. (2010). Hierarchization of myogenic and adipogenic progenitors within human skeletal muscle. *Stem Cells, 28*(12), 2182-2194. doi: 10.1002/stem.537

Pisani, D. F., Dechesne, C. A., Sacconi, S., Delplace, S., Belmonte, N., Cochet, O., . . . Dani, C. (2010). Isolation of a highly myogenic CD34-negative subset of human skeletal muscle cells free of adipogenic potential. *Stem Cells, 28*(4), 753-764. doi: 10.1002/stem.317

Pond, C. M. (1992). An evolutionary and functional view of mammalian adipose tissue. *Proc Nutr Soc, 51*(3), 367-377.

Pope, M., Budge, H., & Symonds, M. E. (2014). The developmental transition of ovine adipose tissue through early life. *Acta Physiol (Oxf), 210*(1), 20-30. doi: 10.1111/apha.12053

Quinn, L. S. (2008). Interleukin-15: a muscle-derived cytokine regulating fat-to-lean body composition. *J Anim Sci, 86*(14 Suppl), E75-83. doi: 10.2527/jas.2007-0458

Rama, P., Matuska, S., Paganoni, G., Spinelli, A., De Luca, M., & Pellegrini, G. (2010). Limbal stem-cell therapy and long-term corneal regeneration. *N Engl J Med, 363*(2), 147-155. doi: 10.1056/NEJMoa0905955

Rasbach, K. A., Gupta, R. K., Ruas, J. L., Wu, J., Naseri, E., Estall, J. L., & Spiegelman, B. M. (2010). PGC-1alpha regulates a HIF2alpha-dependent switch in skeletal muscle fiber types. *Proc Natl Acad Sci U S A, 107*(50), 21866-21871. doi: 10.1073/pnas.1016089107

Raschke, S., & Eckel, J. (2013). Adipo-myokines: two sides of the same coin--mediators of inflammation and mediators of exercise. *Mediators Inflamm, 2013*, 320724. doi: 10.1155/2013/320724

Raschke, S., Elsen, M., Gassenhuber, H., Sommerfeld, M., Schwahn, U., Brockmann, B., . . . Eckel, J. (2013). Evidence against a beneficial effect of irisin in humans. *PLoS One, 8*(9), e73680. doi: 10.1371/journal.pone.0073680

Rebbapragada, A., Benchabane, H., Wrana, J. L., Celeste, A. J., & Attisano, L. (2003). Myostatin signals through a transforming growth factor beta-like signaling pathway to block adipogenesis. *Mol Cell Biol, 23*(20), 7230-7242.

Relaix, F., & Marcelle, C. (2009). Muscle stem cells. *Curr Opin Cell Biol, 21*(6), 748-753. doi: 10.1016/j.ceb.2009.10.002

Relaix, F., Rocancourt, D., Mansouri, A., & Buckingham, M. (2005). A Pax3/Pax7-dependent population of skeletal muscle progenitor cells. *Nature, 435*(7044), 948-953. doi: 10.1038/nature03594

Relaix, F., & Zammit, P. S. (2012). Satellite cells are essential for skeletal muscle regeneration: the cell on the edge returns centre stage. *Development, 139*(16), 2845-2856. doi: 10.1242/dev.069088

Ribeiro, M. O., Bianco, S. D., Kaneshige, M., Schultz, J. J., Cheng, S. Y., Bianco, A. C., & Brent, G. A. (2010). Expression of uncoupling protein 1 in mouse brown adipose tissue is thyroid hormone receptor-beta isoform specific and required for adaptive thermogenesis. *Endocrinology, 151*(1), 432-440. doi: 10.1210/en.2009-0667

Richter, E. A., & Hargreaves, M. (2013). Exercise, GLUT4, and skeletal muscle glucose uptake. *Physiol Rev, 93*(3), 993-1017. doi: 10.1152/physrev.00038.2012

Rodeheffer, M. S., Birsoy, K., & Friedman, J. M. (2008). Identification of white adipocyte progenitor cells in vivo. *Cell, 135*(2), 240-249. doi: 10.1016/j.cell.2008.09.036

Rolfe, D. F., & Brand, M. D. (1996). Contribution of mitochondrial proton leak to skeletal muscle respiration and to standard metabolic rate. *Am J Physiol, 271*(4 Pt 1), C1380-1389.

Romacho, T., Elsen, M., Rohrborn, D., & Eckel, J. (2014). Adipose Tissue and its Role in Organ Crosstalk. *Acta Physiol (Oxf)*. doi: 10.1111/apha.12246

Rosen, E. D., & MacDougald, O. A. (2006). Adipocyte differentiation from the inside out. *Nat Rev Mol Cell Biol, 7*(12), 885-896. doi: 10.1038/nrm2066

Rosen, Evan D, & Spiegelman, Bruce M. (2014). What We Talk About When We Talk About Fat. *Cell, 156*(1–2), 20-44. doi: http://dx.doi.org/10.1016/j.cell.2013.12.012

Rosenwald, M., Perdikari, A., Rulicke, T., & Wolfrum, C. (2013). Bi-directional interconversion of brite and white adipocytes. *Nat Cell Biol, 15*(6), 659-667. doi: 10.1038/ncb2740

Roth, S. M., Martel, G. F., Ferrell, R. E., Metter, E. J., Hurley, B. F., & Rogers, M. A. (2003). Myostatin gene expression is reduced in humans with heavy-resistance strength training: a brief communication. *Exp Biol Med (Maywood), 228*(6), 706-709.

Rothwell, N. J., & Stock, M. J. (1989). Surgical removal of brown fat results in rapid and complete compensation by other depots. *Am J Physiol, 257*(2 Pt 2), R253-258.

Rotter, V., Nagaev, I., & Smith, U. (2003). Interleukin-6 (IL-6) induces insulin resistance in 3T3-L1 adipocytes and is, like IL-8 and tumor necrosis factor-alpha, overexpressed in human fat cells from insulin-resistant subjects. *J Biol Chem, 278*(46), 45777-45784. doi: 10.1074/jbc.M301977200

Rowe, R. W., & Goldspink, G. (1969a). Muscle fibre growth in five different muscles in both sexes of mice. *J Anat, 104*(Pt 3), 519-530.

Rowe, R. W., & Goldspink, G. (1969b). Muscle fibre growth in five different muscles in both sexes of mice. II. Dystrophic mice. *J Anat, 104*(Pt 3), 531-538.

Sacco, A., Doyonnas, R., Kraft, P., Vitorovic, S., & Blau, H. M. (2008). Self-renewal and expansion of single transplanted muscle stem cells. *Nature, 456*(7221), 502-506. doi: 10.1038/nature07384

Sachs, P. C., Francis, M. P., Zhao, M., Brumelle, J., Rao, R. R., Elmore, L. W., & Holt, S. E. (2012). Defining essential stem cell characteristics in adipose-derived stromal cells extracted from distinct anatomical sites. *Cell Tissue Res, 349*(2), 505-515. doi: 10.1007/s00441-012-1423-7

Saito, M., Okamatsu-Ogura, Y., Matsushita, M., Watanabe, K., Yoneshiro, T., Nio-Kobayashi, J., . . . Tsujisaki, M. (2009). High incidence of metabolically active brown adipose tissue in healthy adult humans: effects of cold exposure and adiposity. *Diabetes, 58*(7), 1526-1531. doi: 10.2337/db09-0530

Sakuma, K., & Yamaguchi, A. (2013). Sarcopenic obesity and endocrinal adaptation with age. *Int J Endocrinol, 2013*, 204164. doi: 10.1155/2013/204164

Salibian, A. A., Widgerow, A. D., Abrouk, M., & Evans, G. R. (2013). Stem cells in plastic surgery: a review of current clinical and translational applications. *Arch Plast Surg, 40*(6), 666-675. doi: 10.5999/aps.2013.40.6.666

Sanchez-Gurmaches, J., & Guertin, D. A. (2014a). Adipocyte lineages: tracing back the origins of fat. *Biochim Biophys Acta, 1842*(3), 340-351. doi: 10.1016/j.bbadis.2013.05.027

Sanchez-Gurmaches, J., & Guertin, D. A. (2014b). Adipocytes arise from multiple lineages that are heterogeneously and dynamically distributed. *Nat Commun, 5*, 4099. doi: 10.1038/ncomms5099

Sanchez, J., Nozhenko, Y., Palou, A., & Rodriguez, A. M. (2013). Free fatty acid effects on myokine production in combination with exercise mimetics. *Mol Nutr Food Res, 57*(8), 1456-1467. doi: 10.1002/mnfr.201300126

Sanchis-Gomar, F., Alis, R., Pareja-Galeano, H., Romagnoli, M., & Perez-Quilis, C. (2014). Inconsistency in Circulating Irisin Levels: What is Really Happening? *Horm Metab Res*. doi: 10.1055/s-0033-1363283

Sandoval-Guzman, T., Wang, H., Khattak, S., Schuez, M., Roensch, K., Nacu, E., . . . Simon, A. (2014). Fundamental differences in dedifferentiation and stem cell recruitment during skeletal muscle regeneration in two salamander species. *Cell Stem Cell, 14*(2), 174-187. doi: 10.1016/j.stem.2013.11.007

Schaap, L. A., Koster, A., & Visser, M. (2012). Adiposity, Muscle Mass, and Muscle Strength in Relation to Functional Decline in Older Persons. *Epidemiol Rev*. doi: 10.1093/epirev/mxs006

Schermer, S. J., Bird, J. A., Lomax, M. A., Shepherd, D. A., & Symonds, M. E. (1996). Effect of fetal thyroidectomy on brown adipose tissue and thermoregulation in newborn lambs. *Reprod Fertil Dev, 8*(6), 995-1002.

Schiaffino, S. (2010). Fibre types in skeletal muscle: a personal account. *Acta Physiol (Oxf), 199*(4), 451-463. doi: 10.1111/j.1748-1716.2010.02130.x

Schiaffino, S., Sandri, M., & Murgia, M. (2007). Activity-dependent signaling pathways controlling muscle diversity and plasticity. *Physiology (Bethesda), 22*, 269-278. doi: 10.1152/physiol.00009.2007

Schonfeld, P., & Wojtczak, L. (2012). Brown adipose tissue mitochondria oxidizing fatty acids generate high levels of reactive oxygen species irrespective of the uncoupling protein-1 activity state. *Biochim Biophys Acta, 1817*(3), 410-418. doi: 10.1016/j.bbabio.2011.12.009

Schuelke, M., Wagner, K. R., Stolz, L. E., Hubner, C., Riebel, T., Komen, W., . . . Lee, S. J. (2004). Myostatin mutation associated with gross muscle hypertrophy in a child. *N Engl J Med, 350*(26), 2682-2688. doi: 10.1056/NEJMoa040933

Schulz, T. J., Huang, T. L., Tran, T. T., Zhang, H., Townsend, K. L., Shadrach, J. L., . . . Tseng, Y. H. (2011). Identification of inducible brown adipocyte progenitors residing in skeletal muscle and white fat. *Proc Natl Acad Sci U S A, 108*(1), 143-148. doi: 10.1073/pnas.1010929108

Schulz, T. J., & Tseng, Y. H. (2013). Brown adipose tissue: development, metabolism and beyond. *Biochem J, 453*(2), 167-178. doi: 10.1042/BJ20130457

Seale, P., Bjork, B., Yang, W., Kajimura, S., Chin, S., Kuang, S., . . . Spiegelman, B. M. (2008). PRDM16 controls a brown fat/skeletal muscle switch. *Nature, 454*(7207), 961-967. doi: 10.1038/nature07182

Sekiya, I., Larson, B. L., Vuoristo, J. T., Cui, J. G., & Prockop, D. J. (2004). Adipogenic differentiation of human adult stem cells from bone marrow stroma (MSCs). *J Bone Miner Res, 19*(2), 256-264. doi: 10.1359/JBMR.0301220

Seldin, M. M., Peterson, J. M., Byerly, M. S., Wei, Z., & Wong, G. W. (2012). Myonectin (CTRP15), a novel myokine that links skeletal muscle to systemic lipid homeostasis. *J Biol Chem, 287*(15), 11968-11980. doi: 10.1074/jbc.M111.336834

Sell, H., Dietze-Schroeder, D., Kaiser, U., & Eckel, J. (2006). Monocyte chemotactic protein-1 is a potential player in the negative cross-talk between adipose tissue and skeletal muscle. *Endocrinology, 147*(5), 2458-2467. doi: 10.1210/en.2005-0969

Sen, B., Guilluy, C., Xie, Z., Case, N., Styner, M., Thomas, J., . . . Rubin, J. (2011). Mechanically induced focal adhesion assembly amplifies anti-adipogenic pathways in mesenchymal stem cells. *Stem Cells, 29*(11), 1829-1836. doi: 10.1002/stem.732

Sengenes, C., Lolmede, K., Zakaroff-Girard, A., Busse, R., & Bouloumie, A. (2005). Preadipocytes in the human subcutaneous adipose tissue display distinct features from the adult mesenchymal and hematopoietic stem cells. *J Cell Physiol, 205*(1), 114-122. doi: 10.1002/jcp.20381

Serrano, A. L., Baeza-Raja, B., Perdiguero, E., Jardi, M., & Munoz-Canoves, P. (2008). Interleukin-6 is an essential regulator of satellite cell-mediated skeletal muscle hypertrophy. *Cell Metab, 7*(1), 33-44. doi: 10.1016/j.cmet.2007.11.011

Shabalina, I. G., Petrovic, N., de Jong, J. M., Kalinovich, A. V., Cannon, B., & Nedergaard, J. (2013). UCP1 in brite/beige adipose tissue mitochondria is functionally thermogenic. *Cell Rep, 5*(5), 1196-1203. doi: 10.1016/j.celrep.2013.10.044

Shan, T., Liang, X., Bi, P., & Kuang, S. (2013). Myostatin knockout drives browning of white adipose tissue through activating the AMPK-PGC1alpha-Fndc5 pathway in muscle. *FASEB J, 27*(5), 1981-1989. doi: 10.1096/fj.12-225755

Sharara-Chami, R. I., Joachim, M., Mulcahey, M., Ebert, S., & Majzoub, J. A. (2010). Effect of epinephrine deficiency on cold tolerance and on brown adipose tissue. *Mol Cell Endocrinol, 328*(1-2), 34-39. doi: 10.1016/j.mce.2010.06.019

Smith, SB, & Carstens, GE. (2005). Ontogeny and metabolism of brown adipose tissue in livestock species. *Biology of Growing Animals, 3*, 303-322.

Son, Y. H., Ka, S., Kim, A. Y., & Kim, J. B. (2014). Regulation of Adipocyte Differentiation via MicroRNAs. *Endocrinol Metab (Seoul), 29*(2), 122-135. doi: 10.3803/EnM.2014.29.2.122

Soppela, P., Sormunen, R., Saarela, S., Huttunen, P., & Nieminen, M. (1992). Localization, cellular morphology and respiratory capacity of "brown" adipose tissue in newborn reindeer. *Comp Biochem Physiol Comp Physiol, 101*(2), 281-293.

Spalding, K. L., Arner, E., Westermark, P. O., Bernard, S., Buchholz, B. A., Bergmann, O., . . . Arner, P. (2008). Dynamics of fat cell turnover in humans. *Nature, 453*(7196), 783-787. doi: 10.1038/nature06902

Spangenburg, E. E., & Booth, F. W. (2006). Leukemia inhibitory factor restores the hypertrophic response to increased loading in the LIF(-/-) mouse. *Cytokine, 34*(3-4), 125-130. doi: 10.1016/j.cyto.2006.05.001

Spinella-Jaegle, S., Rawadi, G., Kawai, S., Gallea, S., Faucheu, C., Mollat, P., . . . Roman-Roman, S. (2001). Sonic hedgehog increases the commitment of pluripotent mesenchymal cells into the osteoblastic lineage and abolishes adipocytic differentiation. *J Cell Sci, 114*(Pt 11), 2085-2094.

Stanford, K. I., Middelbeek, R. J., Townsend, K. L., An, D., Nygaard, E. B., Hitchcox, K. M., . . . Goodyear, L. J. (2013). Brown adipose tissue regulates glucose homeostasis and insulin sensitivity. *J Clin Invest, 123*(1), 215-223. doi: 10.1172/JCI62308

Starkey, J. D., Yamamoto, M., Yamamoto, S., & Goldhamer, D. J. (2011). Skeletal muscle satellite cells are committed to myogenesis and do not spontaneously adopt nonmyogenic fates. *J Histochem Cytochem, 59*(1), 33-46. doi: 10.1369/jhc.2010.956995

Steinberg, G. R., O'Neill, H. M., Dzamko, N. L., Galic, S., Naim, T., Koopman, R., . . . Kemp, B. E. (2010). Whole body deletion of AMP-activated protein kinase {beta}2 reduces muscle AMPK activity and exercise capacity. *J Biol Chem, 285*(48), 37198-37209. doi: 10.1074/jbc.M110.102434

Symonds, M. E. (2013). Brown adipose tissue growth and development. *Scientifica (Cairo), 2013*, 305763. doi: 10.1155/2013/305763

Symonds, M. E., Andrews, D. C., & Johnson, P. (1989). The control of thermoregulation in the developing lamb during slow wave sleep. *J Dev Physiol, 11*(5), 289-298.

Takahashi, K., & Yamanaka, S. (2006). Induction of pluripotent stem cells from mouse embryonic and adult fibroblast cultures by defined factors. *Cell, 126*(4), 663-676. doi: 10.1016/j.cell.2006.07.024

Tang, Q. Q., & Lane, M. D. (2012). Adipogenesis: from stem cell to adipocyte. *Annu Rev Biochem, 81*, 715-736. doi: 10.1146/annurev-biochem-052110-115718

Tang, W., Zeve, D., Suh, J. M., Bosnakovski, D., Kyba, M., Hammer, R. E., . . . Graff, J. M. (2008). White fat progenitor cells reside in the adipose vasculature. *Science, 322*(5901), 583-586. doi: 10.1126/science.1156232

Tarnopolsky, M. A., Rennie, C. D., Robertshaw, H. A., Fedak-Tarnopolsky, S. N., Devries, M. C., & Hamadeh, M. J. (2007). Influence of endurance exercise training and sex on intramyocellular lipid and mitochondrial ultrastructure, substrate use, and mitochondrial enzyme activity. *Am J Physiol Regul Integr Comp Physiol, 292*(3), R1271-1278. doi: 10.1152/ajpregu.00472.2006

Tedesco, F. S., Dellavalle, A., Diaz-Manera, J., Messina, G., & Cossu, G. (2010). Repairing skeletal muscle: regenerative potential of skeletal muscle stem cells. *J Clin Invest, 120*(1), 11-19. doi: 10.1172/JCI40373

Teufel, A., Malik, N., Mukhopadhyay, M., & Westphal, H. (2002). Frcp1 and Frcp2, two novel fibronectin type III repeat containing genes. *Gene, 297*(1-2), 79-83.

Thiazolidinediones (TZDs)Nagase, I., Sasaki, N., Tsukazaki, K., Yoshida, T., Morimatsu, M., & Saito, M. (1994). Hyperplasia of brown adipose tissue after chronic stimulation of beta 3-adrenergic receptor in rats. *Jpn J Vet Res, 42*(3-4), 137-145.

Timmons, J. A., Wennmalm, K., Larsson, O., Walden, T. B., Lassmann, T., Petrovic, N., . . . Cannon, B. (2007). Myogenic gene expression signature establishes that brown and white adipocytes originate from distinct cell lineages. *Proc Natl Acad Sci U S A, 104*(11), 4401-4406. doi: 10.1073/pnas.0610615104

Townsend, K., & Tseng, Y. H. (2012). Brown adipose tissue: Recent insights into development, metabolic function and therapeutic potential. *Adipocyte, 1*(1), 13-24. doi: 10.4161/adip.18951

Tran, K. V., Gealekman, O., Frontini, A., Zingaretti, M. C., Morroni, M., Giordano, A., . . . Cinti, S. (2012). The vascular endothelium of the adipose tissue gives rise to both white and brown fat cells. *Cell Metab, 15*(2), 222-229. doi: 10.1016/j.cmet.2012.01.008

Tsigos, C., Papanicolaou, D. A., Kyrou, I., Defensor, R., Mitsiadis, C. S., & Chrousos, G. P. (1997). Dose-dependent effects of recombinant human interleukin-6 on glucose regulation. *J Clin Endocrinol Metab, 82*(12), 4167-4170. doi: 10.1210/jcem.82.12.4422

Uezumi, A., Fukada, S., Yamamoto, N., Ikemoto-Uezumi, M., Nakatani, M., Morita, M., . . . Tsuchida, K. (2014). Identification and characterization of PDGFRalpha+ mesenchymal progenitors in human skeletal muscle. *Cell Death Dis, 5*, e1186. doi: 10.1038/cddis.2014.161

Uezumi, A., Fukada, S., Yamamoto, N., Takeda, S., & Tsuchida, K. (2010). Mesenchymal progenitors distinct from satellite cells contribute to ectopic fat cell formation in skeletal muscle. *Nat Cell Biol, 12*(2), 143-152. doi: 10.1038/ncb2014

van den Berg, S. A., van Marken Lichtenbelt, W., Willems van Dijk, K., & Schrauwen, P. (2011). Skeletal muscle mitochondrial uncoupling, adaptive thermogenesis and energy expenditure. *Curr Opin Clin Nutr Metab Care, 14*(3), 243-249. doi: 10.1097/MCO.0b013e3283455d7a

van Loon, L. J. (2004). Use of intramuscular triacylglycerol as a substrate source during exercise in humans. *J Appl Physiol (1985), 97*(4), 1170-1187. doi: 10.1152/japplphysiol.00368.2004

van Loon, L. J., Koopman, R., Manders, R., van der Weegen, W., van Kranenburg, G. P., & Keizer, H. A. (2004). Intramyocellular lipid content in type 2 diabetes patients compared with overweight sedentary men and highly trained endurance athletes. *Am J Physiol Endocrinol Metab, 287*(3), E558-565. doi: 10.1152/ajpendo.00464.2003

van Marken Lichtenbelt, W. D., Vanhommerig, J. W., Smulders, N. M., Drossaerts, J. M., Kemerink, G. J., Bouvy, N. D., . . . Teule, G. J. (2009). Cold-activated brown adipose tissue in healthy men. *N Engl J Med, 360*(15), 1500-1508. doi: 10.1056/NEJMoa0808718

Vaughan, R. A., Gannon, N. P., Barberena, M. A., Garcia-Smith, R., Bisoffi, M., Mermier, C. M., . . . Trujillo, K. A. (2014). Characterization of the metabolic effects of Irisin on skeletal muscle in vitro. *Diabetes Obes Metab*. doi: 10.1111/dom.12268

Voss, G. J., Kump, D. K., Walker, J. A., & Voss, S. R. (2013). Variation in salamander tail regeneration is associated with genetic factors that determine tail morphology. *PLoS One, 8*(7), e67274. doi: 10.1371/journal.pone.0067274

Wan, D. C., & Longaker, M. T. (2014). Fat or fiction: origins matter. *Cell Metab, 19*(6), 900-901. doi: 10.1016/j.cmet.2014.05.007

Wang, Q. A., Tao, C., Gupta, R. K., & Scherer, P. E. (2013). Tracking adipogenesis during white adipose tissue development, expansion and regeneration. *Nat Med, 19*(10), 1338-1344. doi: 10.1038/nm.3324

Wells, G. D., Noseworthy, M. D., Hamilton, J., Tarnopolski, M., & Tein, I. (2008). Skeletal muscle metabolic dysfunction in obesity and metabolic syndrome. *Can J Neurol Sci, 35*(1), 31-40.

West, C. C., Murray, I. R., Gonzalez, Z. N., Hindle, P., Hay, D. C., Stewart, K. J., & Peault, B. (2014). Ethical, legal and practical issues of establishing an adipose stem cell bank for research. *J Plast Reconstr Aesthet Surg*. doi: 10.1016/j.bjps.2014.01.030

Westerblad, H., Bruton, J. D., & Katz, A. (2010). Skeletal muscle: energy metabolism, fiber types, fatigue and adaptability. *Exp Cell Res, 316*(18), 3093-3099. doi: 10.1016/j.yexcr.2010.05.019

Williams, C. T., Goropashnaya, A. V., Buck, C. L., Fedorov, V. B., Kohl, F., Lee, T. N., & Barnes, B. M. (2011). Hibernating above the permafrost: effects of ambient temperature and season on expression of metabolic genes in liver and brown adipose tissue of arctic ground squirrels. *J Exp Biol, 214*(Pt 8), 1300-1306. doi: 10.1242/jeb.052159

Wrann, C. D., White, J. P., Salogiannnis, J., Laznik-Bogoslavski, D., Wu, J., Ma, D., . . . Spiegelman, B. M. (2013). Exercise induces hippocampal BDNF through a PGC-1alpha/FNDC5 pathway. *Cell Metab, 18*(5), 649-659. doi: 10.1016/j.cmet.2013.09.008

Wu, J., Bostrom, P., Sparks, L. M., Ye, L., Choi, J. H., Giang, A. H., . . . Spiegelman, B. M. (2012). Beige adipocytes are a distinct type of thermogenic fat cell in mouse and human. *Cell, 150*(2), 366-376. doi: 10.1016/j.cell.2012.05.016

Yadav, A., Saini, V., & Arora, S. (2010). MCP-1: chemoattractant with a role beyond immunity: a review. *Clin Chim Acta, 411*(21-22), 1570-1579. doi: 10.1016/j.cca.2010.07.006

Yamada, M., Moriguch, Y., Mitani, T., Aoyama, T., & Arai, H. (2014). Age-dependent changes in skeletal muscle mass and visceral fat area in Japanese adults from 40 to 79 years-of-age. *Geriatr Gerontol Int, 14 Suppl 1*, 8-14. doi: 10.1111/ggi.12209

Yin, H., Pasut, A., Soleimani, V. D., Bentzinger, C. F., Antoun, G., Thorn, S., . . . Rudnicki, M. A. (2013). MicroRNA-133 controls brown adipose determination in skeletal muscle satellite cells by targeting Prdm16. *Cell Metab, 17*(2), 210-224. doi: 10.1016/j.cmet.2013.01.004

Zehentner, B. K., Leser, U., & Burtscher, H. (2000). BMP-2 and sonic hedgehog have contrary effects on adipocyte-like differentiation of C3H10T1/2 cells. *DNA Cell Biol, 19*(5), 275-281. doi: 10.1089/10445490050021186

Zhang, Y., Li, R., Meng, Y., Li, S., Donelan, W., Zhao, Y., . . . Tang, D. (2014). Irisin Stimulates Browning of White Adipocytes Through Mitogen-Activated Protein Kinase p38 MAP Kinase and ERK MAP Kinase Signaling. *Diabetes, 63*(2), 514-525. doi: 10.2337/db13-1106

Zierath, J. R., & Hawley, J. A. (2004). Skeletal muscle fiber type: influence on contractile and metabolic properties. *PLoS Biol, 2*(10), e348. doi: 10.1371/journal.pbio.0020348

Zimmermann, S., Voss, M., Kaiser, S., Kapp, U., Waller, C. F., & Martens, U. M. (2003). Lack of telomerase activity in human mesenchymal stem cells. *Leukemia, 17*(6), 1146-1149. doi: 10.1038/sj.leu.2402962

Zoladz, J. A., & Pilc, A. (2010). The effect of physical activity on the brain derived neurotrophic factor: from animal to human studies. *J Physiol Pharmacol, 61*(5), 533-541.

Zuk, P. A., Zhu, M., Mizuno, H., Huang, J., Futrell, J. W., Katz, A. J., . . . Hedrick, M. H. (2001). Multilineage cells from human adipose tissue: implications for cell-based therapies. Tissue Eng, 7(2), 211-228. doi: 10.1089/107632701300062859

CHAPTER 2. METHODS AND MATERIALS

2.1 Animals

All experimental mice were purchased from the Jackson Laboratory. Pdgfra$^{GFP/+}$ mice (stock 007669) are C57/B6 mixed with 129-S4 background. The aP2-Cre^{+} (stock005069), Myod$^{cre/+}$ (stock 014140), Rosa$^{LSLiDTR/+}$ (stock 007900, simplified as Rosa$^{iDTR/+}$), Rosa$^{LSLeYFP/+}$ (stock 007903, simplified as Rosa$^{eYFP/+}$), and Rosa$^{LSLtdTomato/+}$ (stock 007914, simplified as Rosa$^{td/+}$) mice are of a C57/B6 background. Myf5$^{cre/+}$ mice were provided by University of Ottawa. Mice were housed in the Purdue Lilly Animal Care Facility. The room temperature was set at 27°C and lighting was set on a 12 h light/dark cycle unless specified. Humidity and temperature were automatically controlled. Mice were fed a chow diet and water were freely accessible. All procedures involving the use of animals were approved by the Purdue Animal Care and Use Committee.

According to the strategy shown in **Fig. 23A**, aP2-Cre^{+}/Rosa$^{iDTR/+}$ double heterozygous (aP2-Cre^{+}) mice (F1) were bred. aP2-Cre^{+}/Rosa$^{iDTR/+}$/Pdgfra$^{GFP/+}$ triple heterozygous (Cre+) were bred by back-crossing F1 with the Rosa$^{iDTR/iDTR}$mice, and then crossing the F2 aP2-Cre^{+}/Rosa$^{iDTR/iDTR}$ progeny with Pdgfra$^{GFP/+}$ individual to generate Cre+ F3 progeny. The aP2-Cre^{+} and aP2-Cre F1 were used as experimental and control mice for examining brown fat regeneration, respectively. The Cre+ and Cre– F3

progenies from 3 pairs of F2 breeding pairs were used for examining *Pdgfra* lineage cell activity in regenerating adipose tissue. Myod$^{cre/+}$/Rosa$^{iDTR/+}$/Rosa$^{td/+}$ triple heterozygous mice were created with the same breeding strategy **(Fig. 23B)**.

Mice used for examining *Pdgfra* lineage cells were harvested around embryonic day 17.5 (E17.5), postnatal day 1 (P1), and 2 months of age. Mice used to study brown fat regeneration study were subjected to diphtheria injection at 2 months or 4 months of age. Mice used for muscle in BAT RNA examination and primary adipocyte culture were 2 months old.

2.2 Genotyping

Genotyping was performed according to protocols provided by the Jackson Laboratory. The primers used for genotyping, corresponding band size and annealing temperature are listed in **table. 1**. One 10µl PCR reaction system for genotyping contains 2µl neutralized DNA template, 0.8µl primer mix (20pm), 1µl 10X PCR buffer (Feldan), 0.4µl DMSO, 0.2µl 25mM dNTP (Feldan),0.05µl DNA polymerase (Bio Canada INC) and 6.8µl H_2O.

Table 1: Genotyping primers

Genotype	Primers	Annealing temperature	Band size
aP2-Cre Myf5$^{cre/+}$	F: 5'-GCG GTC TGG CAG TAA AAA CTA TC- 3' R: 5'-GTG AAA CAG CAT TGC TGT CAC TT-3' Internal control F: 5'-CTA GGC CAC AGA ATT GAA AGA TCT- 3' Internal control R: 5'-GTA GGT GGA AAT TCT AGC ATC ATC C- 3'	64°C	Mut671bp WT324bp
iDTR	Common F: 5'-AAA GTC GCT CTG AGT TGT TAT- 3' WT R: 5'-GGA GCG GGA GAA ATG GAT ATG-3' Mutant R: 5'-CAT CAA GGA AAC CCT GGA CTA CTG- 3'	61°C	Mut242bp WT603bp
Pdgfra	WT F: 5'-CCC TTG TGG TCA TGC CAA AC-3' WT R: 5'-GCT TTT GCC TCC ATT ACA CTG G-3' Mutant R: 5'-ACG AAG TTA TTA GGT CCC TCG AC-3'	60°C	Mut242bp WT251bp
Myod$^{cre/+}$	WT F: 5'-CGG CTA CCC AAG GTG GAG AT-3' Mutant F: 5'-GCG GAT CCG AAT TCG AAG TTC C-3' Common R: 5'-TGG GTC TCC AAA GCG ACT CC-3'	62°C	Mut149bp WT343cp
Rosa-td Tomato	WT F: 5'- AAG GGA GCT GCA GTG GAG TA-3' WT R: 5'- CCG AAA ATC TGT GGG AAG TC-3' Mutant F: 5'- GGC ATT AAA GCA GCG TAT CC-3' Mutant R: 5'- CTG TTC CTG TAC GGC ATG G-3'	61°C	Mut196bp WT297bp
Rosa-eYFP	WT F: 5'- AAG GGA GCT GCA GTG GAG TA-3' WT R: 5'- CCG AAA ATC TGT GGG AAG TC-3' Mutant F: 5'- ACA TGG TCC TGC TGG AGT TC-3' Mutant R: 5'- GGC ATT AAA GCA GCG TAT CC-3'	61°C	Mut212bp WT297bp

2.3 Fat dissection

Fat dissection was performed immediately after CO_2 euthanasia of experimental mice according to standard protocol (Lim et al., 2012). The following depots were routinely harvested for experimental examination: isBAT, inguinal white adipose tissue (iWAT), gonadal white adipose tissue (gWAT), tibialis anterior (TA) muscle, extensor digitorum longus (EDL) muscle, soleus (SOL) muscle. For brown adipose tissue dissection, the connective tissues and associated muscles around were carefully removed except

when the BAT was used for studying muscle in BAT. The lymph nodes in iWAT were removed at all times to avoid possible bias.

2.4 SVF culture, differentiation and diphtheria toxin *in vitro* treatment

Harvested BAT or WAT depots were manually minced with dissection scissors for approximately 1 minute. The resulted fat paste was transferred to a 15ml tube and enzymatically digested in 2ml dissociation solution. The dissociation solution contained 1.5mg/ml collagenase I in Dulbecco's Moified Eagle Medium (DMEM). Brown adipose samples were heated in a 37°C water bath for 30 minutes and white adipose for 1.5 hours, with gentle shaking every 5 minutes for both samples. The digesting cells and debris were stopped by culture medium (20% FBS, 1% Hepes, 1% peniciliin/strepomycine (P/S), DMEM), passed through a 100μm cell strainer, and spun down at 15000rpm. Supernatant was discarded and the resulting palette was resuspended by 6ml of culture medium and transferred to culture dishes. The cells were cultured in an incubator at 37°C with 5% CO_2. Medium was changed every other day.

For spontaneous adipocyte differentiation, cells were plated in culture medium with reduced Fetal bovine serum (5% FBS) for up to 14 days until 30% confluence on a 10cm culture plate. For standard insulin induced differentiation, cells that reached 80% confluence were induced by induction medium (10% FBS, 0.3nM dexamethasone (Sigma), 0.63mM 3-isobutyl-1-methylxanthine (Sigma), 2.85nM human insulin for 4 days with only one change of medium. The cells were then differentiated with differentiation medium (10% FBS, 0.197nM insulin and 10nM triiodothyronine) for up to 6 days.

Diphtheria toxin (DT) (Calbiochem) powder was dissolved in DMSO to make 1mg/ul stock. Cultured SVF were treated with 200ng/ml DT in culture medium for 2 days before induction.

2.5 SVF transplantation

$Pdgfra^{GFP/+}$ mice isBAT SVF were isolated and the final cell palette from isBAT of 1 animal was re-suspended in 150µl PBS with 1ng/ml basoc fibroblast growth factor. A total volume of 50µl suspended cells was immediately injected into 1 GPF^{-} WT acceptor underneath the isBAT area or forelimb skin pouch. The animal was sedated during this procedure with an IP injection of 100µl ketamine cocktail per 10g body weight. The ketamine cocktail contained 1 part of Xylaxzine (10mg/ml), 9 parts of Ketamine (100ml/ml), and 90 parts of 0.9% injectable saline. After 21 days or 3 months, the isBAT and forelimb areas were examined under fluorescent microscope for any GFP^{+} cells that had developed into new adipose or integrated into the pre-existing fat depots.

2.6 Brown fat damage and regeneration

To chemically damage brown fat, aP2-Cre^{+}/$Rosa^{iDTR/+}$ mice were used since their mature adipocytes express DT receptor and are subjected to DT damage. DT working solution was made by dissolving 2µl of stock solution in 1ml saline. Animal were sedated by ketamine cocktail, shaved, and disinfected with iodine before a 0.5cm incision was made on the back skin to expose isBAT. To get an even distribution of the drug and to reduce leakage, 60µl 2ng/µl DT in saline was injected into the isBAT at 2 different

locations. An insulin injection needle/syringe was used and injection sites were specifically picked to avoid major blood vessels in isBAT. Any isBAT that had blood vessel rupture was not used in the experiment. After toxin injection, the wound was immediately sutured with surgical glue and wiped with iodine. After DT injection for 3 days, 21 days, 30 days or 3 months, isBAT were harvested and subjected to further examination.

2.7 Muscle damage and regeneration

Mice were first sedated with a ketamine cocktail. The hind legs were shaved to better locate TA muscle position. Cardiotoxin (CTX, 2.5µl/g/animal, 10µM, Sigma) was then injected into the belly of the TA muscle on one side and saline was injected into the other side as a control. The mice were then allowed to recover for 14 or 21 days. Cryostat and Hematoxylin and Eosin (H&E) staining was then performed to visualized the morphology of the damaged and control TAs.

All tissues harvested (such as isBAT, P1 mouse and TA muscles) were collected and merged in an optimal cutting temperature compound (O.C.T.) using dry ice-cooled 2-methol-butane. Transversal cryosections (10µm) were obtained by a Leica CM1850 cryostat on superfrost plus glass slides. The sections were washed with PBS, emerged in Hematoxylin for 5min, rinsed with deionized water, and then incubated in eosin for 2 minutes. Slides were then dried with 75%, 95% and 100% alcohol for 1 minute each, placed in Xylene for 5 minutes and mounted with cytoseal. Unused slides were stored in -20°C.

Due to the fragility of WAT and regenerated isBAT, WAT and regenerated isBAT samples were sent to Purdue Veterinary School Pathology lab for paraffin sectioning at 3µm thickness and processed with H&E staining according to the pathology lab standard protocol.

2.8 Immunohistochemistry

Fresh or frozen slides were washed with PBS to remove O.C.T. 4% poly formaldehyde (PFA) were applied for 10 minutes, followed by 100mM glycine for 5 minutes, and washed with PBS for 3 times. The resulting slides were then immersed in blocking buffer (5% goat serum, 2% BSA, 0.2% triton X-100 and 0.1% sodium azide in PBS) for 1 hour at room temperature and then incubated in blocking buffer diluted primary antibodies overnight under 4 °C. After the primary antibody incubation, slides were washed with PBS 3 times, and PBS diluted secondary antibodies (1:1000) with DAPI (1:1000) were applied for 1 hour at room temperature. Final products were rinsed 3 times with PBS, mounted with Dako fluorescent mounting media (Glostrup, Denmark) and imaged with Coolsnap HQ CCD camera (photometrics, USA) driven by IP Lab software (Scanalytics Inc, USA) using a Leica DMI 6000B fluorescent microscope. Primary antibodies were: Mf20 1:20(made in lab), Ki67 (BD bioscience 550609) 1:500, Laminin 1:1000, BrdU (Alfa Aesar) 1:500, typeIIA, typeIIB, typeI, GFP 1:10000.

2.9 Oil-Red-O staining

The Oil-Red-O staining stock solution was made by dissolving 0.25g Oil-Red-O powder (Sigma) in 50ml isopropanol, filtered through a normal chemical filter, and stored in a 4 °C cooler. Working solution was made fresh each time when staining was performed due to its instability. Working solution was made by mixing 3 parts of the Oil-Red-O stock with 2 parts of ddH_2O (distilled water) and filtered through 2 layers of chemical filters. Typically, 1ml working solution was used per well of a 6-well-plate, and 0.5ml was used per well of a 12-well-plate. Each time, no less than 5ml total volume of working solution was made to account for the residue on filters.

Mature adipocytes on the culture dish were harvested and fixed in 4% PFA for 5 minutes at room temperature or as long as overnight in 4 °C until all plates were collected. Fresh adipose cryosections were fixed with 4% PFA for 15 minutes at room temperature. For whole mount, adipose tissues were cut into $2mm^3$ cubes and fixed with 4% PFA for at least 30 minutes at room temperature. After fixation, cells/tissues were quickly rinsed 3 times with PBS and Oil Red O working solution was applied for 10 minutes. The working solution was then removed and replaced with ddH_2O for 10 minutes. The resulting cells/tissues were then counter stained with DAPI (1:1000) for 30 minutes and washed 3 times with PBS for 5 minutes each. The finished products were covered with 50% glycerol. The sections were further covered with glass coverslip and sealed with nail polish around the edges.

2.10 BrdU *in vivo* proliferation assay

Eighty microliters of l 25mg/ml BrdU (Alfa Aesar, MA, USA) solution in saline was IP injected daily into 2-month-old individuals for 7 continuous days housed in 4 °C cold room or at room temperature. Brown adipose tissue and intestine were harvested and cryo-sectioned. The sections were fixed at room temperature with cold 70% ethanol for 10 minutes, rinsed with PBS 3 times for 5 minutes each, incubated in 40°C with 1.5N HCl for 1 hour, and rinsed with PBS twice for 5 minutes each. The resulting slides were then subjected to immunohistochemistry as described previously.

2.11 Cold treatment

For cold proliferation experiments, mice were housed in a cool room at 4°C for 3 or 7 days. Only 1 mouse was housed per cage to ensure adequate exposure to cold. Standard chow diet and water were freely accessible.

2.12 Fluorescence activated cell sorting (FACS)

The SVF of Pdgfra$^{GFP/+}$ moue various fat depots (isBAT, iWAT, gWAT) were isolated as previously described. Suspended cells were plated on a culture dish for 45 minutes to remove hematopoietic and blood vessel lineage cells. After pre-plating, cells were enzymatically digested by 0.05% trypsin, cell pallets were collected and re-suspended in 200µl PBS with 2% FBS, and stained with 5µl Pacific blue conjugated Stem cell antigen1 (Sca1, 5µl, biolegend) antibody on ice for 20 minutes. Cells were then washed with PBS containing 2% FBS twice for 5 minutes each and placed on ice before sorting. WT isBAT

cells were isolated and used as negative control. WT isBAT cells were isolated, stained, and used as background control. Pdgfra^{GFP+} isBAT cells without staining were used for GFP^{+} gating. The sorted population was then cultured and differentiated according to the SVF culture and differentiation procedure.

2.13 Quantitative polymerase chain reaction

Quantitative polymerase chain reaction (qPCR) analysis was performed using a Roche Lightcycler 480 system. Total RNA was extracted by trizol and 4 µg of RNA were converted into cDNA using MMLV reverse transcriptase and random hexamer primers. For each qPCR reaction, 5µl SYBR Green Mastermix (Roche), 0.2µl of each primer (20µM) and 4.6µl cDNA (2ng/ul) was mixed. Relative fold changes were calculated using the $2^{-\Delta\Delta CT}$ method and 18s gene was used as a housekeeping control. Primers used are listed in **Table 2**.

Table 2: q-PCR primer

18s	F: 5'-AGT CCC TGC CCT TTG TAC ACA- 3' R: 5'-CGA TCC GAG GGC CTC ACT- 3'
Pdgfra	F: 5'-TGC TGG AACCGA TCC GAG GGC CTC ACT AGT GAG CCC GAG A- 3' R: 5'-AGG CCA CCT TCC CAG TCC TTC A- 3'
aP2	F: 5'-CCG ACT GAC TAT TGT AGT GGT TAG TG- 3' R: 5'-TCA CCG CAG ACG ACA GGA AGG T- 3'
Ucp1	F: 5'-GGC CCT TGT AAA CAA CAA AAT AC- 3' R: 5'-GGC AAC AAG AGC TGA CAG TAA AT- 3'
Cidea	F: 5'-TGT TCT TCT GTA TCG CCC AGT- 3' R: 5'-GCC GTG TTA AGG AAT CTG CTG- 3'
Prdm16	F: 5'-CAG CAC GGT GAA GCC ATT C- 3' R: 5'-GCG TGC ATC CGC TTG TG- 3'
Myod	F: 5'-GGC TAC GAC ACC GCC TAC TA- 3' R: 5'-CGA CTC TGG TGG TGC ATC TG- 3'
Myog	F: 5'- TGC CCA GTG AAT GCA ACT CC- 3' R: 5'- TTG GGC ATG GTT TCG TCT GG- 3'
Leptin	F: 5'-GTG GCT TTG GTC CTA TCT GTC- 3' R: 5'-CGT GTG TGA AAT GTC ATT GAT CC- 3'
Dlk1	F: 5'-CCT GGC TGT GTC AAT GGA GT- 3' R: 5'-TGG CAG TCC TTT CCA GAG AA- 3'

2.14 Western blot

Total protein was isolated from cells using RIPA buffer (pH8.0 50mM Tris-HCL, 150mMNaCl, 1%NP-40, 0.5% sodium deoxycholate and 0.1% SDS). Concentrations were determined by BCA Protein Assay Reagent (Pierce Biotechnology, Rockford, IL). Proteins adjusted to the same concentrations and volumes were separated by sodium dodecyl sulfate PAGE (SDS-PSGE), transferred to a polyvinylidene fluoride (PVDF) membrane (Millipore Corporation, Billerica, MA), blocked with 4% milk, and incubated with the diluted first antibodies under 4°C overnight. Primary antibodies were typically used with 1: 500 dilutions, except GAPDH primary antibody (Santa Cruz, CA) was used with 1:2500

dilutions. Band detection was performed using enhanced chemiluminescence (ECL) western blotting substrate (Pierce Biotechnology, Rockford, IL) and detected with a FluorChem R protein imaging system (Protein Simple, CA, USA).

2.15 SeeDB tissue clarification

Standard See deep brain (SeeDB) tissue clarification was performed according to online protocol (Ke & Imai, 2014). Briefly, isBAT were fixed in 4%PFA overnight, washed 3 times with PBS for 10 minutes each time, incubated in sequential increasing concentration of fructose solution (20%, 40%, and 60%) on a seesaw shaker each for 6 hours. The sample was then transferred into 80% and then 100% fructose for incubation, each for 12 hours with shaking. The sample was then merged in SeeDB solution for 48 hours. SeeDB solution was made by mixing 20.25g fructose with 100ul α-thioglycerol and 5 ml of ddH_2O. The tissue was then imaged using a Leica DMI 6000B fluorescent microscope and pieced in a Photoshop program.

2.16 Image analysis

Stained single cell signals and GFP^+ signals were manually counted in software Photoshop CS3 using Analysis-Count plug in. DAPI nucleus signals were converted to black and white signals and quantified in software Image J using ITCN plugin. Three dimensional (3D) reconstruction was performed in 3D Max with manual modelling using transverse section pictures as frameworks. Confirmation 3D construction was done in

Image Pro using stacking property based on another independent set of transverse section pictures.

2.17 Statistics

Data are presented as mean ± s.e.m.. Number of repeats represents biological repeats unless indicated. P-values were calculated using a two-tailed student t-test (* $P<0.05$, ** $P<0.01$, ***$p<0.005$).

References

Ke, M. T., & Imai, T. (2014). Optical clearing of fixed brain samples using SeeDB. *Curr Protoc Neurosci, 66*, Unit 2 22. doi: 10.1002/0471142301.ns0222s66

Lim, S., Honek, J., Xue, Y., Seki, T., Cao, Z., Andersson, P., . . . Cao, Y. (2012). Cold-induced activation of brown adipose tissue and adipose angiogenesis in mice. *Nat Protoc, 7*(3), 606-615. doi: 10.1038/nprot.2012.013

CHAPTER 3. RESULTS

3.1 Result1: Embryonic and adult brown adipose progenitors are distinct populations

3.1.1 Progenitor/stem cells in BAT

Although studies suggest that classic BAT precursors are located in pericytic niches (Cinti & Morroni, 1995; Gupta et al., 2012; Tran et al., 2012), systemic examination of BAT stem cells and their contribution to BAT *in vivo* is lacking. Consistent with previous study, our study suggests the isBAT, which is the most abundant and well established classical BAT depot in mice, contains adipogenic progenitors that differentiate into mature adipocytes in culture (**Fig. 6, 11 & 14**).

3.1.1.1 *Pdgfra*$^{+}$ cells do not contribute to embryonic BAT adipogenesis

The cell surface protein Pdgfrα is a widely accepted WAT adipose precursor marker. FACS sorting of white adipose progenitors is frequently based on Pdgfrα and Sca1 (Pretheeban, Lemos, Paylor, Zhang, & Rossi, 2012). Supporting this notion, *in vivo* lineage tracing proves that mature subcutaneous white adipocytes are derived from the *Pdgfra* lineage (Berry & Rodeheffer, 2013). In addition, *Pdgfra*$^{+}$ progenitors form both WAT and Beige adipose *in vivo* and *in vitro* (Lee, Petkova, Mottillo, & Granneman, 2012). This prompts us to question whether BAT adipocytes are from the *Pdgfra*$^{+}$ population.

To examine if BAT is formed by *Pdgfra*$^{+}$ cells during development, Pdgfra$^{GFP/+}$mice were bred. These mice have a H2B-eGFP (Histone 2B-enhanced green fluorescent protein) reporter gene insertion (or knock-in) into the endogenous *Pdgfra* locus, which functionally interrupts Pdgfrα protein. Pdgfra$^{GFP/GFP}$ mice were not used due to their embryonic lethality, since *Pdgfra*-expressing cells are critical for neurogenesis and angiogenesis during development (Hoch & Soriano, 2003; Zhang et al., 2009). The Pdgfra$^{GFP/+}$ mice have a normal phenotype and are fertile. Their *Pdgfra*$^{+}$ cells express nucleus located H2B-GFP fusion protein, and the fluorescence pattern mimics the endogenous expression. Theoretically, since the H2B has a slow turnover rate, the GFP fusion protein is stable for months, which can be used for lineage tracing. The persistent expression of GFP in mature adipocytes in adult animals **(Fig. 5A)** and in cell culture **(Fig. 11)** also suggests that the H2B-GFP is stable *in vivo* because mature adipocytes do not express Pdgfrα. In this case, the GFP+ population potentially represents the *Pdgfra* lineage cells.

To examine embryonic BAT, we first validated the method for accessing developing BAT histologically. Myf5$^{cre/+}$/Rosa^{eYFP+} mice, whose cells from the *Myf5* lineage express enhanced yellow florescent protein (eYFP), were killed on postnatal day 1 (P1) and their anterior torso were sectioned. During this early stage of BAT formation, several lobulated structures that were densely labeled with YFP were identified within the interscapular region towards the dorsal side of the spine **(Fig. 1A)**. Because BAT and skeletal muscle share a common *Myf5* origin, the YFP expression confirms the presence of the premature BAT. These lobes of BAT were closely located to each other. They are

likely the premature forms of different BAT depots such as isBAT,sBAT, cBAT, and paBAT (Sanchez-Gurmaches & Guertin, 2014). Morphologically, these lobulated structures appeared darker than the surrounding tissues in the H&E staining **(Fig. 1B)**. This was an expected result since the premature fat tissues are compacted with a large amount of interstitial cells and preadipocytes. The preadipocytes during this stage have not yet accumulated large lipid droplets, resulting in a relatively dense cell distribution in premature BAT. In addition, the GFP patterns of each lobulated structure were similar **(Fig. 3A)**. This reveals that various BAT depots contain similar percentage of *Pdgfra*$^{+}$ cells. Together the data shows that developing BAT is lobulated, possesses a myogenic origin, and is distributed with *Pdgfra*$^{+}$ cells evenly among depots.

Next we characterized and quantified the GFP^{+} cells in E17.5 **(Fig. 2)** and P1 **(Fig. 3)** developing isBAT. If isBAT adipocytes originate from the *Pdgfra*$^{+}$ population, most of the isBAT cells are expected to be GFP^{+} due to the slow turnover rate of H2B-eGFP. However, in the early developmental stage of BAT at E17.5, the majority of the isBAT cells are GFP^{-} **(Fig. 2B-D)**. This clearly demonstrates that isBAT does not develop from *Pdgfra*$^{+}$ precursors. Interestingly, some GFP^{+} cells are located in isBAT dispersedly or around hollow structures which are potentially blood vessels from the “primitive structure” of fat pads **(Fig. 2B)**. Consistent with our finding, previous studies have shown that the *Pdgfra* lineage cells are frequently identified close to vasculature structures in various depots, and so are the ASCs (Cai, Lin, Hauschka, & Grottkau, 2011; Cinti & Morroni, 1995; Gupta et al., 2012; Tran et al., 2012). These findings point to the possibility that a certain population of *Pdgfra*$^{+}$ progenitors is preserved in developing

BAT vascular structures. On P1 when BAT starts to mature and express BAT functional genes, only 6.50 ± 0.76% cells were GFP^+ **(Fig. 3)**. The GFP^+ population was again a small fraction of the total cell number and distributed loosely in isBAT. Data obtained from E17.5 and P1 isBAT together suggests that the majority of developing BAT adipocytes are from the *Pdgfra* negative population. In conclusion, *Pdgfra*$^+$ cells are not the main source of embryonic BAT development.

3.1.1.2 *Pdgfra*$^+$ cells represent a small fraction of adult BAT

Although previous findings showed that adult subcutaneous WAT and its precursors are almost completely from the *Pdgfra* lineage (Berry & Rodeheffer, 2013), our data shows that adult BAT only contains a small population of *Pdgfra*$^+$ cells **(Fig. 4)**. Specifically, in mature isBAT from the 2-month-old individuals, 2.93 ± 0.09% cells were GFP^+. This percentage was low and was significantly lower than P1 ($P=0.0098$, $N=3$). The difference between adult and P1 isBAT can be due to the proliferation of GFP^- cells, loss/slow proliferation of GFP^+ cells or both, which was not tested in this study. In contrast, mature iWAT had a high percentage of GFP^+ cells **(Fig. 5A)** representing 59.22 ± 1.10% of the total population **(Fig. 5B)**. The GFP^+ percentage in mature iWAT was 20 times higher than isBAT ($P= 0.0000009$, $N=3$), which indicates that the majority of subcutaneous WAT cells but not the BAT cells originates from the *Pdgfra*$^+$ cells.

Our data does not contradict with the previous lineage tracing study by Berry and his colleagues since their *in vivo* data obtained did not account for the interstitial cells in WAT. Membrane targeted fluorescent reporter used by the previous study is

ideal for delineating mature adipocytes but is difficult to distinguish the small interstitial cells in between fat cells. These interstitial cells likely constitute the GFP^- population in our $Pdgfra^{GFP/+}$ model. Overall, *Pdgfra*$^+$ cells are a small fraction of mature BAT cells but a big portion of mature WAT cells, which indicates that most cells in BAT are not developmentally originated from the *Pdgfra* lineage as their counterparts in WAT.

3.1.1.3 *Pdgfra*$^+$ cells are abundant in BAT SVF culture

Classic BAT contains ASCs that can give rise to functional brown adipocytes. BAT ASCs are highly proliferative in SVF cell culture and have adipogenic potentials (Nechad, 1983). The adipocytes derived from BAT SVF culture are functional brown adipocytes expressing BAT signature genes such as *Ucp1* and *Cidea* (Cannon & Nedergaard, 2001). They are richer in mitochondria number comparing to counterparts from WAT SVF culture (Nechad, 1983). In our BAT SVF culture, ASCs appeared as spindle shaped fibroblast-like cells **(Fig. 6A)**. Upon adipogenic differentiation, these cells formed multiloculated mature isBAT adipocytes whose lipid content can be stained by Oil-Red-O in red **(Fig. 6B)**. Our data confirms a successfully established BAT SVF culture and differentiation assay.

On the contrary to the *in vivo* data which showed a low percentage of GFP^+ cells **(Fig. 2-4)**, *Pdgfra*$^+$ cells represented the majority of BAT SVF *in vitro* **(Fig. 7-10)**. *Pdgfra*$^+$ cells are thereby a major source of BAT progenitors in culture. Only 5 hours after isolation (cells not attached to the plate were excluded by pre-plating), 52.08 ± 2.09% SVF cells from $Pdgfra^{GFP/+}$ isBAT SVF were GFP^+ **(Fig. 7 left)**. After 1.5 days of culture, the

percentage increased to 67.93 ± 9.24% **(Fig. 7 right)**. Five days of culture yielded ~90% cells with GFP expression, which represented the vast majority of BAT SVF **(Fig. 8)**. In fact, 3 days of culture were sufficient to yield high proportion of GFP^+ cells in both isBAT and iWAT SVF **(Fig. 9)**. The *Pdgfra* expression in isBAT SVF was validated by immunostaining showing widely expressed Pdgfrα protein in dividing and differentiating BAT SVF cells **(Fig. 10)**. These together illustrate that *Pdgfra*$^+$ cells are enriched in BAT SVF and are BAT progenitors *in vitro*.

In addition, *Pdgfra*$^+$ cells are proliferative and highly expandable *in vitro*. The number of GFP^+ cells increased after a short **(Fig. 7 GFP panel)** or prolonged **(Fig. 8 GFP panel)** culture. For example, in the prolonged culture with a 5 day interval, the GFP^+ percentage was significantly higher on D5 (90.40 ± 1.25%) than on D1 (49.90 ± 2.75%) with P=0.0002, N=3 **(Fig. 8)**, and the increase of GFP^+ percentage was accompanied by an increase of GFP^+ cell number **(Fig. 8)**. This indicates that *Pdgfra*$^+$ population is proliferative and expands faster than other populations in BAT SVF culture. The data infers that *Pdgfra*$^+$ cells represent BAT and WAT progenitors *in vitro*.

Furthermore, most of the differentiated isBAT adipocytes *in vitro* are GFP^+. Typically, isBAT differentiation is induced by an insulin cocktail, but because chemical modification may induce not only adipocyte progenitors, but other adipogenic cells to form adipocytes, we allowed isBAT SVF spontaneously differentiate for a week. As expected, 95.2% of mature adipocytes are GFP^+ after differentiation **(Fig. 11D)**. This suggests that *Pdgfra*$^+$ cells are adipogenic, and more importantly, most of the spontaneously formed adipocytes are from *Pdgfra* lineage. In addition, the full process

of culture and differentiation of isBAT SVF took 14 days and the GFP persisted until the end of the differentiation period **(Fig. 11)**. This confirms the stability of H2B-eGFP protein for reliable lineage tracing.

3.1.2 Characteristics of *Pdgfra*$^{+}$ BAT progenitors

We next evaluated the ability of *Pdgfra*$^{+}$ progenitors to be incorporated into adipose tissues *in vivo*. Freshly isolated isBAT SVF from Pdgfra$^{GFP/+}$ mice were injected into isBAT and asWAT depots of WT hosts. After 21 days, GFP^{+} cells were found in both isBAT and asWAT **(Fig. 12)**. These GFP^{+} cells appear in clusters **(Fig. 12 left panels)**, suggesting possible replication after survival. Within the cluster, the GFP^{+} signals were parted by mature adipocytes **(Fig. 12 right panels)**. This GFP pattern is similar to adipocyte nucleus distribution *in vivo* and thus points to the possibility that the *Pdgfra*$^{+}$ cells form mature adipocytes after transplantation. In fact, the ability of *Pdgfra*$^{+}$ cells to form adipocytes *in vivo* has been indirectly demonstrated by previous studies showing that *Pdgfra* mRNA is highly expressed in the CD24^{+} BAT ASCs (Berry & Rodeheffer, 2013) and the CD24^{+} adipose progenitors possess *in vivo* adipogenic potential (Rodeheffer, Birsoy, & Friedman, 2008). Our data and previous studies further support that at least a population of *Pdgfra*$^{+}$ BAT progenitors are stem cells that can contribute to brown adipocytes *in vivo*. It is also greatly possible that many GFP^{+} cells become interstitial cells.

Cell culture results show that *Pdgfra*$^{+}$ stem cell populations in SVF of various adipose depots are adipogenic. SVF cells collected from Pdgfra$^{GFP/+}$ mice were sorted based on GFP and Sca1 expression **(Fig. 13, 15 and 17)**. The FACS separation went well,

indicated by the present of green cells in cultured GFP^+ fractions and the absence of GFP signals in the cultured GFP^- fraction **(Fig. 14, 16 and 18 right panels)** although this does not rule out the possibility that the GFP^+ fraction contains GFP^- cells. Consistent with GFP pattern in adult isBAT depot, the fraction of GFP^+ cells from isBAT SVF was ~2% **(Fig. 13)** which was low comparing to IMAT and IWAT **(Fig. 15&17)**. This indicates that *Pdgfra*$^+$ cells represent a small population of SVF cells in addition to representing a small population of total cells in BAT tissues. The low GFP^+ percentage corresponds well with the rare quantity of stem cells preserved in adult tissues. Importantly, only the cells from $GFP^+/Sca1^+$ fraction of isBAT SVF were adipogenic *in vitro* upon adipogenic differentiation, forming mutiloculated mature adipocytes **(Fig. 14 upper left)**. This indicates that the *Pdgfra*$^+$ stem cells are indeed adult isBAT ASCs *in vitro*. IMAT and iWAT SVF differentiation also showed that $GFP^+/Sca1^+$ cells have the most adipogenic potential **(Fig. 16 and 18 upper left)**. Culture of GFP^- population generates few (IMAT) to no (iWAT) adipocytes upon insulin cocktail induced adipogenic differentiation. Our data in IMAT and iWAT are consistent with other studies showing *Pdgfra* can be used as a sorting criterion for WAT ASCs (Macdougald, 2014), and fibroblastic *Pdgfra*$^+$ cells in IMAT are significantly more adipogenic than *Pdgfra*$^-$ cells (Uezumi et al., 2014). These together illustrated that *Pdgfra* lineage cells in BAT, WAT and IMAT SVF possess adipogenic potential.

3.1.3 Cold exposure does not increase BAT *Pdgfra*$^{+}$ cells

The existence of BAT stem cells and the seasonal dynamics of BAT in hibernating species lead to our hypothesis that BAT possesses regenerative ability under certain stimuli such as cold exposure and damage. Early studies using radio labeling of nucleotides have shown that in rats, cold treatment induces 70 times more proliferation index of BAT preadipocytes (L. Bukowiecki, Collet, Follea, Guay, & Jahjah, 1982). Another early study showed that total DNA content and mitochondria activity increases after β3 adrenergic receptor stimulation in BAT(Nagase et al., 1994), suggesting a proliferation of BAT cells under neuronal stimulus.

However, cold induced BAT cell proliferation was rarely detected in our study. D7 after continuous cold exposure of 2-month-old Pdgfra$^{GFP/+}$ mice, 0.56 ± 0.27% of isBAT cells were proliferating as indicated by positive Ki67 staining **(Fig. 19)**. This suggests that few cells proliferate after 7 days of cold exposure. Among the 0.56% of cells, hardly any cells were GFP^{+}/Ki67^{+} (0%, **Fig. 19 and Fig. 18A**). Therefore, isBAT cells rarely undergo cell division in cold, and the majority of proliferating cells are *Pdgfra* negative. This result was further confirmed by no difference in GFP^{+} percentage observed in cold treated and control mice isBAT **(Fig. 21)** (P=0.32, N=3). However, some Ki67^{+} cells were found next to GFP^{+} cells **(Fig. 18B)**, suggesting a relationship between the dividing cells and the *Pdgfra*$^{+}$ population. Overall, the degree of cell proliferation in cold treated BAT is low.

To access the accumulative proliferation of isBAT in cold, BrdU were i.p. injected daily into the mice subjected to 7 days of cold exposure. 1.08 ± 0.44% of isBAT cells have proliferated in cold compared to 1.09 ± 0.60% at room temperature condition **(Fig. 22)**, confirming no increase of mitotic division in cold treated isBAT (P=0.99, N=3).Together, our data shows that cold exposure does not increase isBAT progenitor proliferation.

3.1.4 BAT regeneration

3.1.4.1 BAT is affectively damaged by genetic ablation

In the case of regeneration, aP2-Cre^{+} Rosa$^{iDTR/+}$ Pdgfra$^{GFP/+}$ triple heterozygous (Cre+) and aP2-Cre^{+}/Rosa$^{iDTR/+}$ double heterozygous (aP2-Cre^{+}) mice were created for the purpose of specifically damaging isBAT **(Fig. 23A)**. The Rosa$^{iDTR/+}$ Pdgfra$^{GFP/+}$ (Cre–) and Rosa$^{iDTR/+}$ (aP2-Cre) littermates were recruited as controls. The adipocyte protein 2 (aP2) has been extensively used as mature adipocyte reporter (Shan, Liu, & Kuang, 2013), and therefore mature BAT adipocytes in the aP2-Cre^{+} mice express DT receptor and are theoretically damaged by DT injection. Cells of aP2-Cre individuals are not responsive to DT treatment, thus aP2-Cre^{+} and aP2-Cre mice represent damage models and intact controls, respectively. In Cre+ and Cre– mice, cells from *Pdgfra* lineage are marked with nucleus located GFP (not shown in the breeding strategy).

Local delivery of DT in 2-month-old mice in isBAT resulted in isBAT damage. On day 3 after injection, isBAT morphology was dramatically changed from full of evenly distributed multiloculated adipocytes **(Fig. 24B)** to a fibrotic appearance with enlarged spaces/cavities and abundant interstitial cells infiltrated **(Fig. 24A)**. The weight of

damaged isBAT was markedly decreased **(Fig. 25A)** coupled with the loss of cellular lipid content **(Fig. 25B-C)**, suggesting that isBAT damage was successful.

Pdgfra lineage cells proliferate vigorously in isBAT on D3 after injection. Many $GFP^+/Ki67^+$ cells were identified in isBAT after damage **(Fig. 26, white arrows)**, which were not found in intact controls. Some proliferating cells were GFP^- **(Fig. 26, red arrows)**. This suggests that many cells proliferate in damaged isBAT, including *Pdgfra*$^+$ population. DT induced damage significantly increases GFP^+ cell percentage in isBAT from 4.44 ± 0.72% to 9.22 ± 1.27% **(Fig. 27)** (P=0.007, N=3). Owing to the fact that about half of BAT progenitors are from aP2 lineage (Shan, Liu, & Kuang, 2013) and could be killed by DT, the GFP percentage could have been even higher if the aP2 is more stringently expressed by mature adipocytes (for example, if $Adiponectin^{Cre}$ is used). However, how many proliferating *Pdgfra*$^+$ cells are BAT progenitors are not known.

3.1.4.2 BAT regenerates after 30 days

To test if isBAT can regenerate, isBAT damage was made by local DT delivery, and then the experimental animals recovered in their home cages for 30 days. After 30 days, isBAT from aP2-Cre^+ and aP2-Cre mice were harvested. Considering the number and functionality of adult stem cells are commonly age dependent, animals at 2 different ages (2-month-old and 4-month-old) were recruited for the regeneration study.

Surprisingly, contrary to the situation upon damage, the isBATs from 4-month-old aP2-Cre^+ mice were bigger and significantly heavier after regeneration compared to the aP2-Cre littermates **(Fig. 28A)** (0.083 ± 0.03 g vs. 0.161 ± 0.037 g, p=0.0095, N=3).

BAT adipocytes underwent hypertrophy resulting in isBAT adipocytes acquiring a morphology resembling WAT adipocytes **(Fig. 29)**. Similar trends were found in the 2-month-old mice. The isBAT adipocytes of aP2-Cre^{+} mouse exhibited larger sizes and significantly increased weights (0.045 ± 0.002 g vs. 0.055 ± 0.001g) compared to aP2-Cre controls **(Fig. 28B)** (P=0.006, N=3). The magnitude of the increase in weight and size was smaller in the 2-month-old individuals than in the 4-month-old mice **(Fig. 28)**. Together, all of these results suggest that isBAT can regenerate through hypertrophy, but the regenerative capacity is age dependent. Whether hyperplasia occurs during this process is impractical to be measured due to the heterogeneity of adipocytes.

The percentage of GFP^{+} cells was significantly higher in isBAT of Cre+ mice compared to Cre– controls **(Fig. 30)** (P=0.01, N=3). This suggests that the *Pdgfra* lineage cells, which may include mature adipocytes generated from the adult BAT progenitors, increases in percentage after 30 days of regeneration. In 4-month-old individuals, GFP^{+} percentage in isBAT was 7.80 ± 0.41% in Cre+ individuals and 4.66 ± 0.60% in intact controls **(Fig. 30B)**. Similar trend was found in younger mice at 2 month of age (P=0.04, N=3). Cre+ isBAT has 4.65 ± 0.57% of GFP^{+} cells and the Cre– one has 2.93 ± 0.09% of GFP^{+} cells **(Fig. 30C)**. The degree of increment in D30 samples (4.65 ± 0.57%) was smaller than D3 samples (9.22 ± 1.27%) **(Fig. 27&30)**. This suggests that the regenerating isBAT has a higher percentage of *Pdgfra*$^{+}$ cells comparing to controls. In addition, GFP cells exist in larger proportion to total cell number in older animal (4.66 ± 0.60%) compared to the young (2.93 ± 0.09%), which indicates an accumulation of *Pdgfra* lineage cells after aging.

Although GFP$^+$ cells of BAT SVF differentiate into mature adipocytes *in vitro*, the increased GFP$^+$ cells in the regenerating BAT are not likely mature adipoctyes derived from the *Pdgfra*$^+$ cells. Firstly, the GFP$^+$ percentage was low (<10%, **Fig. 30**). A replacement of dramatically lost adipocytes **(Fig. 25)** during regeneration should result in a large percentage of GFP$^+$ cells in regenerating BAT, which was not found in our case. Furthermore, GFP percentage declines later on (D30) comparing to early stage of regeneration (D3) **(Fig. 27&30)**, suggesting a clearance of *Pdgfra* lineage population which should not occur if many Pdgfra lineage cells form mature BAT adipocytes. Based on the above inference, *Pdgfra*$^+$ adult BAT progenitors do not actively contribute to BAT regeneration.

3.1.4.3 BAT regeneration persists after 90 days

90 days after DT injection, isBAT from aP2-Cre$^+$ mouse remained larger in size **(Fig. 31A left)** and heavier by weight (0.079 ± 0.008 g vs. 0.182 ± 0.019 g, p=0.002, N=7) **(Fig. 31C)**. This indicates that isBAT regeneration is retained after a prolonged period. The augmentation in size and weight was again a result of isBAT hypertrophy clearly indicated by enlarged isBAT adipocytes **(Fig. 32A)**. This was indirectly reflected by decreased nucleus number (DAPI signal) per field in isBAT from Cre+ mouse comparing to the control **(Fig. 33C)**. The ability to accumulate lipid in isBAT was also restored. Oil-Red-O staining showed that each enlarged adipocyte in Cre+ individual accumulates much more lipid content compared to the Cre– control. This is dramatically different than D3 samples, in which the lipid accumulation of damaged isBAT was lost **(Fig. 25B)**.

Together, these data indicate that isBAT regeneration remains 90 days after damage and is largely contributed by isBAT adipocyte hypertrophy.

Although regenerated isBAT was larger and heavier, there was no difference in *Pdgfra* lineage cell percentage between regenerated and intact BAT **(Fig 34A- B)**. Cell counting revealed significantly fewer GFP^+ cells and DAPI signals per field in Cre+ isBAT comparing to Cre– controls **(Fig. 34C)**. This is due to the increased adipocyte size as previously described **(Fig. 32)**. However, the GFP/DAPI percentages were not different in Cre+ and Cre– mice (7.11 ± 0.44% vs. 6.43 ± 0.25%, p=0.19, n=22) **(Fig. 34B)**. This is interesting because the proportion of *Pdgfra*$^+$ cell increases during damage and early regeneration, but resets to the default level after 90 days of regeneration. It suggests that the *Pdgfra*$^+$ cells exert functions during the isBAT regeneration, but do not contribute to new adipocyte formation on a large scale, if there is any adipogenesis occurring. This further infers that the increase of *Pdgfra*$^+$ percentage in D3 and D30 samples was not contributed by mature adipocytes formed by *Pdgfra* lineage BAT progentitors. Therefore, the *Pdgfra*$^+$ cells proliferating during regeneration are likely supportive cells facilitating tissue restoration.

Previous studies have proved that surgical removal of BAT or genetic ablation of BAT results in compensatory growth of WAT (Rothwell & Stock, 1989). This phenotype was identified after isBAT regeneration. aP2-Cre^+ mice had bigger iWAT **(Fig. 31A upper right)** and gWAT **(Fig. 31A bottom right)** with significantly greater weights in comparison to the Cre– controls **(Fig. 31C)** (P=0.01 for iWAT and P=0.003 for gWAT, N=7). This reveals that isBAT function is not fully recovered during regeneration despite

its overgrown state in size and weight. The loss of BAT possibly leads to altered body metabolism and lipid accumulation in other fat depots in the body. Distinct from WAT depots, body weights and TA muscle weights were not affected by isBAT damage and regeneration **(Fig. 31B- C)**. No significant changes were found in liver morphology **(Fig. 31A middle)**. The effect of isBAT damage promotes compensatory growth of WAT but does not affect muscle, liver or whole body phenotypes 90 days after isBAT damage.

Then we asked how isBAT function is altered by toxin induced regeneration process. Quantitative PCR was performed to access BAT and WAT related gene expression. Consistent with the fact that regenerated isBAT appears larger and "whiter" morphologically **(Fig. 32A)**, BAT related genes such as *Ucp1*, *Cidea*, *Prdm16*, *Pgc1a* were repressed significantly ($p<0.05$, $N=3$) while the WAT related gene leptin was up regulated for 2.5 folds **(Fig. 34)**. *Ucp1* expression was down regulated for ~25%, which is considered a large reduction because the basal level of Ucp1 in BAT is high. *Cidea*, *Prdm16*, and *Pgc1a* mRNA expression were all reduced to about half of the original. Genes related to adipogenic differentiation and adipose precursors such as *aP2*, *Pdgfra* and *Dlk1* exhibited inconsistent changes indicating complex involvement of these genes during regeneration. Together these show that regenerated isBAT undergoes a "whitening" process.

3.1.5 Conclusion and discussion

3.1.5.1 BAT stem cells

Our study of the *Pdgfra*$^+$ cells in isBAT leads to a surprising conclusion— The majority of BAT cells *in vivo* originate from *Pdgfra* negative cells, whereas BAT precursors *in vitro* are from *Pdgfra* positive cells. In developing and mature BAT, *Pdgfra*$^+$ cells take up less than 7% of total cell number. The percentage is higher in the early developmental stage and lower in the mature stage. But the overall percentage is low. This proves that during development, the majority of the cells in isBAT are not from the *Pdgfra*$^+$ lineage. On the contrary, culture of mature isBAT SVF shows that *Pdgfra*$^+$ population quickly expands *in vitro*. In addition, only the GFP$^+$/Sca1+ population differentiates into mature adipocytes. These indicate that the *Pdgfra* lineage cells are indeed adipogenic precursors in adult isBAT, although they do not seem responsive to cold stimuli or contribute to regeneration after injury. We thereby conclude that embryonic and adult isBAT stem cells are distinct populations. Adult ASCs contribute to BAT adipogenesis to a limited extent.

Our data strongly suggests that adult stem cells of classical BAT are from *Pdgfra* lineage. The fact that ~95% mature adipocytes arise from GFP$^+$ cells shows that the majority of BAT adipocytes formed *in vitro* are from the *Pdgfra* lineage. Furthermore, because GFP$^+$ SVF cells from mature isBAT can survive, expand and be incorporated into adipose depots by transplantation, *Pdgfra* lineage cells in adult BAT are highly possible to contain an adipogenic stem cell population *in vivo*. Lastly, the FASCs sorting showing

only GFP$^+$/Sca1+ BAT SVF cells from adult animal are adipogenic thus indicates that the co-expression of *Pdgfra* and *Sca1* is a molecular characteristic of adult BAT precursors. The combination of these two markers can be useful for isolating adult BAT stem cell population. Thus we conclude that adult BAT stem cells are from *Pdgfra* lineage.

The regeneration and cold stimuli data reveals that adult isBAT stem cells do not necessarily contribute to BAT dynamic. In the 7 day cold challenge, less than 1% of the cells proliferated. The low proliferation rate means that cold environment does not greatly stimulate hyperplasia of any cell type in mature mouse isBAT cells, including BAT stem cells. The adult BAT stem cells are therefore not necessary for cold up-regulation of BAT function. This phenomenon is against previous studies showing dramatic increase of proliferating cells in cold treated rat isBAT(L. J. Bukowiecki, Geloen, & Collet, 1986). The inconsistency may be due to age or species differences. In the regeneration models, although the *Pdgfra* lineage cells containing potential isBAT stem cells proliferate dramatically during early stage (3-30 days), the percentage falls to default after 90 days. This means that the *Pdgfra* lineage population may exert function during regeneration, but do not dramatically contribute to new adipocyte formation in regenerated isBAT. This is similar to the case of muscle regeneration, where muscle injury increases the number of interstitial *Pdgfra*$^+$ expressing cells **(Fig. 35)**. The *Pdgfra*$^+$ cells disappear while regeneration is near completion **(Fig. 36)**. These *Pdgfra*$^+$ cells are adipogenic *in vitro* and believed to form IMAT *in vivo* (Uezumi, Fukada, Yamamoto, Takeda, & Tsuchida, 2010). They are needed for muscle regeneration but do not form

muscle cells. The function and activation condition of adult isBAT progenitors needs further exploration.

Apart from cold and injury, HFD and β3 Adr stimulation are other approaches to induce isBAT function and possibly progenitor proliferation *in vivo*, which was not included in this study. A more stringent lineage tracing using membrane targeted reporter with *Pdgfra* driven Cre recombinant would be ideal for verifying the contribution of *Pdgfra* lineage cells to isBAT. The *in vivo* adipogenic ability of isBAT *Pdgfra*$^{+}$ lineage cells to from functional adipocytes can be tested by sorting out and transplanting *Pdgfra*$^{+}$ cytoplasmic or membrane fluorescent BAT SVF cells into WTs. The study of classic BAT stem cells is still in its infancy.

3.1.5.2 BAT regenerative capacity

Our study shows that classic BAT possesses a certain extent of regenerative capability. Upon toxin treatment, isBAT structure is damaged and the ability to store lipids is attenuated. This is mainly due to the death of mature adipocytes. However, after 30 and 90 days of resting, isBAT weight is recovered and even overgrows for more than 2 fold through adipocyte hypertrophy. Lipid accumulation is increased in the regenerating adipocytes. This regeneration of isBAT is not a result of proliferation of adult progenitors but instead due to hypertrophy of adipocytes either from remaining mature cells or by de novo differentiation of preadipocytes. It is also possible that some *Pdgfra*- precursors proliferate and differentiate into mature adipocytes during regeneration to compensate for the loss of BAT. Although the weight and lipid content is

recovered, the regenerated BAT becomes “whiter” than before, losing its mutilocular morphology and shifting its gene expression pattern towards WAT. In conclusion, isBAT has the ability to regenerate in terms of weight, size and lipid content, but not function. Adult BAT stem cells within the *Pdgfra*$^{+}$ pool do not contribute to this process by participating adipogenesis. The contribution of adult BAT progenitors to BAT is still unclear.

3.2 Result 2: Skeletal muscle and skeletal muscle precursors are structurally associated with brown adipose tissue

3.2.1 Skeletal muscle and muscle precursors in brown adipose

Skeletal muscle and classic BAT are closely related. They originate from the *Myf5* lineage cells from the mesenchyme. White adipocytes, however, are derived from mostly non-*Myf5* lineage. This suggests a closer developmental relationship of BAT with muscle than with WAT (Timmons et al., 2007). An *In vitro* study has showed that loss of Prdm16 switches BAT cells to skeletal muscle and vice versa (Seale et al., 2008). A recent study argues that without genetic modification, a cell secretive factor-bone morphogenetic protein 6 induces C2C12 cells to differentiate into adipocyte-like cells and express BAT characteristic genes such as *Ucp1* and *Pgc1α* (Sharma et al., 2014). These lines of evidence lead us to examine if skeletal muscle and skeletal muscle precursors are involved in BAT structurally and functionally.

3.2.1.1 Existence of satellite cells in brown fat culture

Satellite cells are identified in isBAT SVF culture. Before differentiation, a population of round and bright cells is commonly found in BAT SVF which is usually constituted by spindle shaped and fibroblast-like cells **(Fig. 37A)**. These round-shape cells are enriched in the GFP-/Sca1+ population from BAT SVF sorting **(Fig. 14)**. After myogenic differentiation, tubular structures that are similar to mature myotubes, which occasionally twitch in the culture, are formed by these cells **(Fig. 37B white arrows)**. These serve as a strong piece of evidence supporting the presence of myogenic progenitors in BAT primary cell culture. Therefore, we conclude that satellite cells exist in BAT SVF.

3.2.1.2 Existence of skeletal muscle in and near the brown adipose

The existence of satellite cells in isBAT SVF prompts us to consider whether these myogenic cells are from skeletal muscle contamination in BAT or transformation of BAT SVF to muscle progenitor cells. By carefully sectioning adult and embryonic isBAT to examine for mature muscles in isBAT, we discovered a discrete piece of muscle imbedded in mature isBAT **(Fig. 38A)**. This means there are mature skeletal muscles in adult isBAT. We then sectioned embryonic BAT. As expected, premature muscles in between the lobes of embryonic BAT were identified **(Fig. 38B)**. This indicates that during development, muscle and BAT are structurally intertwined. In conclusion, skeletal muscles and BAT are structurally associated during developmental and mature stages.

3.2.2 Characteristics of muscle near brown adipose

3.2.2.1 Location of muscle in BAT

The location and characteristics of the muscle associated with BAT is important because it indicates whether the existence of skeletal muscle and satellite cells in BAT is random or not. We found in more than 15 animals that two pieces of skeletal muscles are connected to the posterior site of mature isBAT and are anatomically difficult to distinguish from isBAT and its associated WAT **(Fig. 39)**. It is evident that the existence of skeletal muscle in BAT is not a coincidence. The location of the skeletal muscle in isBAT makes it difficult to get clean cuts of BAT. Therefore, the satellite cells in isBAT culture are possibly a contamination of the connected muscle.

To see if skeletal muscle structurally overlaps with isBAT, 3D reconstruction based on 15 sequential sections obtained from an isBAT was performed by computation **(Fig. 40A)**. The sequential sections are manually aligned in 3D Max software. Muscle and isBAT are outlined and built into plane frameworks separately based on their histological appearance in the H&E sections. The plane frameworks are then connected along the Z axis and smoothened out **(Fig. 40B)**. After rendering, a large piece of skeletal muscle was shown to overlap with isBAT **(Fig. 41A, muscle in red and isBAT in blue)**. Another independent set of isBAT sequential sections were reconstructed in another way using Z-stack function in the Image Pro software **(Fig. 40C)**. Briefly, muscle in H&E sections is manually marked in red while the BAT part is colored orange (background is set to black). Automatic alignment was then done based on a common center point,

which is the center of each section. Comparison of 3D reconstruction by these two approaches shows similar location of muscle in BAT which is consistent with 3D Max reconstruction.

Based on the 3D reconstruction, the muscle in BAT appears to be an insertion of the nearby skeletal muscle **(Fig. 41)**. It is a large piece of thin muscle sandwiched by the two lobes of upper and lower isBAT, consistent with the previously identified muscles in tissue dissection **(Fig. 39)**. No discrete clumps of muscles in the isBAT were detected after sectioning more than 15 mice (10 from C57/B6 or 129, 1 from Albino and 4 from Agoti strain). This suggests that isBAT cells do not transform into muscle islets that are completely merged in isBAT. Muscles in BAT are inserted parts of the nearby muscles.

SeeDB tissue clarification method was employed to detect muscle in BAT on a fluorescent basis. $Myod^{cre/+}/Rosa^{iDTR/+}/Rosa^{td/+}$ triple heterozygous ($Myod^{cre/+}$) mice were created for this purpose **(Fig. 23B)**. The *Myod* gene encodes a member of myogenic regulatory protein family which is specifically expressed in mature myocytes and activated satellite cells. Cells from *Myod* lineage in the triple heterozygous mice express diphtheria toxin receptor and red fluorescent protein at the same time. Upon fat clarification, red fluorescent signal representing skeletal muscle can be observed under a microscope through the fat. Two large and symmetrical pieces of muscles are identified in the lateral side of SeeBD processed isBAT. This confirms that our localization of skeletal muscle in isBAT by disection and in 3D reconstruction is accurate, and muscles in BAT do not appear by chance **(Fig. 42)**. It is also clear that the direction of the myofibers in the inserted piece of muscle is along the posterior-anterior axis **(Fig.**

42) which indicates that the muscles overlapped with isBAT do not start or end in BAT. We observed no mature adipocytes expressing red fluorescent protein, and no separate clumps of muscles were detectable. The combined data indicates that muscle in BAT is a thin piece of skeletal muscle inserted from a nearby muscle.

3.2.2.2 Fiber type of muscle in BAT

Muscle in BAT has an intricate myofiber type. The inserted muscle mainly consists of typeIIA and typeIIB muscles, which are typical fast twitch muscles **(Fig. 43A)**. Muscles towards the lateral edge that overlap with but do not penetrate isBAT have mix fiber types including slow twitch typeI muscle and fast twitch TypeIIA and typeIIB muscles **(Fig. 43B)**. Whether this characteristic is affected by being located in or near the BAT is unknown.

3.2.3 Elimination of myogenic cells in brown adipose culture

Since there are skeletal muscles closely located to BAT, methods for isolating pure BAT becomes essential in studying BAT without muscle contamination. After understanding the location and lineage origin of muscle in BAT, separating out pure BAT SVF cells without myogenic cells becomes possible.

To culture “pure” BAT SVF, isBAT is anatomically divided into two parts -BAT with muscle and BAT without (w/o) muscle **(Fig. 44A)**. After culture and myogenic differentiation, no tubular mature myotubes (stained in red by Mf20) were found in the culture of BAT without muscle part **(Fig. 44B left and C left)**, whereas the culture of BAT with muscle part contained numerous mature myotubes **(Fig. 44B right and C right)**.

Gene expression examination shows significantly less myogenic signature genes such as *Myod* and *Myog* in the culture of BAT w/o muscle part **(Fig. 45A)** compared to the BAT with muscle part. In contrast, BAT related genes such as Ucp1, Pgc1a and adipose related genes such as *leptin*, *aP2* are significantly enriched **(Fig. 45 B-C)** ($p<0.01$, N=3). In fact, anatomically separating out isBAT w/o muscle parts readily eliminates the myogenic gene expression. Similarly, we observed that *Myod* and *Myog* expression was high in the BAT with muscle and whole BAT without separation, whereas BAT without muscle part had low expression of *Myod* and *Myog* comparable to EWAT **(Fig. 48)**. *Myf5* and *aP2* were not dramatically affected **(Fig. 47)**. These lines of evidence show that by anatomically separating out isBAT muscle, pure isBAT SVF culture can be obtained without muscle contamination efficiently.

An alternative way to obtain pure BAT SVF is by lineage depletion in culture. Whole isBAT SVF from $Myod^{cre/+}$ mice was cultured and treated with DT 2 days before differentiation. Upon myogenic differentiation, no myotubes formed in the treatment group while the control group showed many mature myotubes from the *Myod* lineage in red **(Fig. 48)**. Lineage depletion of myogenic cells is an effective way to obtain pure BAT SVF culture without muscle contamination.

3.2.4 Conclusion and discussion

In addition to a close relationship in lineage origin, skeletal muscle and classic BAT are structurally associated. During the developmental and adult stage, isBAT resides near skeletal muscles, but does not have the ability to switch to skeletal muscles. We

identified myogenic stem cells in BAT SVF, located the skeletal muscle in adult isBAT, and discovered that muscle inserted in BAT has characteristics of fast twitch fiber types. Finally, we developed approaches to obtain pure BAT SVF culture by eliminating myogenic cell population.

Given the close anatomical location of BAT and skeletal muscle, the myogenic signature gene in BAT cells may be a result of contamination from nearby muscles. In 2007, Timmons and colleagues discovered myogenic genes in cultured primary BAT SVF such as *Myf5*, *Myod* and *Myog* (Timmons et al., 2007), as confirmed by micro array. These genes are up-regulated in BAT SVF compared to WAT SVF during the first 4 days of culture, and disappeared afterwards. Timmons group propose SIRT1 as the upstream regulator of *Myod*, which inhibits myogenic gene expression in the culture later on. The authors tried to exclude the possibility of skeletal muscle cell contamination by immunohistological staining *Myf5* in primary SVF samples, and compared to samples artificially contaminated with myoblasts. The staining pattern was not convincing, and no other procedures were taken to prevent muscular contamination. Therefore we suspect that skeletal muscle may affect be the BAT SVF gene profile in this study. This is supported by a recent research showing that mature BAT and BAT SVF do not contain *Myod* lineage cells by *in vitro* lineage tracing and mRNA profiling (Sanchez-Gurmaches & Guertin, 2014). We hereby emphasize the importance of obtaining pure BAT tissue or cells without muscle contamination in studying muscle-BAT origin and potential interactions.

We also suspect that muscle-BAT switch by artificial modification of Prdm16 expression may be partially due to skeletal muscle contaminant. Patrick Seale and colleagues found that knocking down Prdm16 by shRNA promotes primary BAT SVF to undergo myogenic differentiation (Seale et al., 2008). There is a possibility that Prdm16 does not directly mediate an inter-conversion of BAT cells to muscle cells, but inhibits adipogenic differentiation BAT preadipocytes and promotes myogenic differentiation of satellite cells that co-exist in culture. Because myogenesis inhibits adipogenesis, this further inhibits primary BAT SVF adipogenic differentiation, resulting in an illusion of a "switch" of fat cells to muscle cells. This notion is supported by an *in vivo* lineage depletion study showing no conversion of classic BAT depot to muscle in mice with Prdm16 knockout in mature adipoctyes (Cohen et al., 2014). But it is still worth noting that *Myod* and *Igf2* double mutant mice have increased Prdm16 expression with a dramatic hypertrophy of BAT depot (Borensztein et al., 2012), suggesting a positive effect of Prdm16 on BAT adipogenesis. Therefore, the conversion of primary BAT cells to skeletal muscles may be questionable if muscle contaminant in BAT SVF is not eliminated.

BAT may also in turn affect muscle. This is partially reflected by a preferred fast twitch fiber type in the deeply inserted muscle in isBAT compared to the parts simply overlap with BAT. Possible explanations of this fiber type characteristic are: 1. BAT influences nearby muscle function by direct contact, signaling, or adipokine secretion. Since the inserted part of muscle is relatively thin and small, it is very likely that the surrounding BAT adipocytes influence the piece muscle by signaling or secretive factors,

finally changing muscle characteristics like fiber types. However, whether this occurs and the possible mechanism is not known. 2. Fast twitch skeletal muscle is developed on purpose to somehow support BAT function. Fast muscle may play a role in rapid cold responses such as shivering, which may activate and induce BAT function. BAT depots are anatomically located in “sockets” surrounded by skeletal muscles (isBAT as an example), or deeply embedded in the joint of several muscles (cBAT as an example). This provides an ideal condition for skeletal muscle secretive factors and signaling molecules to reach BAT. It is already known that skeletal muscles promote Ucp1 expression and induces beige fat formation in WAT through up-regulation of irisin (Bostrom et al., 2012). Local action of myokines like irisin may be needed for BAT development and function. 3. The muscle in BAT is developed from a specially arranged progenitor population which is anatomically distinct from other muscles. This is less likely since the lateral parts of the muscle in BAT have mixed fiber types. The reason why fast twitch fiber type is more desired in BAT is not known. Whether it is a result of BAT effect or a need for specific actions only offered by fast muscle is not clear. In conclusion, a potential crosstalk exists between skeletal muscle and classic BAT.

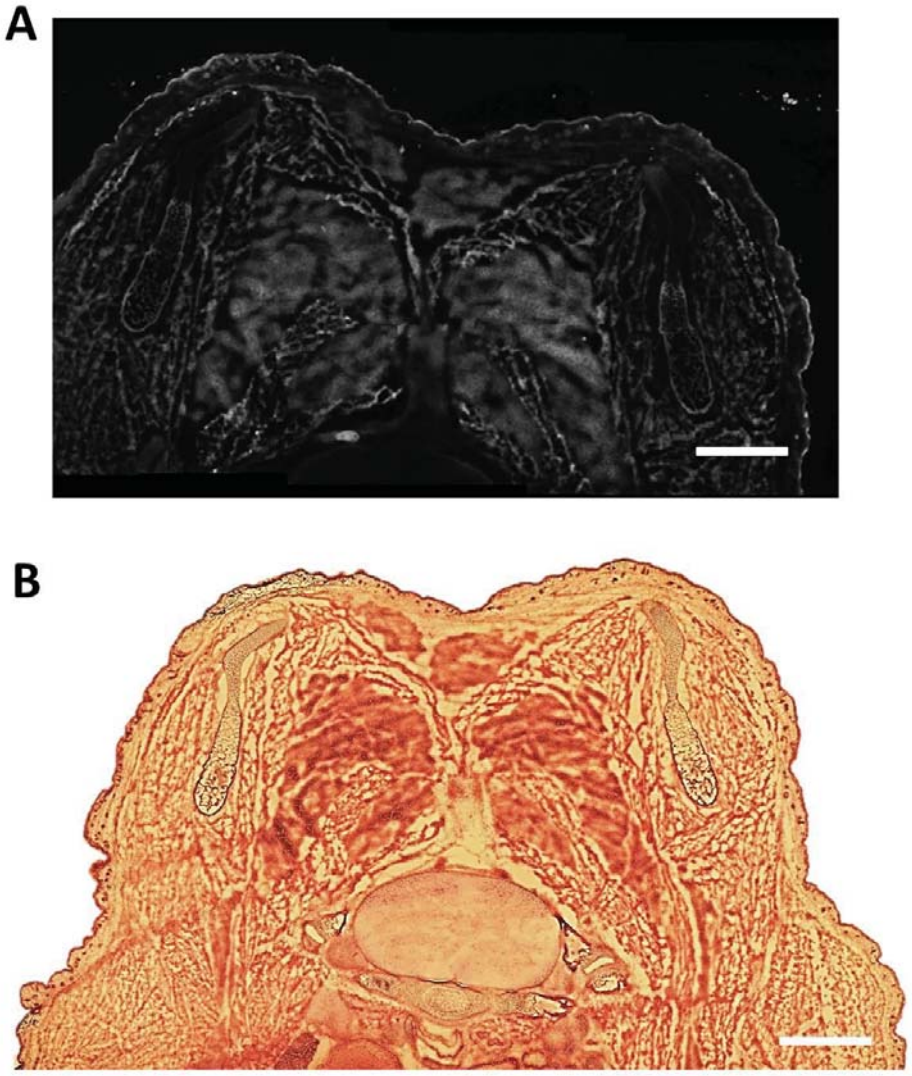

Figure 1: isBAT morphology at P1

(A) Fluorescent picture of Myf5$^{cre/+}$/Rosa$^{eYFP/+}$ mouse isBAT region at P1. (B) H&E section of mouse isBAT region at P1. Scale bar 100µm.

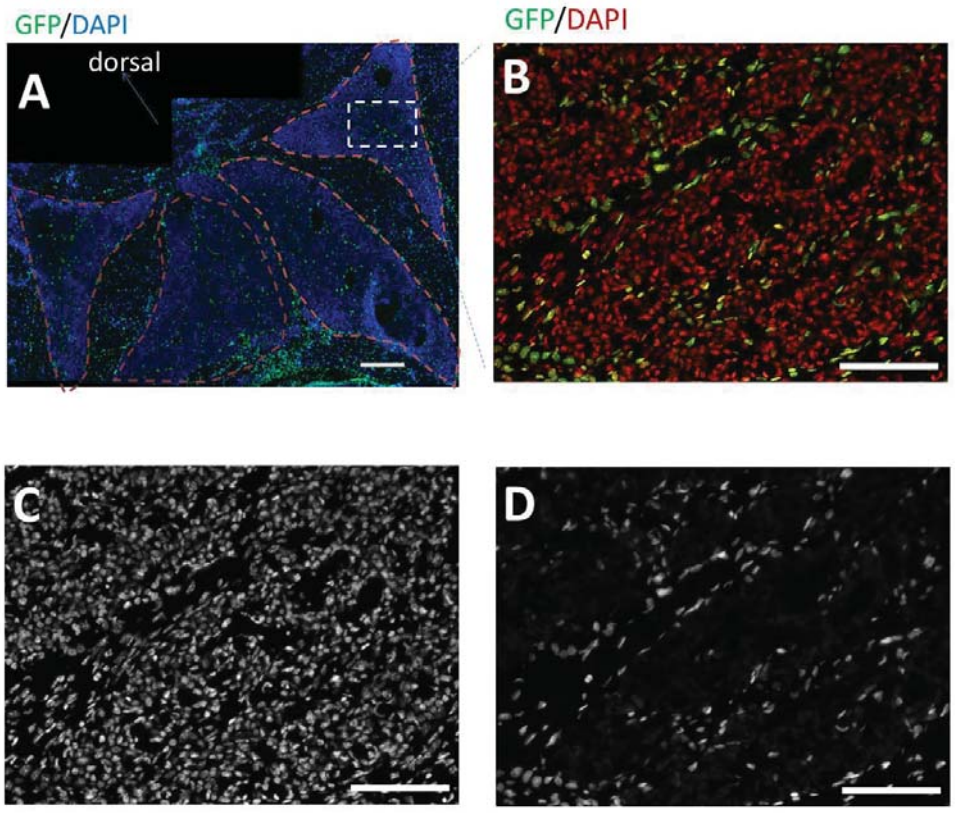

Figure 2: GFP^{+} cells in isBAT of Pdgfra$^{GFP/+}$ mouse at E17.5

(A) Picture of isBAT at P1. White box shows a sample enlarged region. Scale bar 100µm. (B) isBAT at E17.5 with merged colors. Scale bar 10µm. (C) DAPI staining of nucleus. Scale bar 10µm. (D) GFP^{+} cells. Scale bar 10µm.

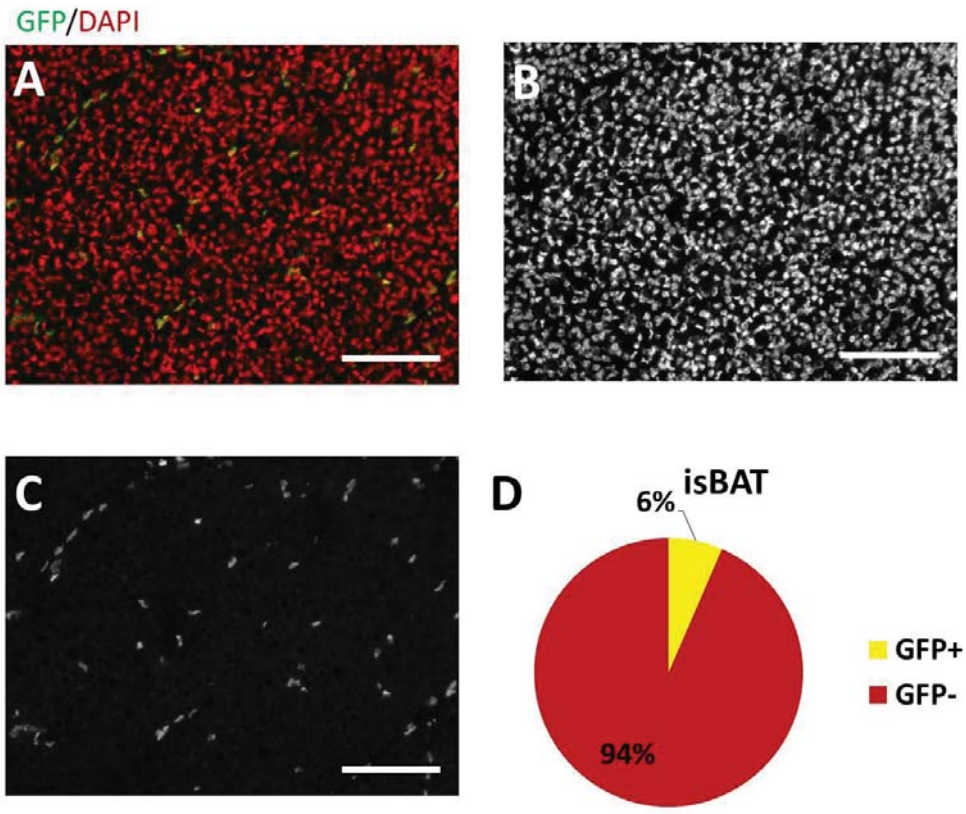

Figure 3: GFP^{+} cell in isBAT of Pdgfra$^{GFP/+}$ mouse at P1

(A) isBAT at P1 with merged colors. Scale bar 10µm. (B) DAPI staining of nucleus. Scale bar 10µm. (C) GFP^{+} cells. Scale bar 10µm. (D) Quantification by pie chart. N=3.

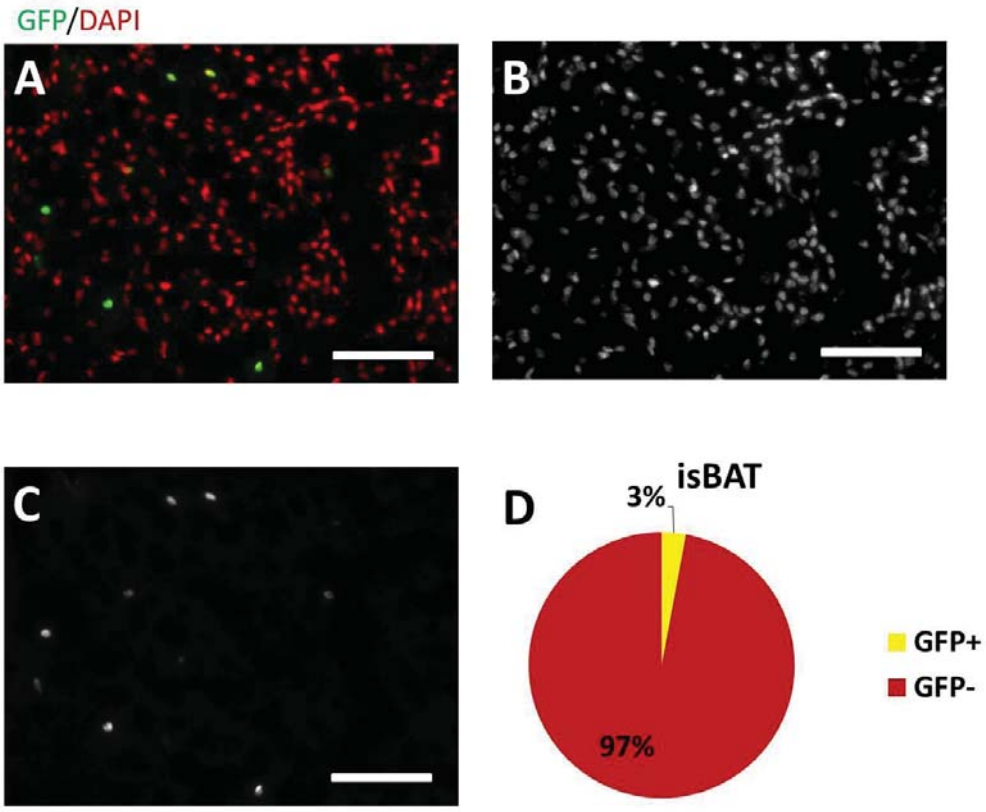

Figure 4: GFP^{+} cell in 2-month-old (mature) isBAT of Pdgfra$^{GFP/+}$ mouse

(A) Mature isBAT with merged colors. Scale bar 10μm. (B) DAPI staining of nucleus, scale bar 10μm. (C) GFP+ cells. Scale bar 10μm. (D) Quantification by pie chart. N=3.

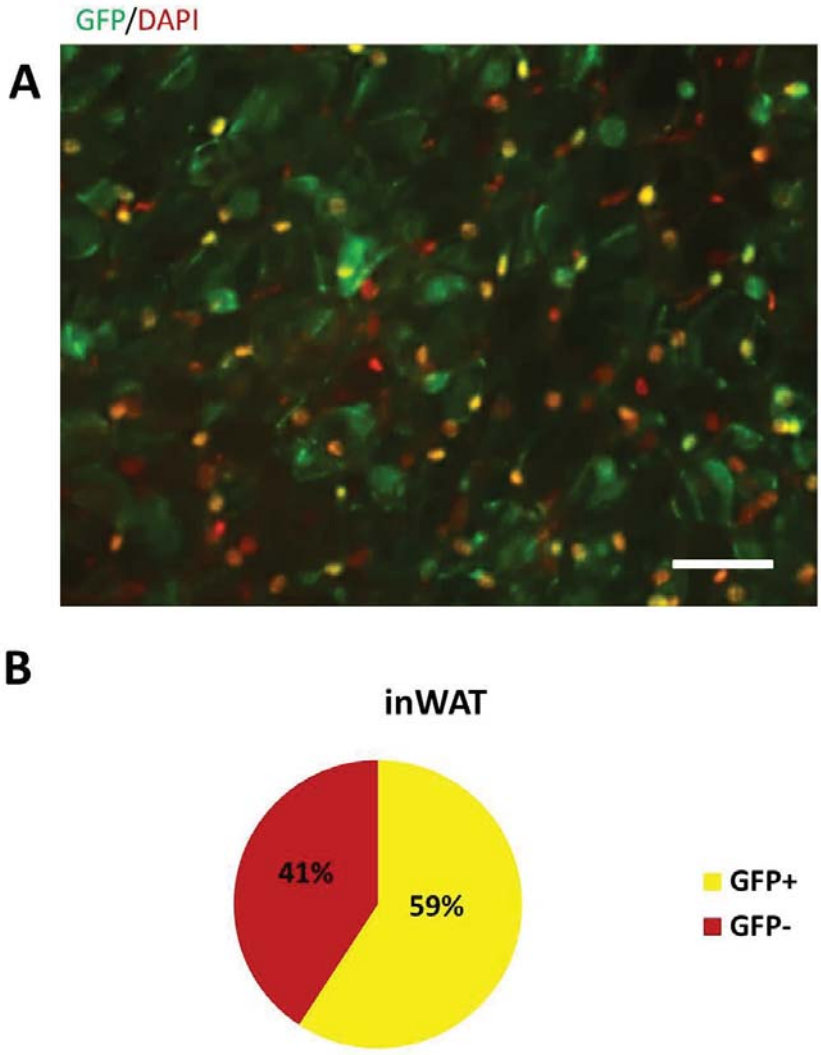

Figure 5: GFP^{+} cell in mature inWAT of Pdgfra$^{GFP/+}$ mouse

(A) Whole mount picture of inWAT. Scale bar 10µm. (B) Quantification by pie chart. N=3.

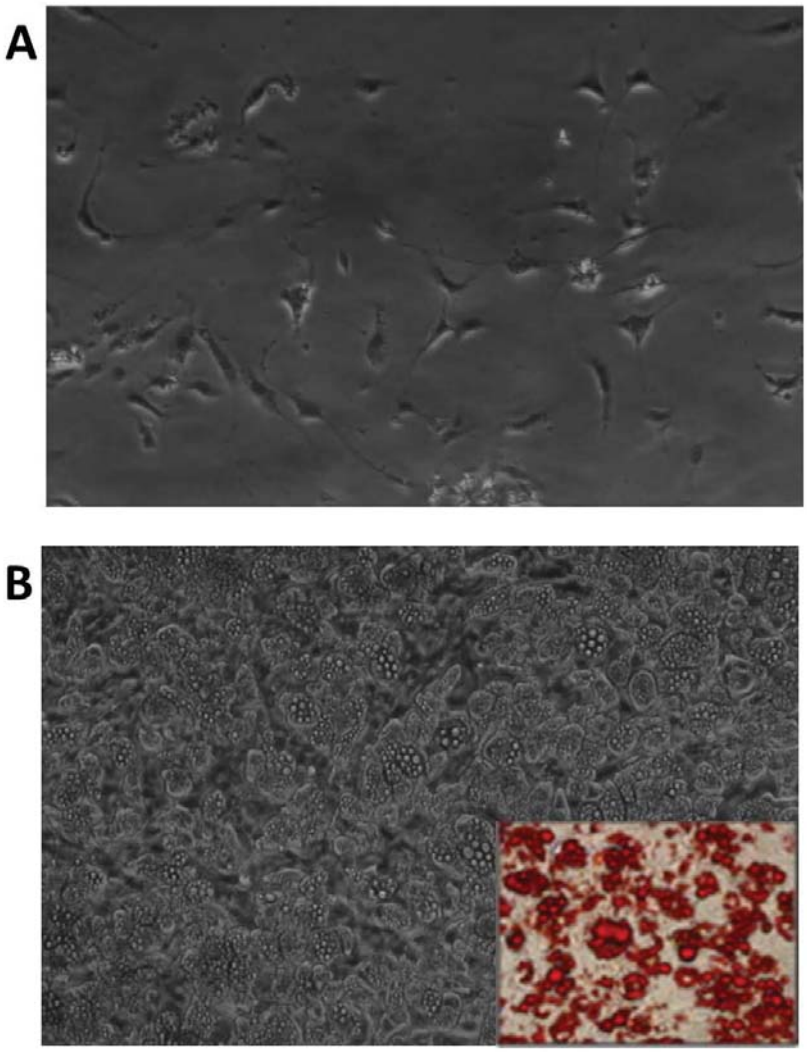

Figure 6: Isolation and differentiation of isBAT SVF

(A) Isolation of isBAT SVF on D2. (B) Differentiation of isBAT on D4. Boxed region shows mature SVF adipocyte Oil-Red-O staining.

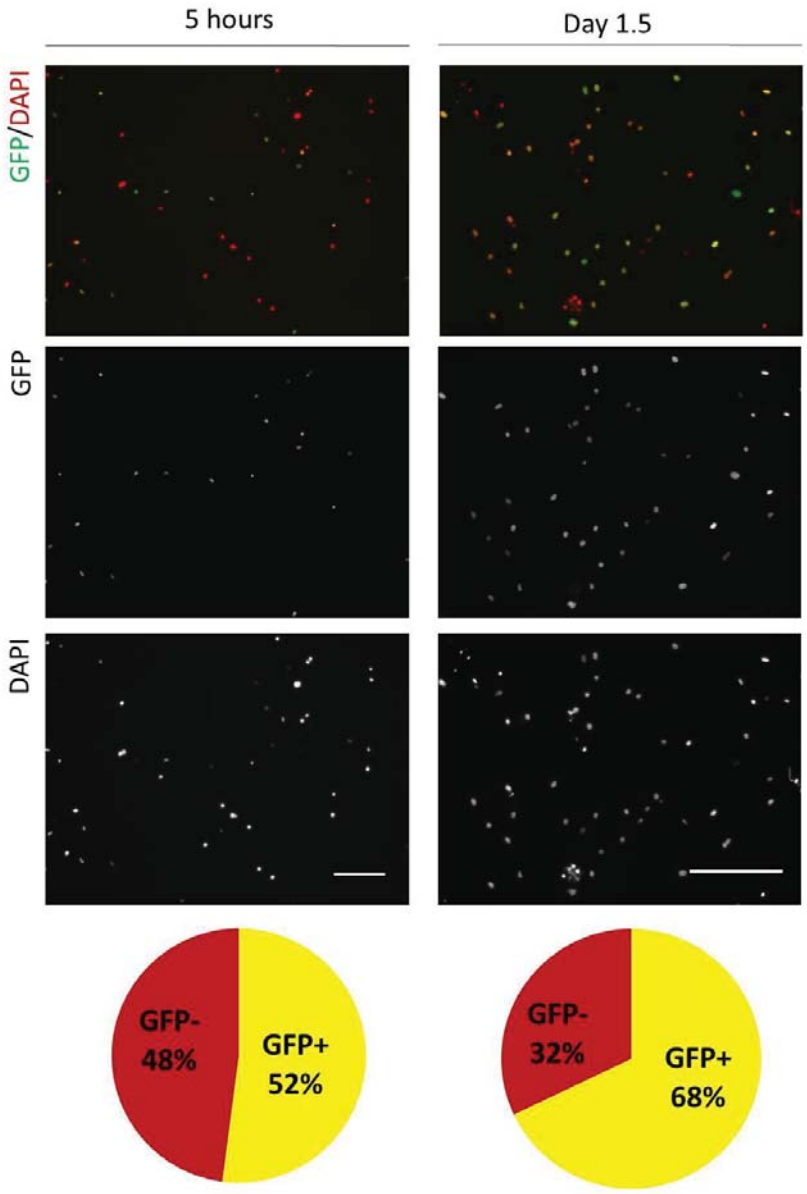

Figure 7: GFP^{+} cells in Pdgfra$^{GFP/+}$ mouse isBAT SVF culture at 5h and D1.5

Left panel shows 5h pictures and quantification; right panel shows D1.5 pictures and quantification. Scale bar 10µm, N=3.

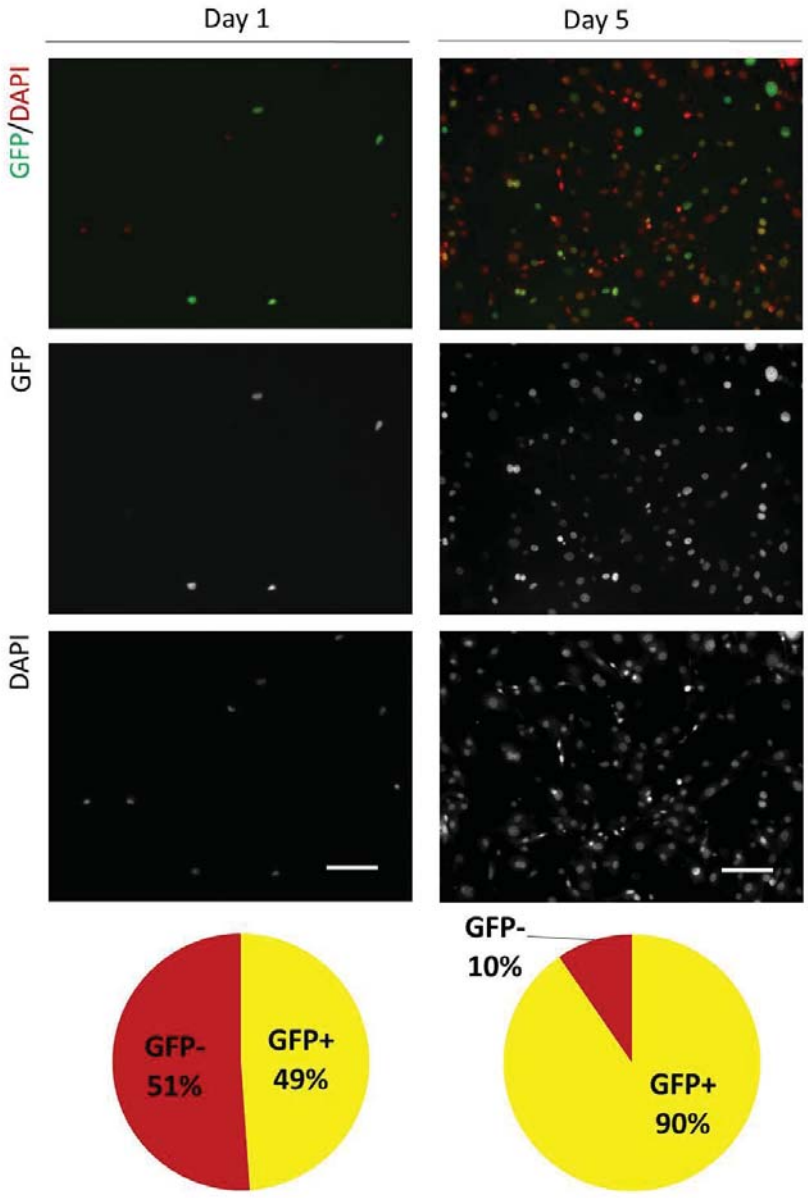

Figure 8: GFP^{+} cells in Pdgfra$^{GFP/+}$ mouse isBAT SVF culture at D1 and D5

Left panel shows D1 pictures and quantification; right panel shows D5 pictures and quantification. Scale bar 10µm, N=3.

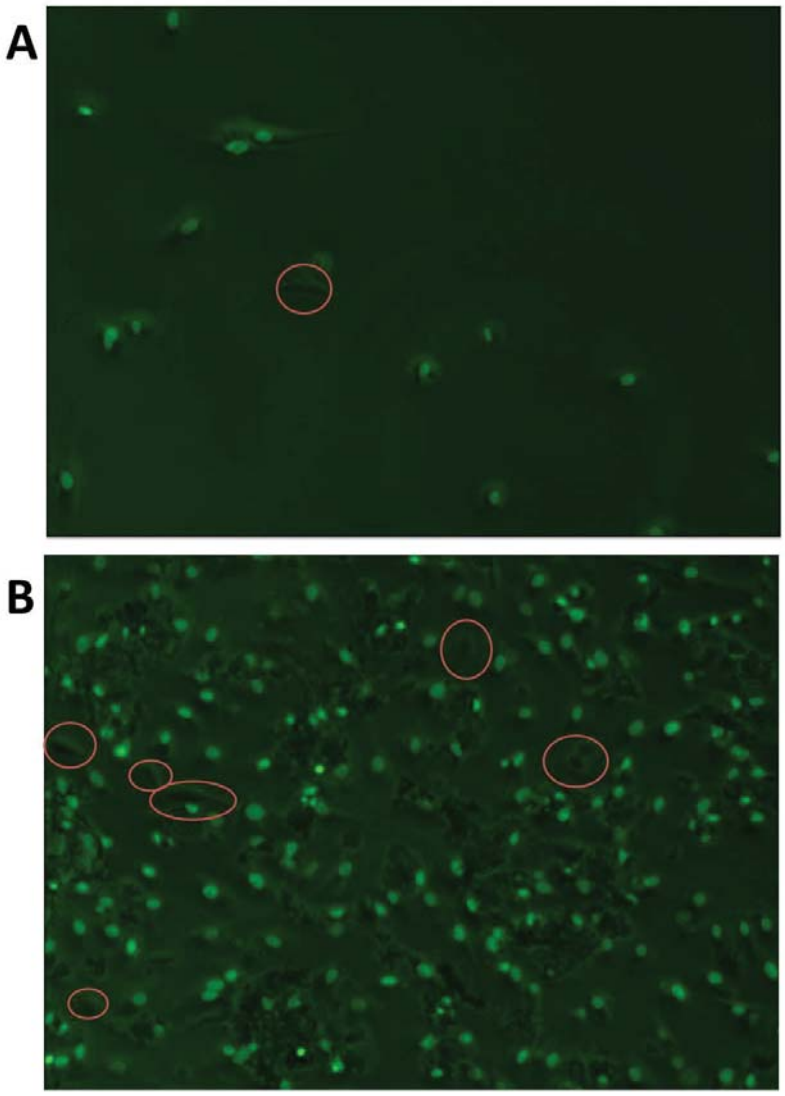

Figure 9: GFP^{+} cells in isBAT and iWAT SVF culture of Pdgfra$^{GFP/+}$ mouse

(A) isBAT culture, the circle indicates a GFP^{+} cell. (B) iWAT culture, the circles indicate GFP^{+} cells.

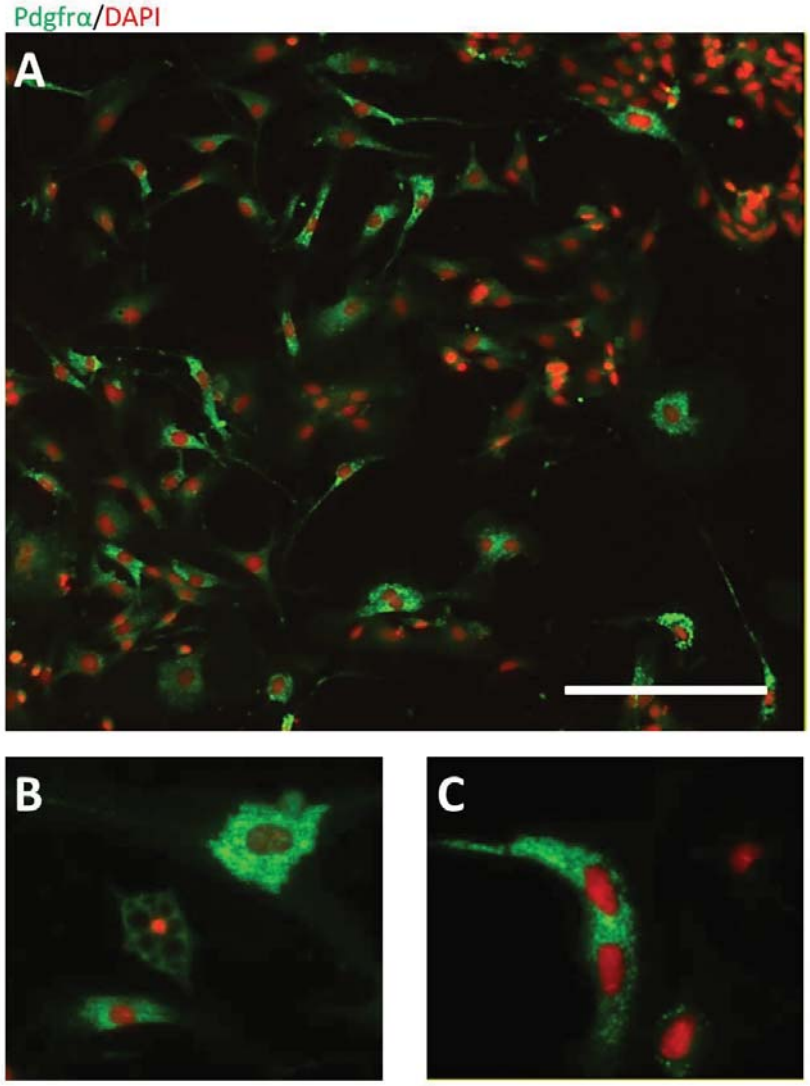

Figure 10: Pdgfrα staining of isBAT SVF culture on D3

(A)Picture of Pdgfrα staining, scale bar 10µm. (B) Pdgfrα is stained in mature adipocytes and undifferentiated preadipocytes. (C) Pdgfrα is stained in dividing cells.

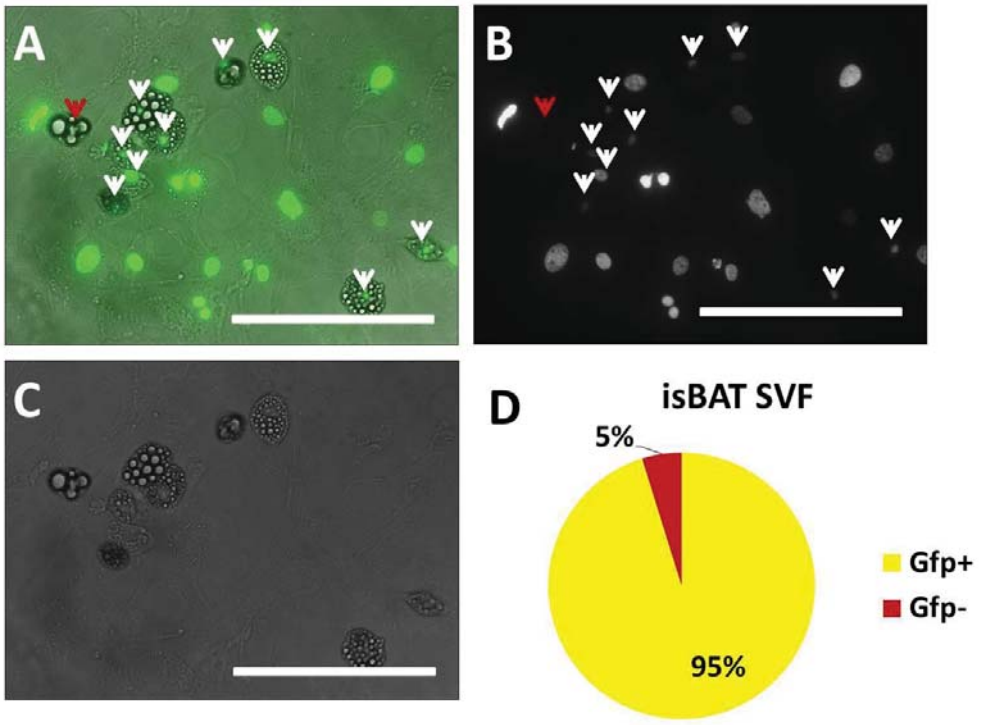

Figure 11: GFP^{+} cells in spontaneous differentiated isBAT SVF of Pdgfra$^{GFP/+}$ mouse

(A) Merged picture, white arrows indicate GFP^{+} mature adipocytes, red arrow indicates a GFP- mature adipocyte. Scale bar 10µm. (B) Green fluorescent channel. Scale bar 10µm. (C) Phase contrast channel. Scale bar 10µm. (D) Quantification by pie chart, N=2.

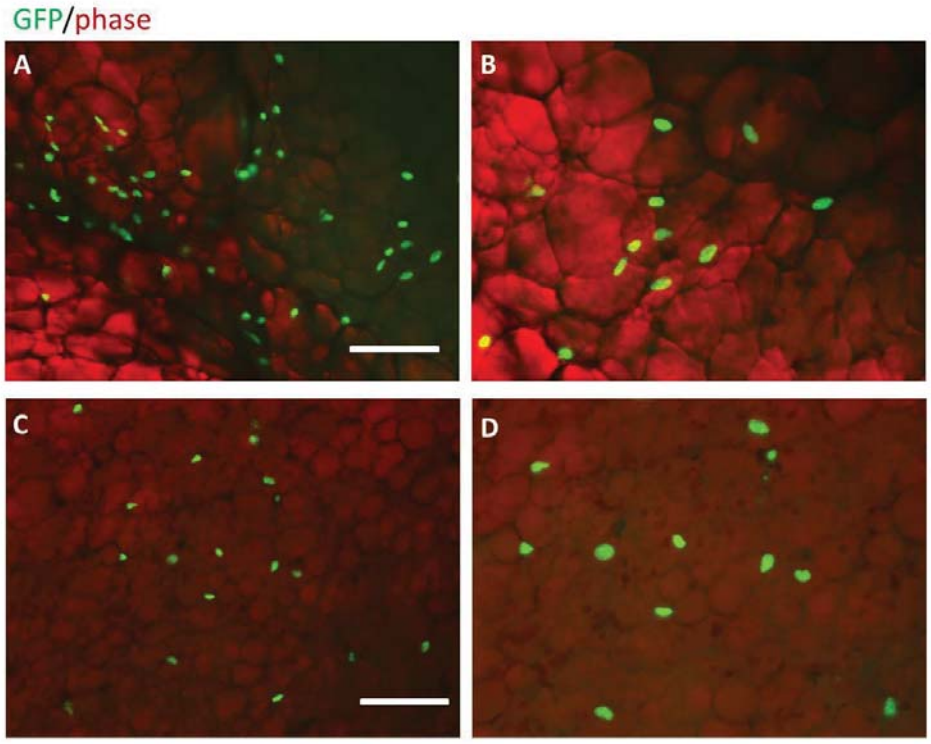

Figure 12: GFP$^+$ isBAT SVF cell transplantation in isBAT and asWAT of WT individual on D21 after transplantation

(A) Transplantation in asWAT, scale bar 10µm. (B) Enlarged asWAT picture. (C) Transplantation in BAT, scale bar 10µm. (D) Enlarged isBAT picture.

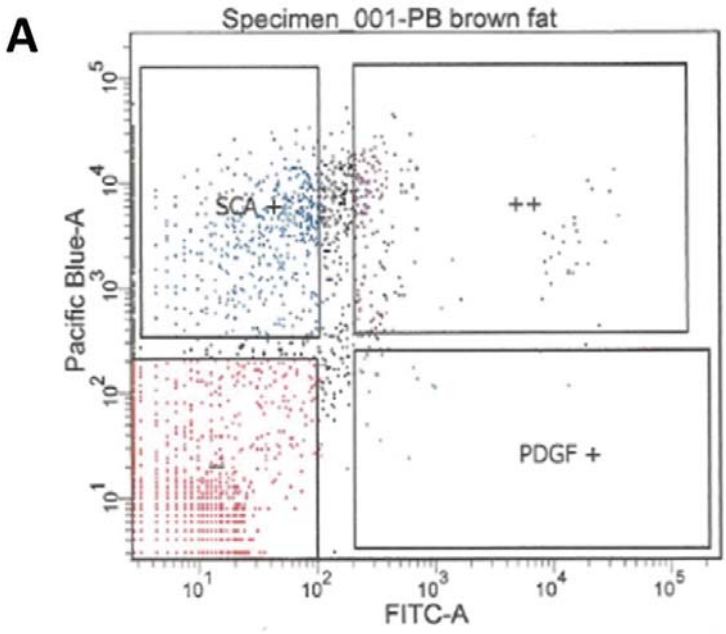

B Tube: PB brown fat

Population	#Events	%Parent	%Total
All Events	10,000	####	100.0
Scatter Gate	9,976	99.8	99.8
SSC Gate	9,851	98.7	98.5
FSC Gate	9,795	99.4	98.0
SCA +	482	4.9	4.8
++	178	1.8	1.8
--	8,568	87.5	85.7
PDGF +	17	0.2	0.2

Figure 13: FACS of isBAT SVF

(A) Subpopulations of isBAT SVF. (B) Sorted isBAT SVF subpopulation percentages.

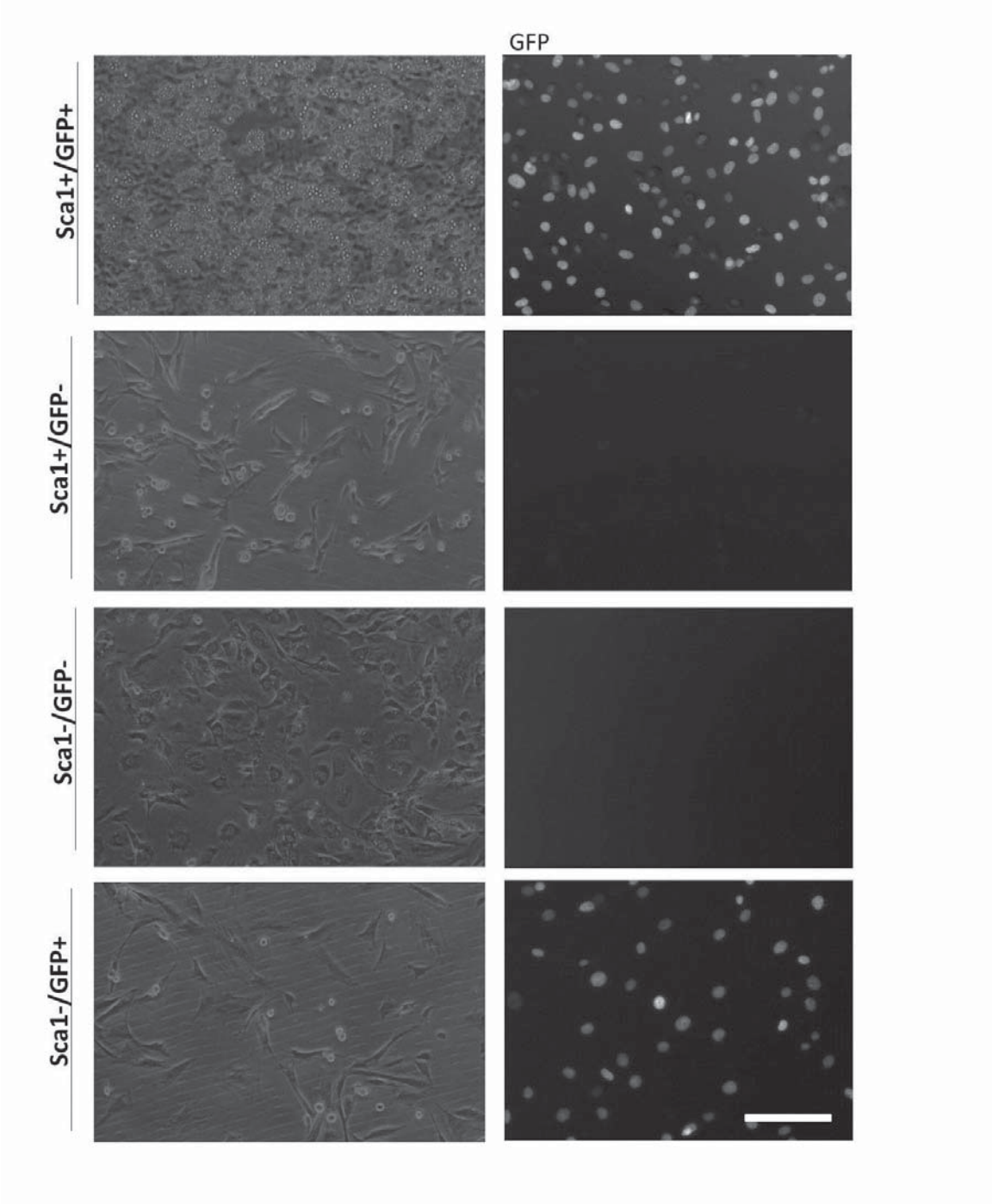

Figure 14: Culture of isBAT SVF subpopulations

Left panel shows phase contrast picture, right panel shows GFP signals taken 2 days later.

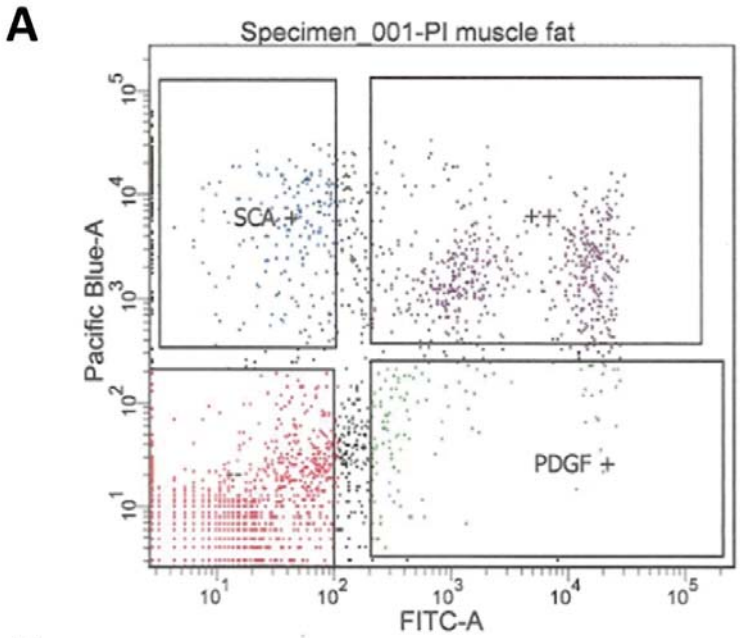

B

Tube: PI muscle fat

Population	#Events	%Parent	%Total
All Events	10,000	####	100.0
Scatter Gate	9,832	98.3	98.3
SSC Gate	9,512	96.7	95.1
FSC Gate	9,348	98.3	93.5
SCA +	203	2.2	2.0
++	570	6.1	5.7
--	6,061	64.8	60.6
PDGF +	125	1.3	1.2

Figure 15: FACS of IMAT SVF

(A) Subpopulations of IMAT SVF. (B) Sorted IMAT SVF subpopulation percentages.

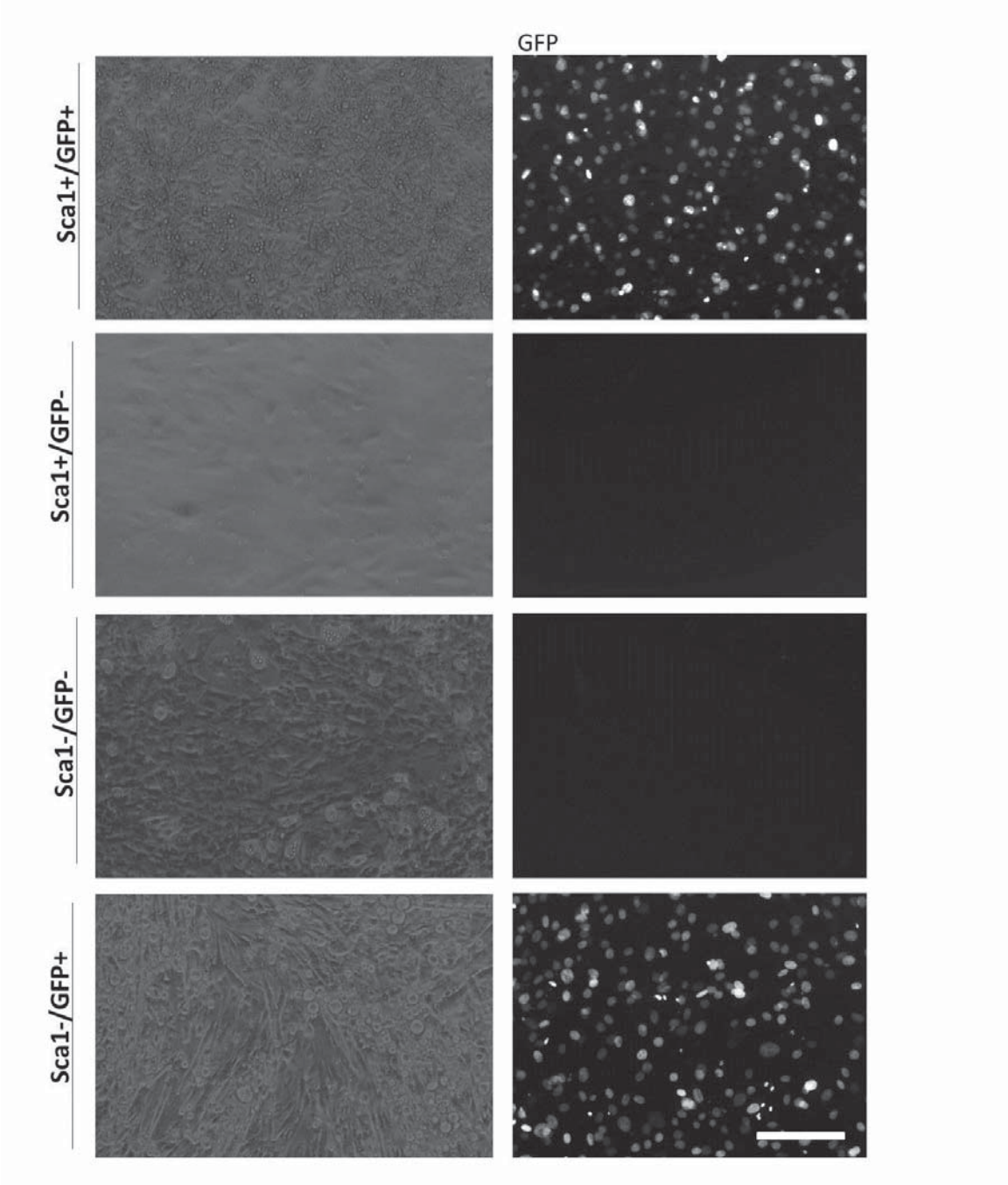

Figure 16: Culture of iMAT SVF subpopulations

Left panel shows phase contrast picture, right panel shows GFP signals taken 2 days later.

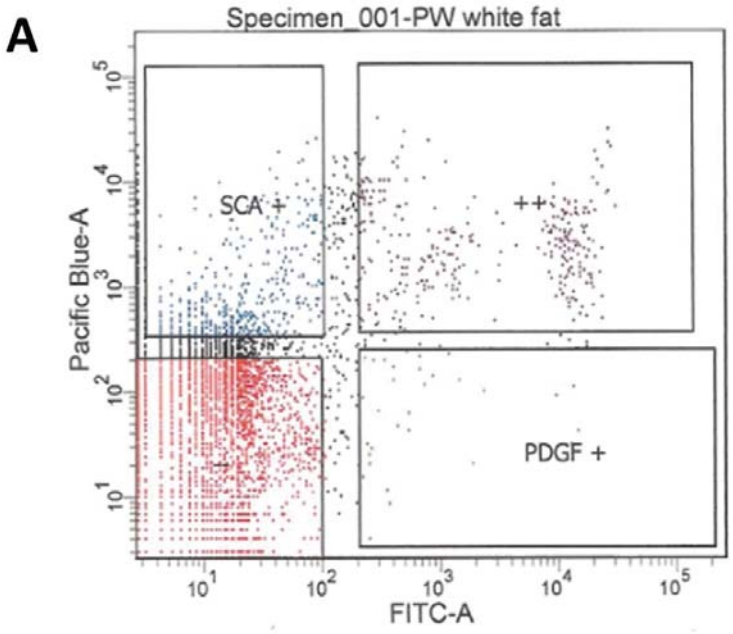

B

Tube: PW white fat

Population	#Events	%Parent	%Total
All Events	10,000	####	100.0
Scatter Gate	9,916	99.2	99.2
SSC Gate	9,287	93.7	92.9
FSC Gate	9,229	99.4	92.3
SCA +	477	5.2	4.8
++	307	3.3	3.1
--	7,122	77.2	71.2
PDGF +	32	0.3	0.3

Figure 17: FACS of iWAT SVF

(A) Subpopulations of iWAT SVF. (B) Sorted iWAT SVF subpopulation percentages.

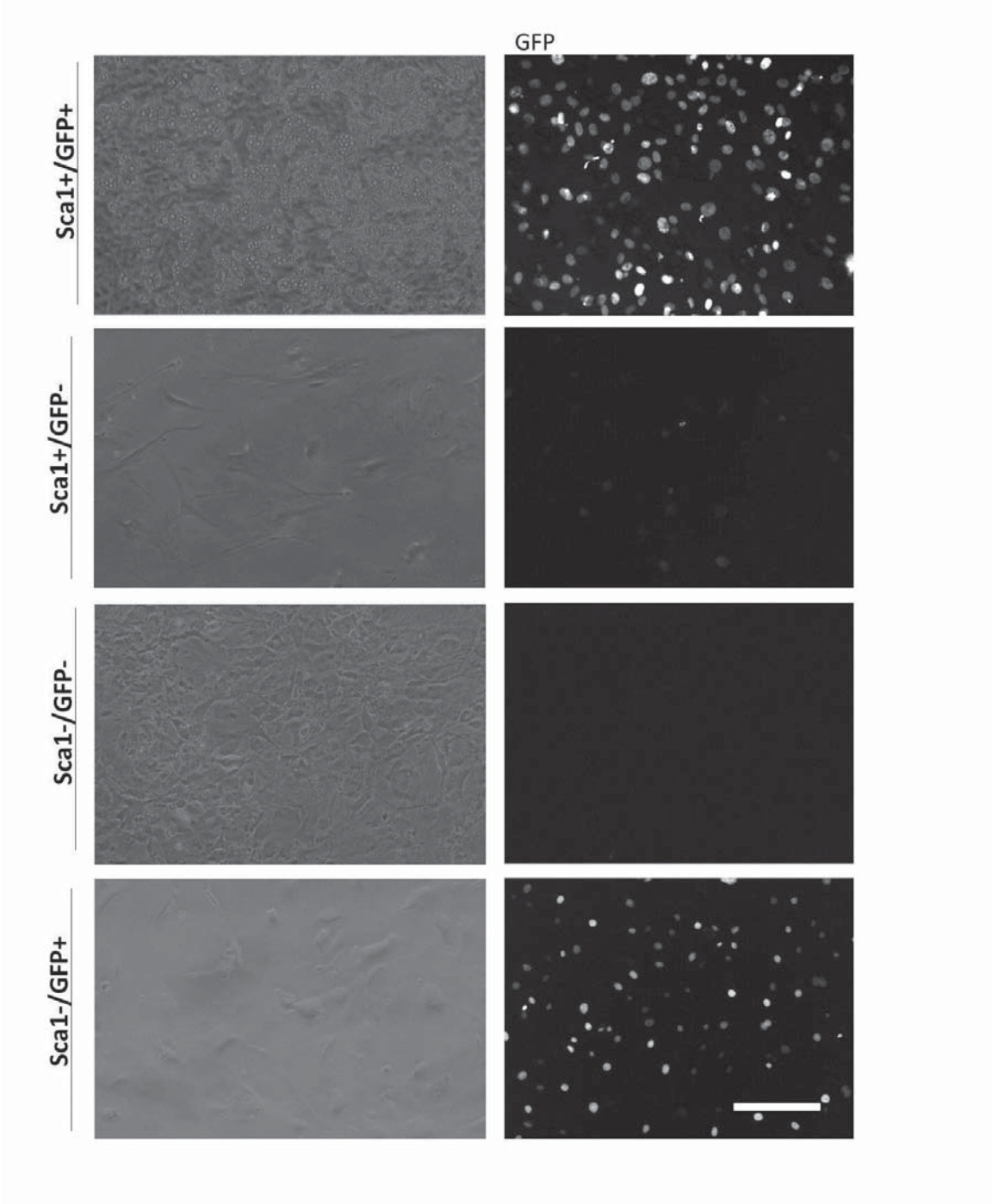

Figure 18: Culture of iWAT SVF subpopulations

Left panel shows phase contrast picture, right panel shows GFP signals taken 2 days later.

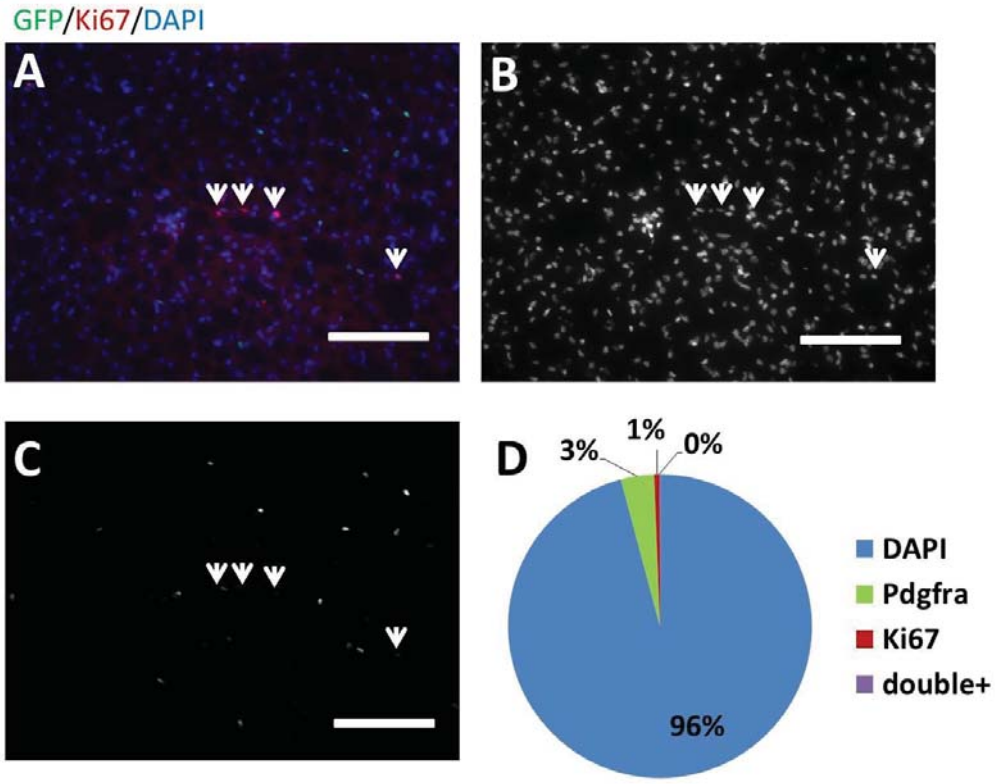

Figure 19: Majority of GFP^{+} cells are Ki67- in isBAT of Pdgfra$^{GFP/+}$ mouse on D7 after cold treatment

(A) Merged picture, scale bar 10µm. (B) DAPI staining of nucleus, scale bar 10µm. (C) GFP^{+} cells, scale bar 10µm. (D) Quantification by pie chart, N=3.

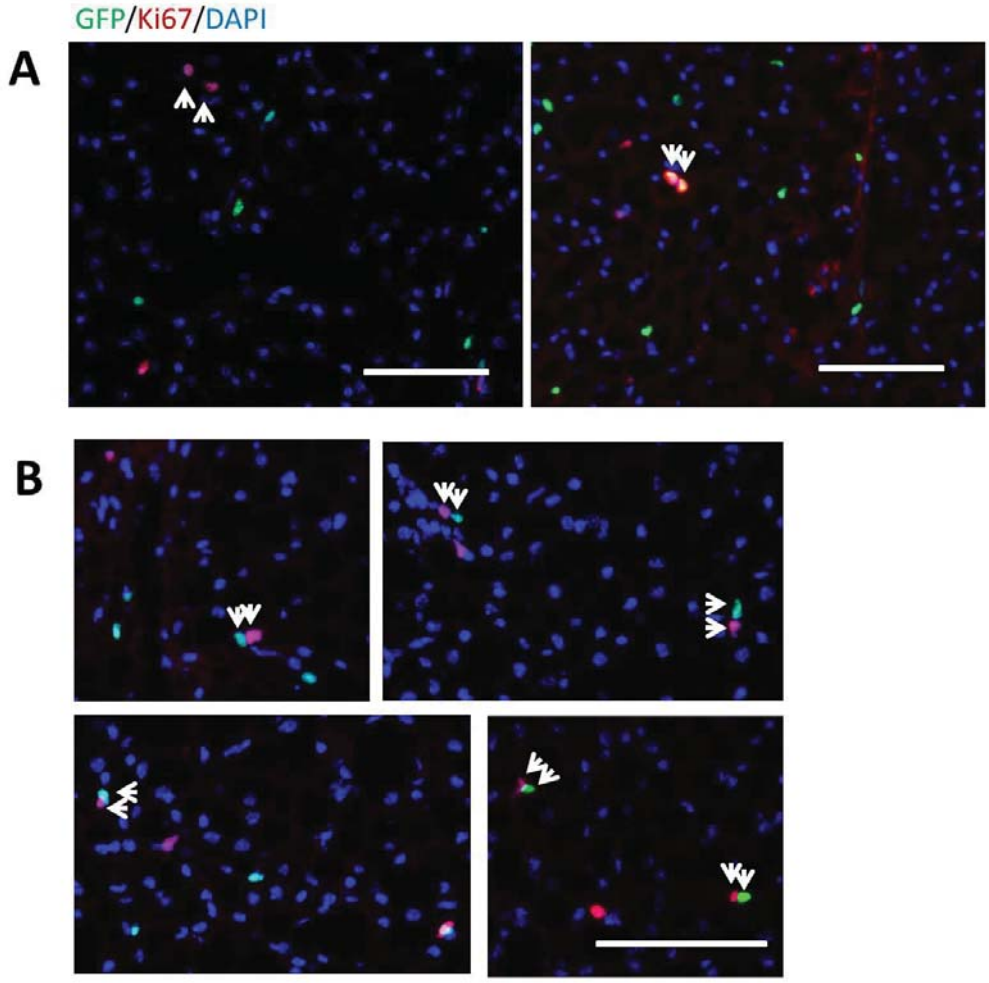

Figure 20: Small population of GFP$^+$ cells are Ki67+ or near Ki67+ cells

(A) Few GFP$^+$ cells are proliferating. Arrows indicate co-localization. Scale bar 10µm. (B) Some GFP$^+$ cells are near Ki67+ population. Arrows indicate closely localized cells. Scale bar 10µm.

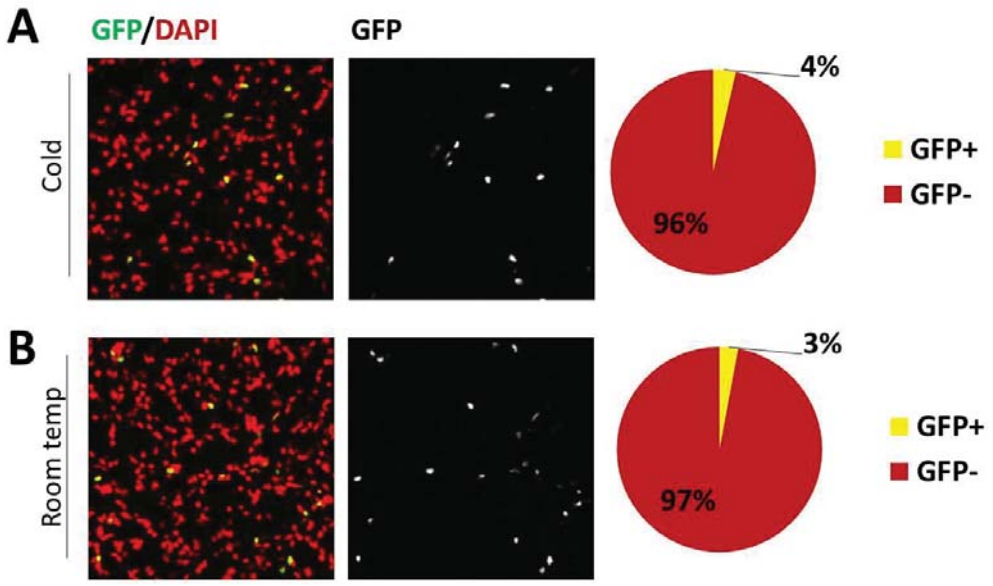

Figure 21: GFP+ cells in isBAT of PdgfraGFP mouse on D7 in cold

(A) Picture and quantification of GFP+ cells in isBAT in cold. (A) Picture and quantification of GFP+ cells in isBAT at room temperature. N=3.

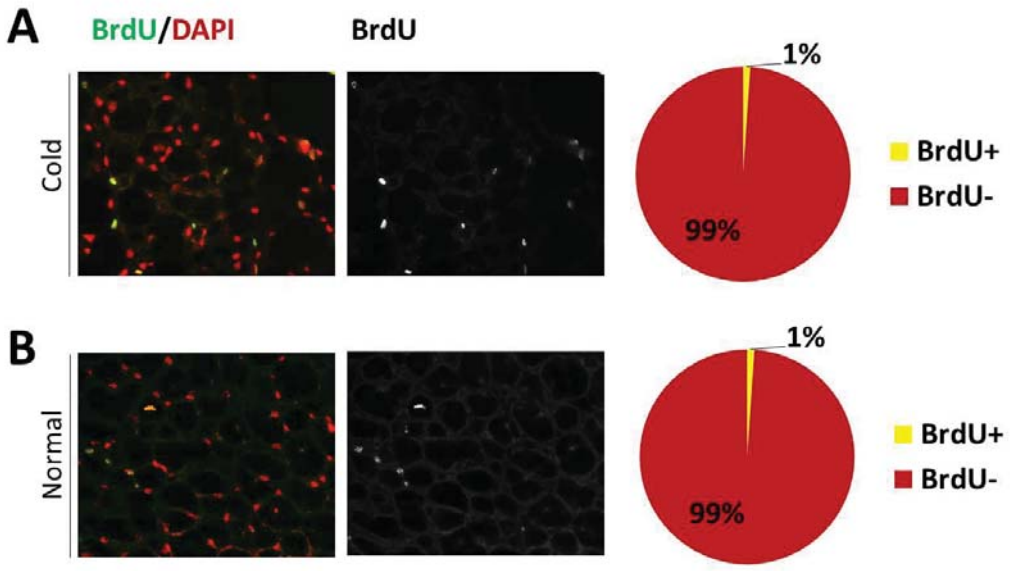

Figure 22: BrdU+ cells in isBAT on D7 in cold

(A) Picture and quantification of BrdU+ cells in isBAT in cold. (A) Picture and quantification of BrdU+ cells in isBAT at room temperature. N=3.

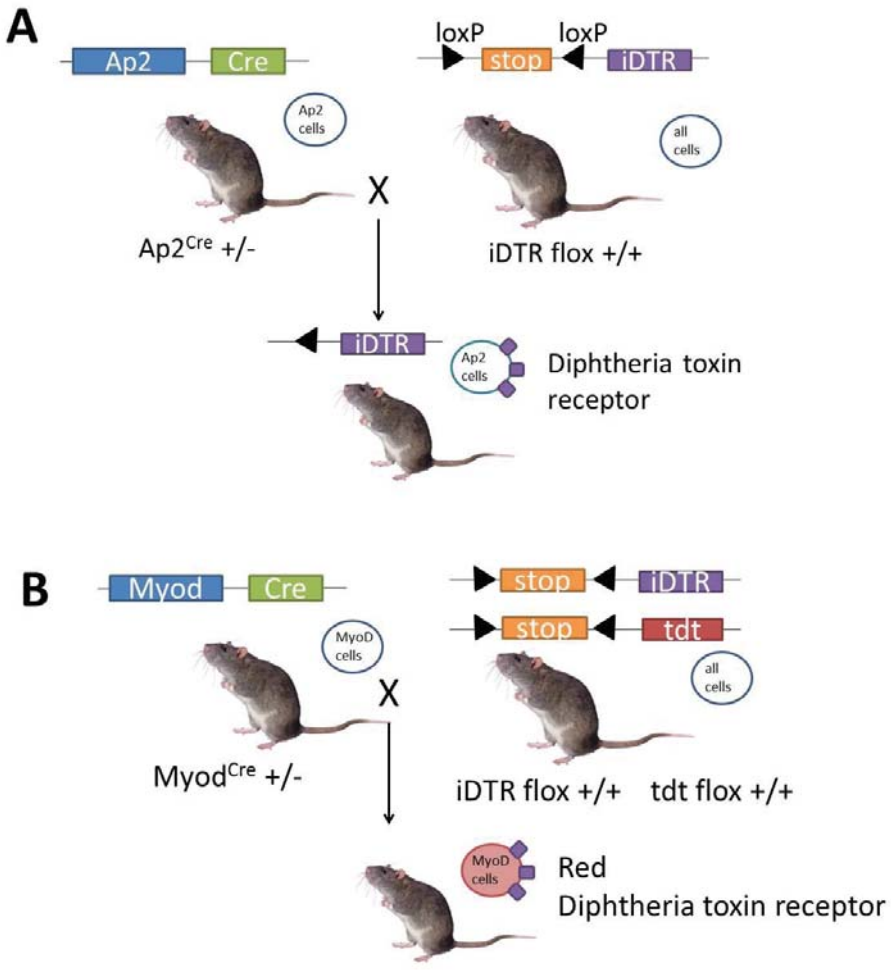

Figure 23: Strategy of mouse breeding

(A) Breeding strategy of aP2-cre^{+}/Rosa$^{iDTR/+}$ (aP2-Cre^{+}) mice. Rosa$^{iDTR/+}$ (aP2-Cre) littermates are controls. (B) Breeding strategy of Myod$^{cre/+}$/Rosa$^{iDTR/+}$/Rosa$^{td/+}$ (Myod$^{cre/+}$) mice. Rosa$^{iDTR/+}$/Rosa$^{td/+}$ (Myod$^{+/+}$) littermates are controls.

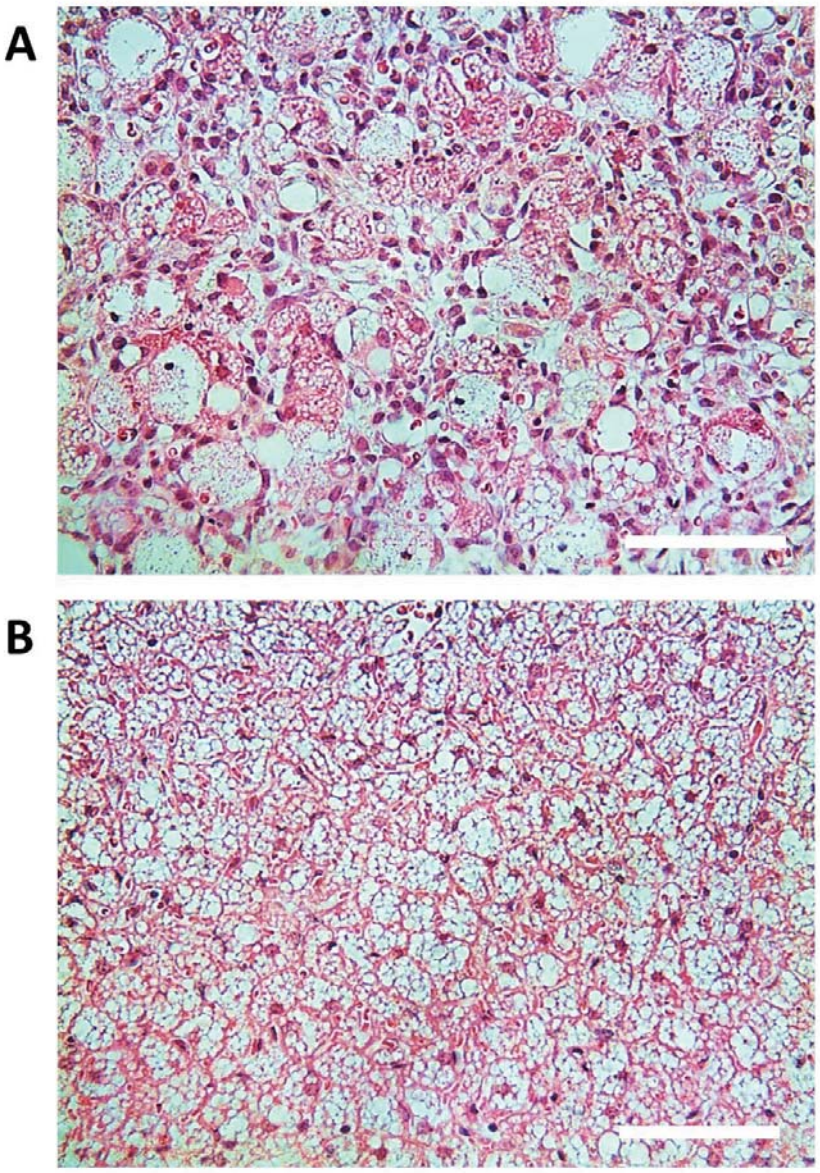

Figure 24: H&E sections of DT treated isBAT on D3 after injection

(A) aP2-cre^{+} mouse isBAT. Scale bar 10µm. (B) aP2-Cre mouse isBAT. Scale bar 10µm.

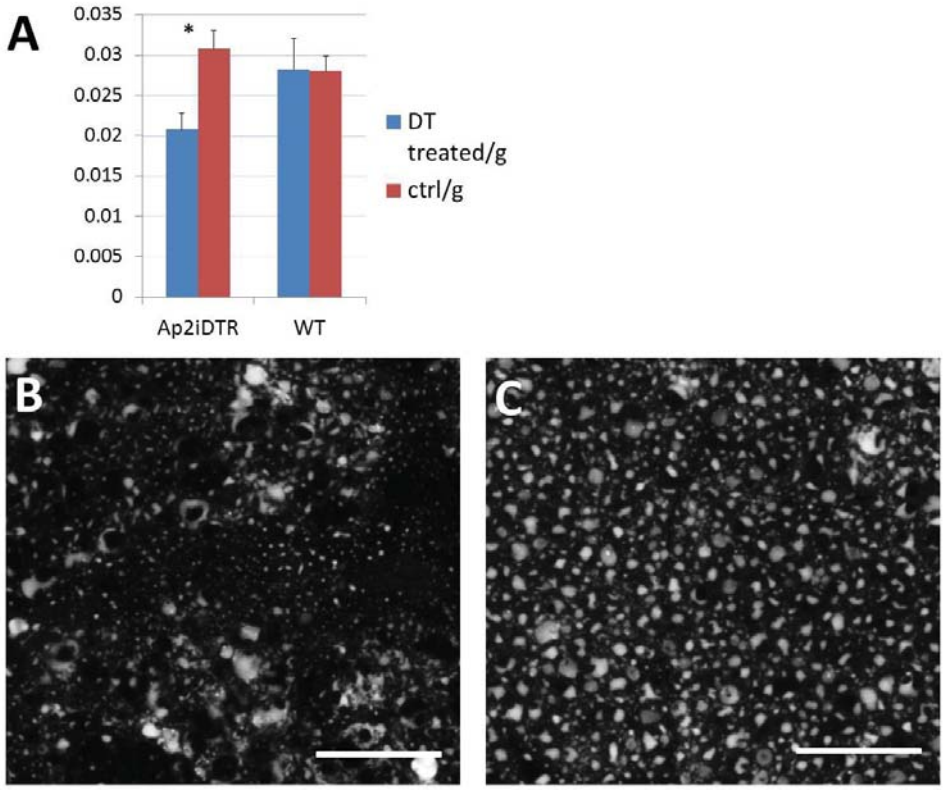

Figure 25: Weight and lipid distribution of DT treated isBAT on D3 after injection

(A) DT or saline control treated isBAT weight, error bar represents SEM, *p<0.05, **p<0.01, N=5. (B) Oil-Red-O staining of aP2-Cre^{+} mouse isBAT, scale bar 10µm. (B) Oil-Red-O staining of aP2-Cre mouse isBAT, scale bar 10µm.

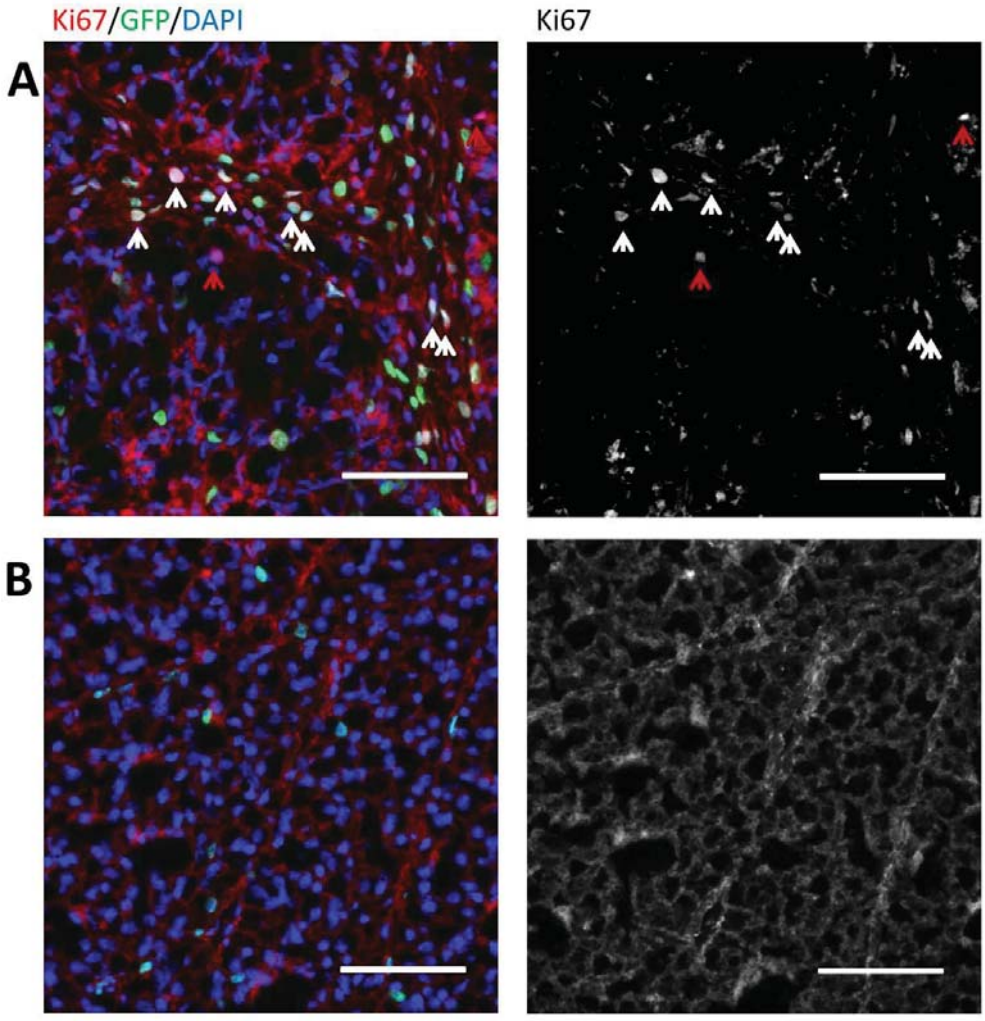

Figure 26: Proliferating GFP^{+} cells in isBAT on D3 after DT treatment

(A) aP2-Cre^{+} Rosa$^{iDTR/+}$ Pdgfra$^{GFP/+}$ mouse isBAT. White arrows indicate ki67+/GFP^{+} cells, and red arrows indicate Ki67+/GFP- cells. (B) Rosa$^{iDTR/+}$ Pdgfra$^{GFP/+}$ mouse isBAT. Scale bar 10µm.

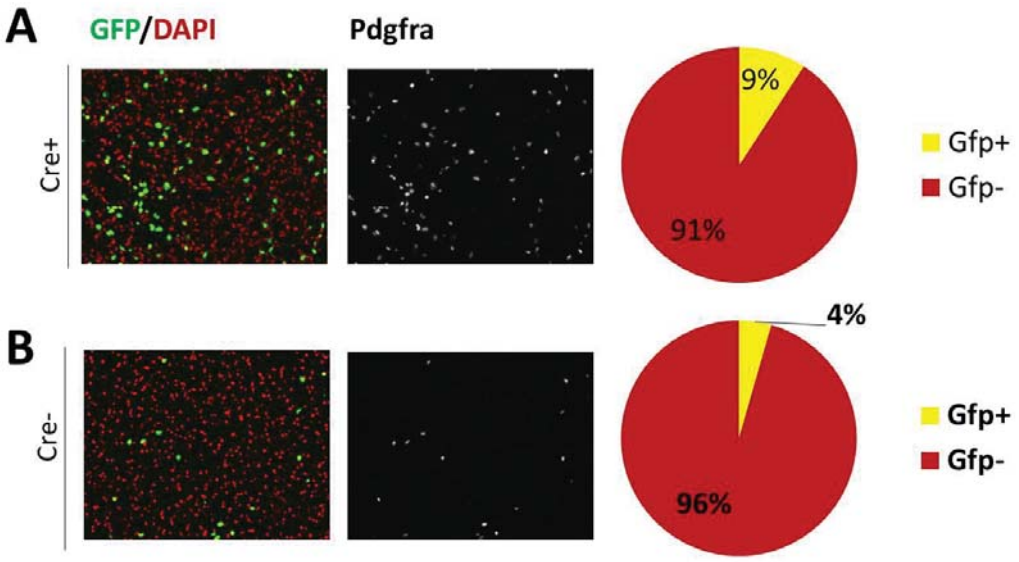

Figure 27: GFP$^+$ cells in isBAT on D3 after DT injection

(A) Picture and quantification of GFP$^+$ cells in aP2-Cre$^+$/Rosa$^{iDTR/+}$/Pdgfra$^{GFP/+}$ mouse isBAT. (B) Picture and quantification of GFP$^+$ cells in Rosa$^{iDTR/+}$/Pdgfra$^{GFP/+}$ mouse isBAT. N=3.

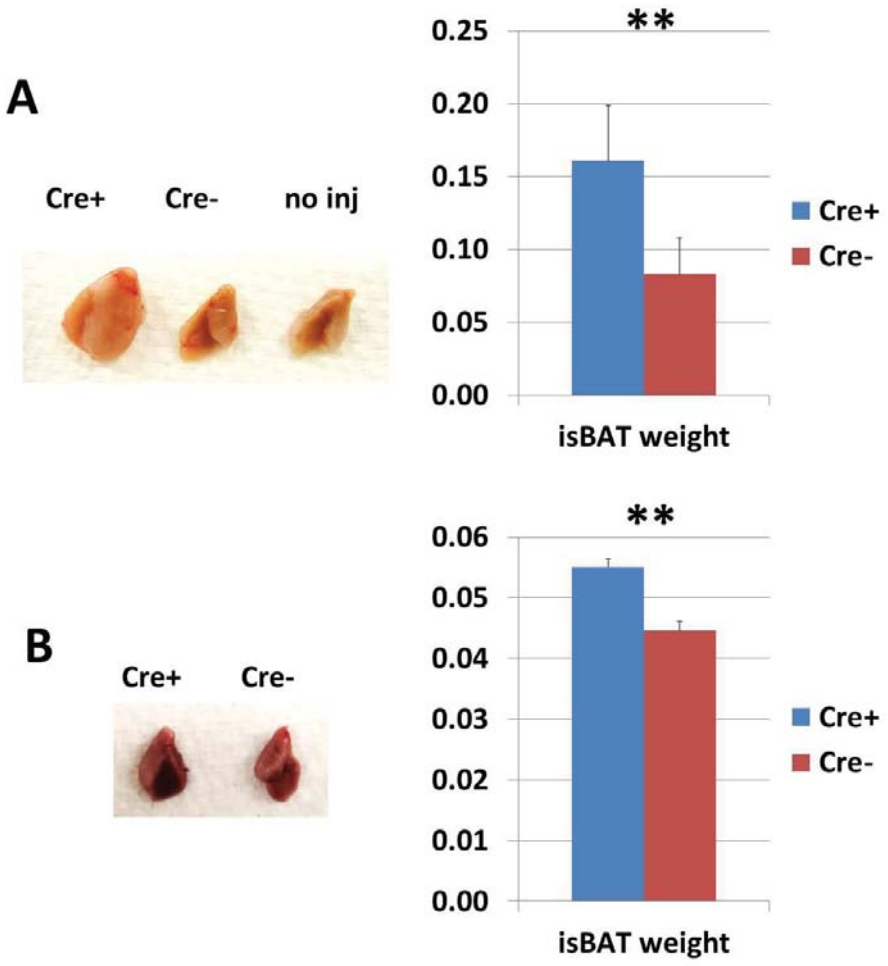

Figure 28: Regeneration of isBAT on D30 after DT injection

(A) Picture and quantification of 4-month-old mice aP2-Cre^{+} and aP2-Cre mice isBAT, error bar represents SEM, *p<0.05, **p<0.01, N=4. (B) Picture and quantification of 2-month-old mice aP2-Cre^{+} and aP2-Cre isBAT, error bar respresents SEM, *p<0.05, **p<0.01, N=3.

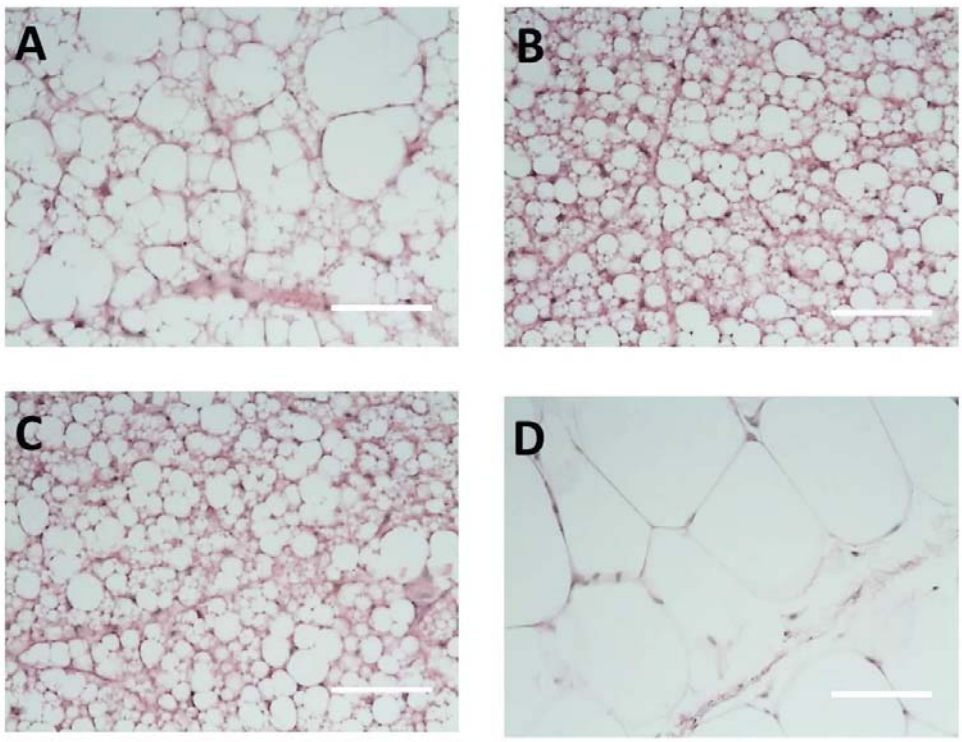

Figure 29: H&E sections of 4-month-old mouse adipose tissues on D30 after DT treatment

(A) isBAT of aP2-Cre^{+} mouse. (B) isBAT of aP2-Cre mouse. (C) isBAT of aP2-Cre^{+} mouse with no injection. (D) iWAT of aP2-Cre^{+} moue. Scale bar 10µm.

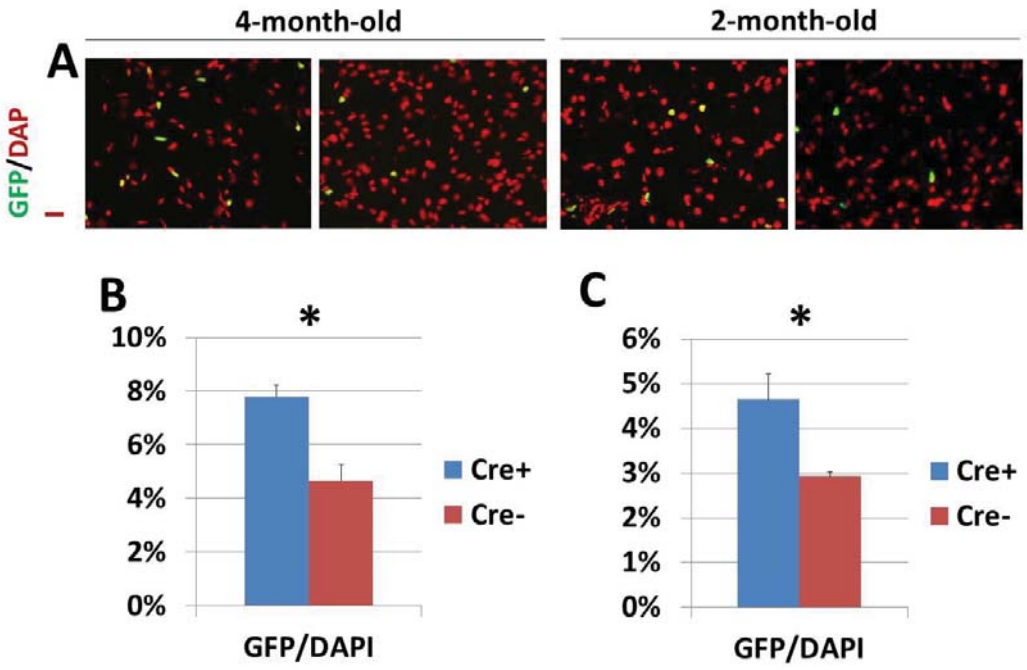

Figure 30: GFP$^+$ cells in isBAT on D30 after DT injection

(A) GFP$^+$ cells in 4-month-old or 2-month-old aP2-Cre$^+$/Rosa$^{iDTR/+}$/Pdgfra$^{GFP/+}$ (left) and Rosa$^{iDTR/+}$/Pdgfra$^{GFP/+}$ (right) mice isBAT, scale bar 10µm. (B) GFP$^+$ cell percentage of 4-month-old mice. (C) GFP$^+$ cell percentage of 2-month-old mice. Error bar represents SEM, *p<0.05, **p<0.01, N=3.

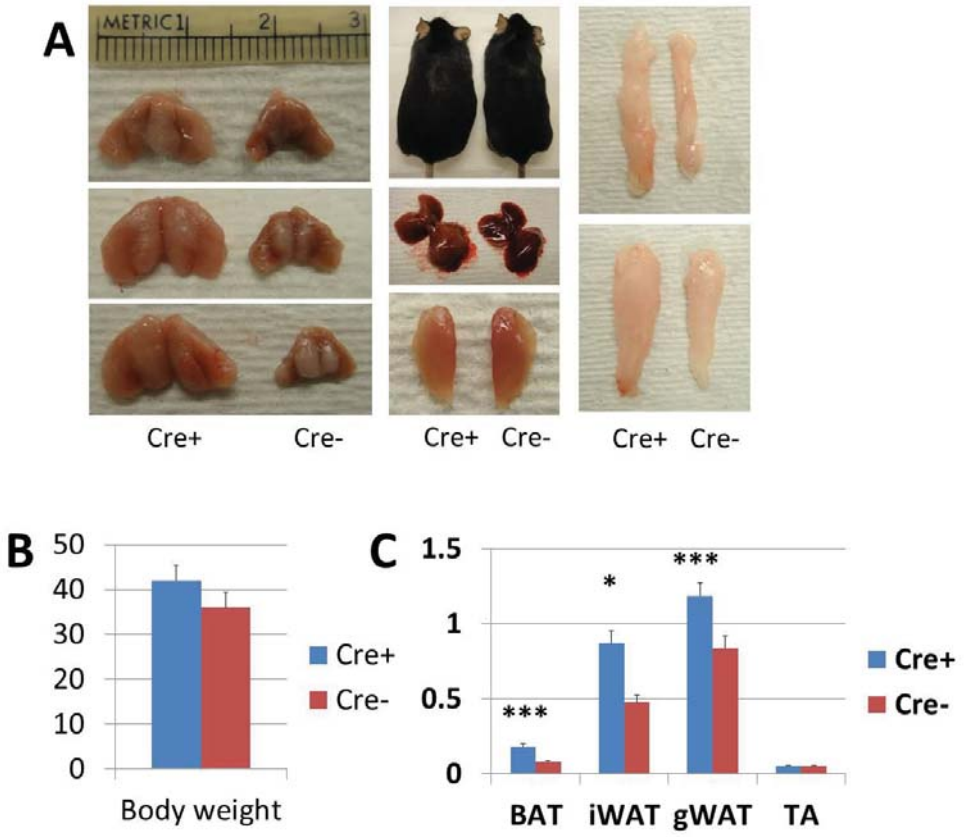

Figure 31: Regeneration of isBAT and effects on other tissues on D90 after DT injection

(A) Pictures of aP2-Cre^{+} and aP2-Cre 4-month-old mice and organs, ruler unit in cm. (B) Quantification of body weight, N=5. (C) Quantification of tissue weights, N=7. Error bar represent SEM, *p<0.05, **p<0.01.

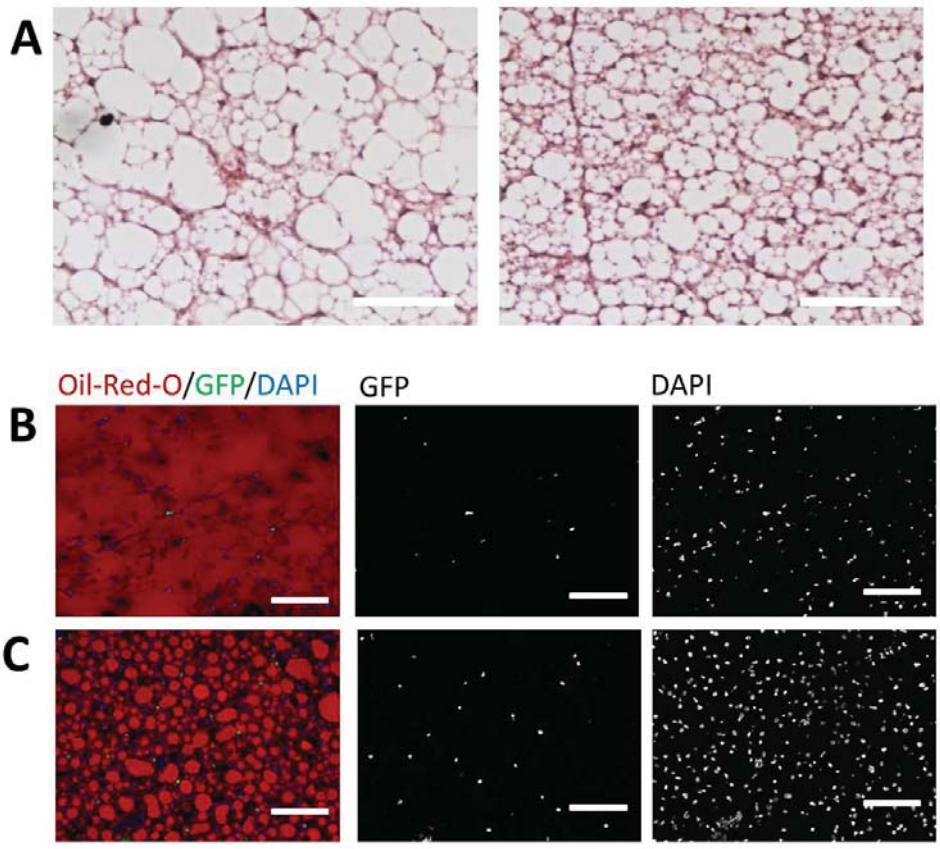

Figure 32: GFP^{+} cell and lipid distribution in isBAT on D90 after DT treatment

(A) aP2-Cre^{+}/Rosa$^{iDTR/+}$ (left) and Rosa$^{iDTR/+}$ (right) mice isBAT H&E section. Scale bar 10µm. (B) aP2-Cre^{+}/Rosa$^{iDTR/+}$ Pdgfra$^{GFP/+}$ mouse isBAT. Scale bar 20µm. (C) Rosa$^{iDTR/+}$/Pdgfra$^{GFP/+}$ mouse isBAT. Scale bar 20µm.

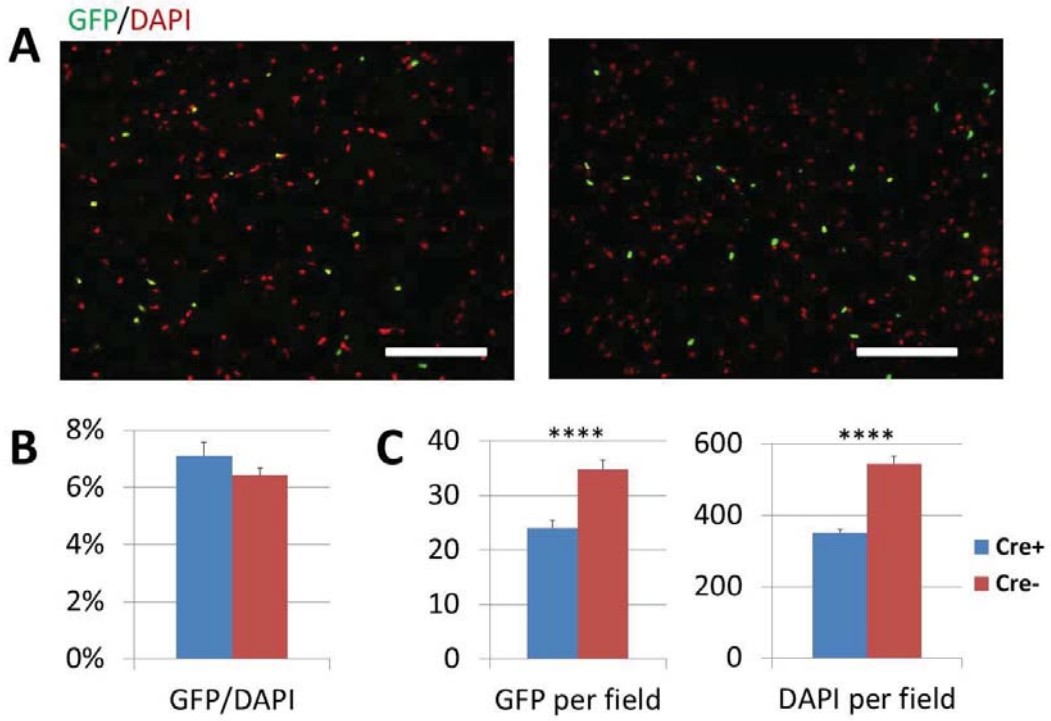

Figure 33: GFP$^+$ cell percentage and nucleus number in isBAT on D90 after DT injection

(A) GFP$^+$ cells in aP2-Cre$^+$/Rosa$^{iDTR/+}$/Pdgfra$^{GFP/+}$ (left) and Rosa$^{iDTR/+}$/Pdgfra$^{GFP/+}$ (right) isBAT. Scale bar 10μm. (B) Quantification of GFP/DAPI. Error bar represents SEM, *p<0.05, **p<0.01, n=22. (C) Quantification of GFP$^+$ cells per field and DAPI per field. Error bar represents SEM, *p<0.05, **p<0.01, n=22.

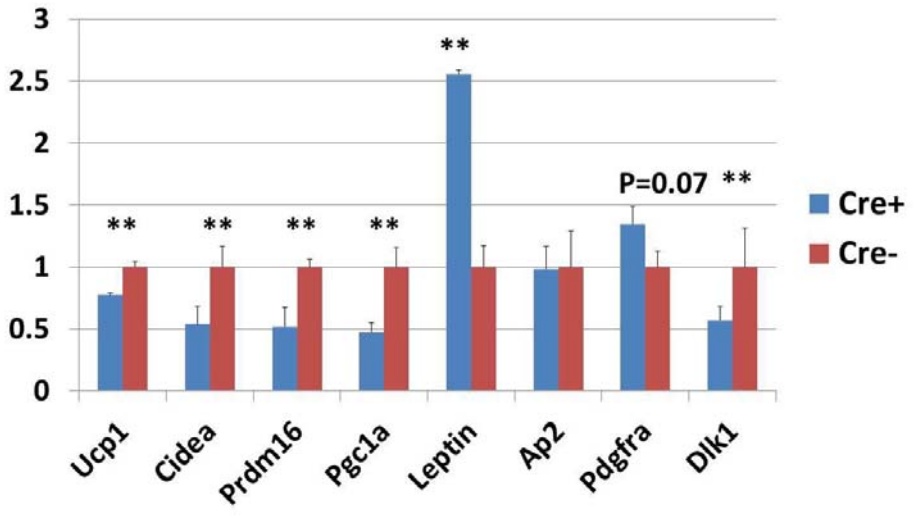

Figure 34: Whitening of isBAT on D90 after DT injection

qPCR of Cre+ and Cre– isBAT. Error bar represents SEM, *p<0.05, **p<0.01, N=3.

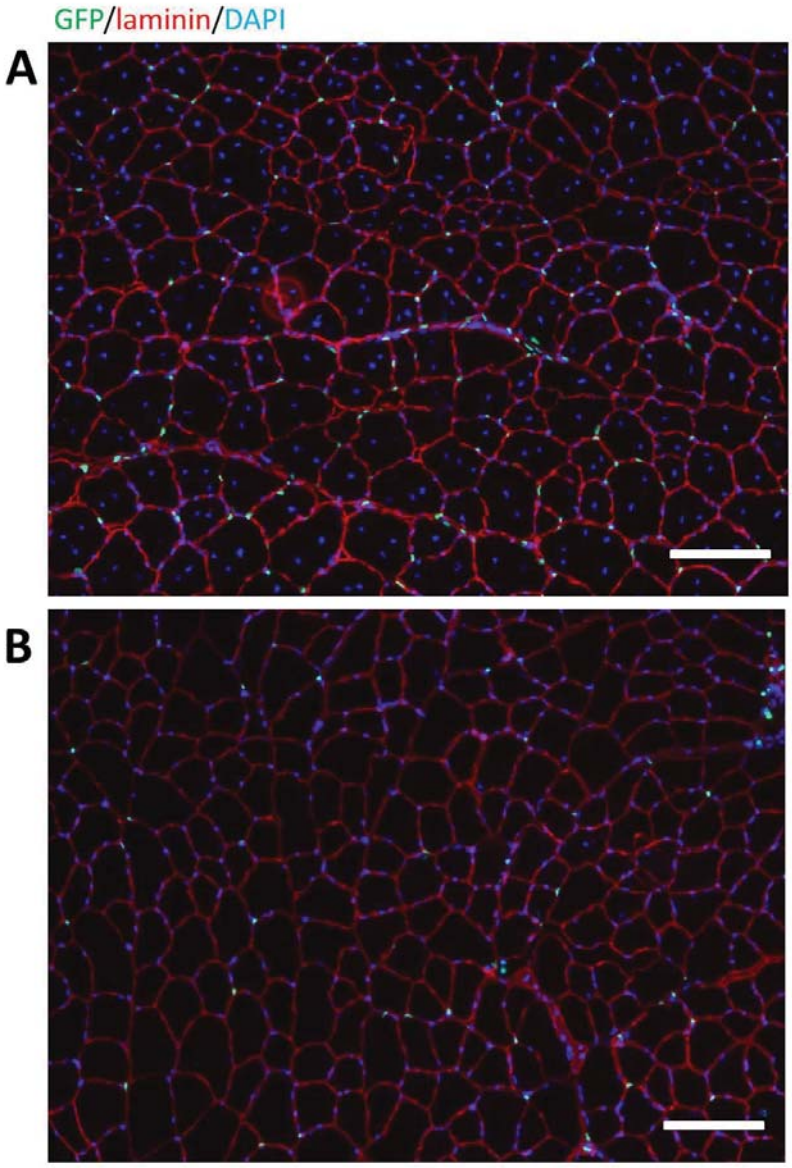

Figure 35: GFP^{+} cells in regenerating muscles of Pdgfra$^{GFP/+}$ mouse

(A) CTX 21 day TA muscle section. (B) No CTX control TA muscle section. Scale bar 10µm.

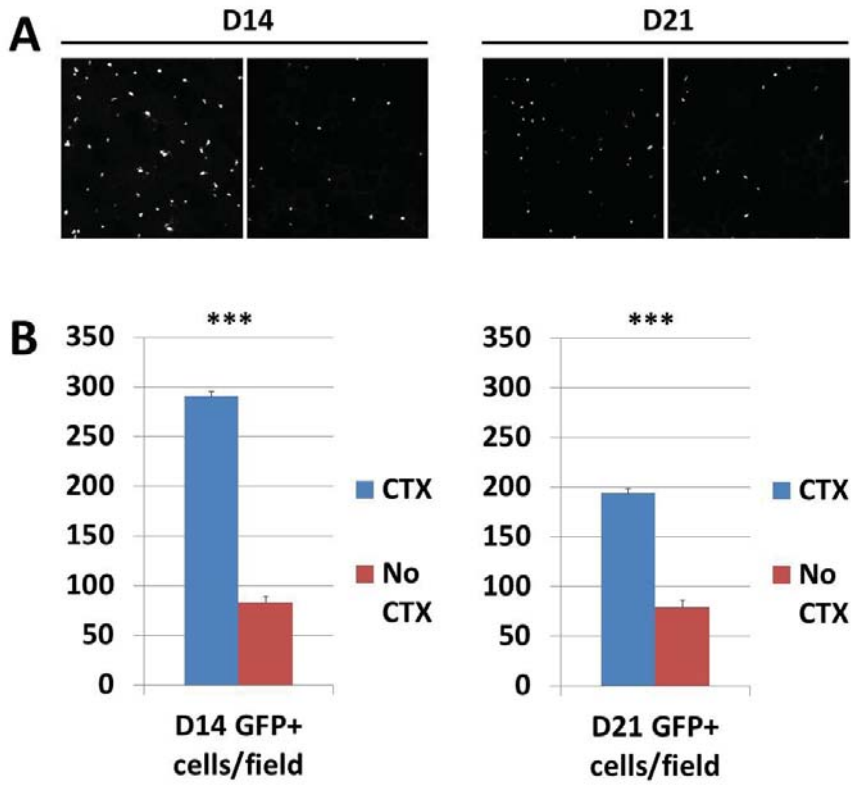

Figure 36: GFP$^+$ cells in regenerating TA

(A) GFP$^+$ cells in regenerating (left) and intact (right) TA on D14 or D21.(B) Quantification of GFP$^+$ cells per field. Error bar represents SEM, *p<0.05, **p<0.01, ***p<0.005, N=3.

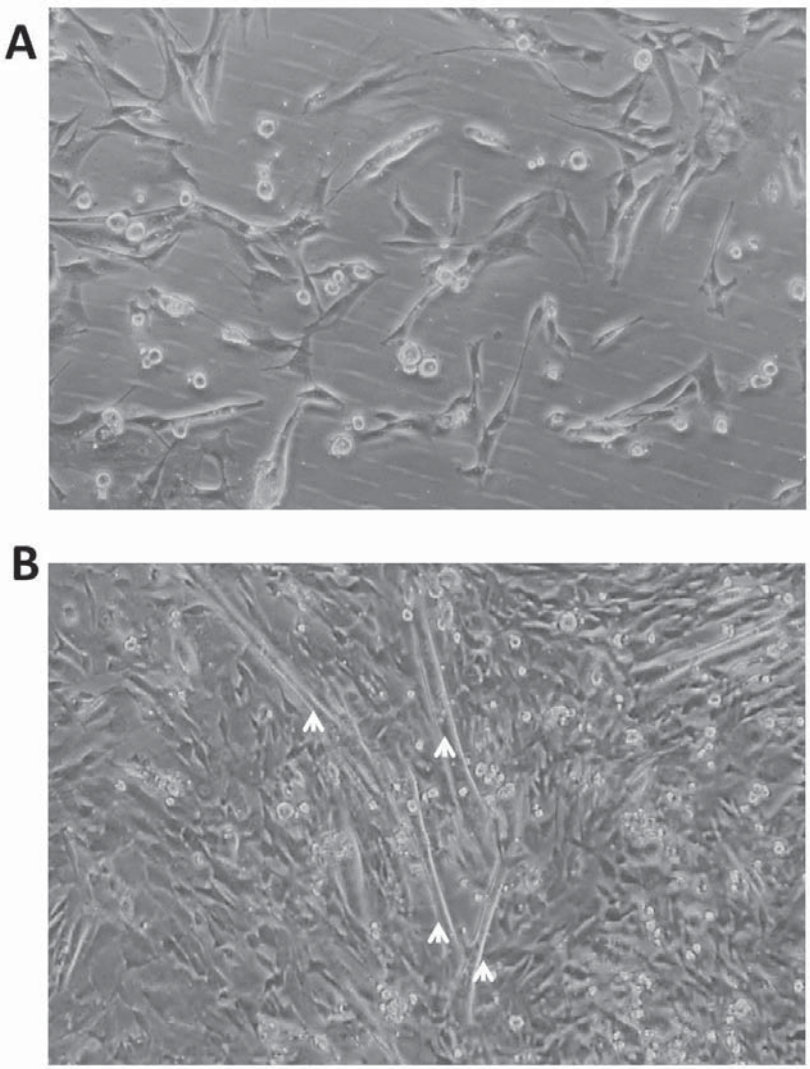

Figure 37: Myogenic cells in isBAT SVF culture

(A) isBAT SVF culture before myogenic differentiation. (B) isBAT SVF after 2 days of myogenic differentiation. Arrows indicate myotubes.

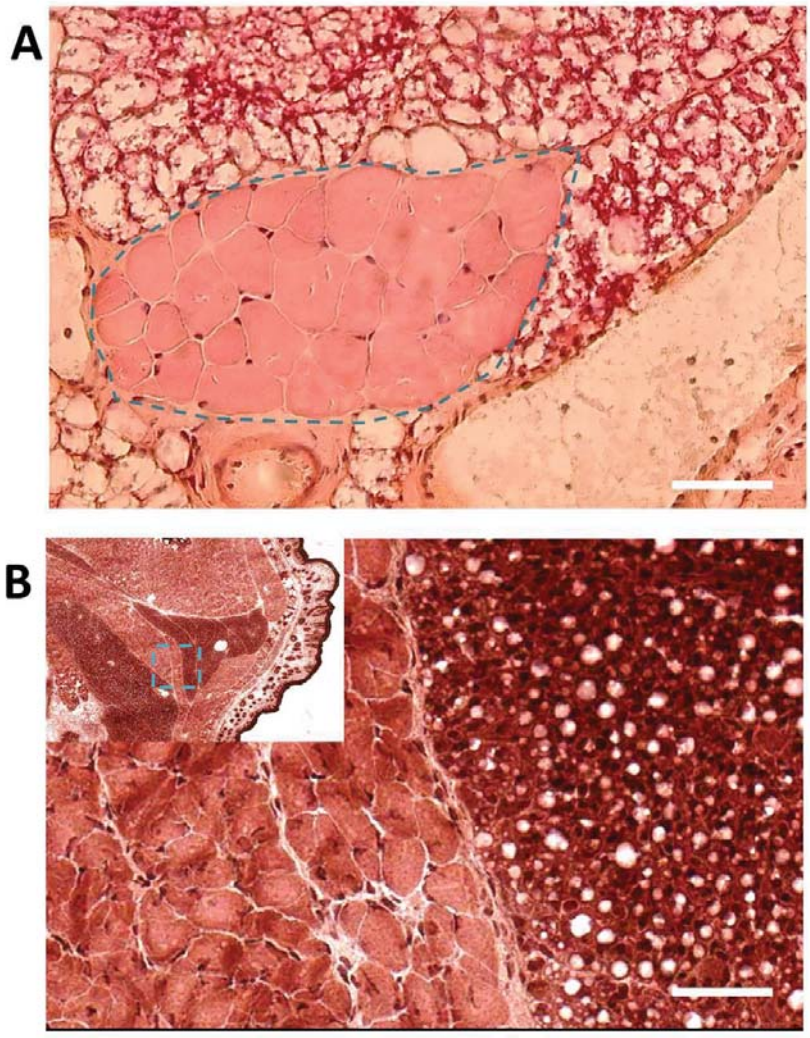

Figure 38: Skeletal muscle in adult and embryonic BAT

(A) Skeletal muscle islet in adult isBAT (section by Weiyi Liu). (B) Skeletal muscle near BAT in E17.5 mouse embryo. Box region is enlarged. Scale bar 10µm.

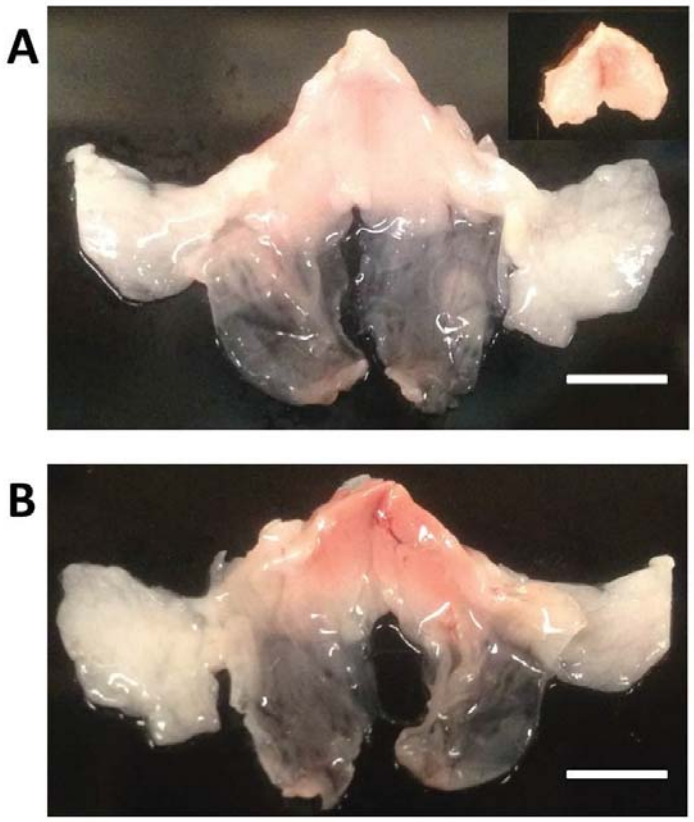

Figure 39: Mature isBAT with associated muscles

(A) Dorsal view. Boxed region represents the same isBAT after removing connected WAT and muscles. (B) Ventral view. Scale bar 5mm.

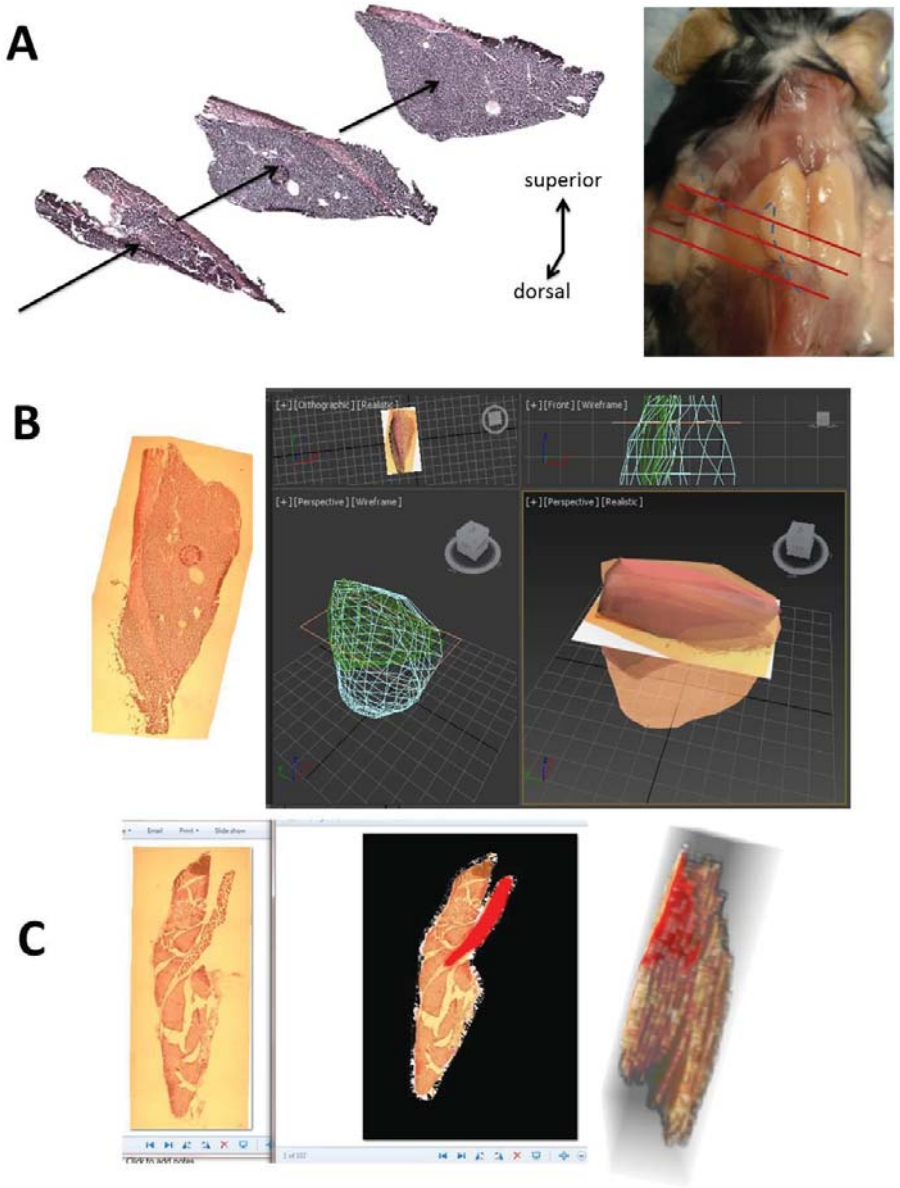

Figure 40: Strategy of 3D reconstruction for muscle in isBAT

(A) Direction of cutting cryosections. (B) 3D reconstruction in 3D MAX software. (C) 3D reconstruction by stacking in Image Pro software.

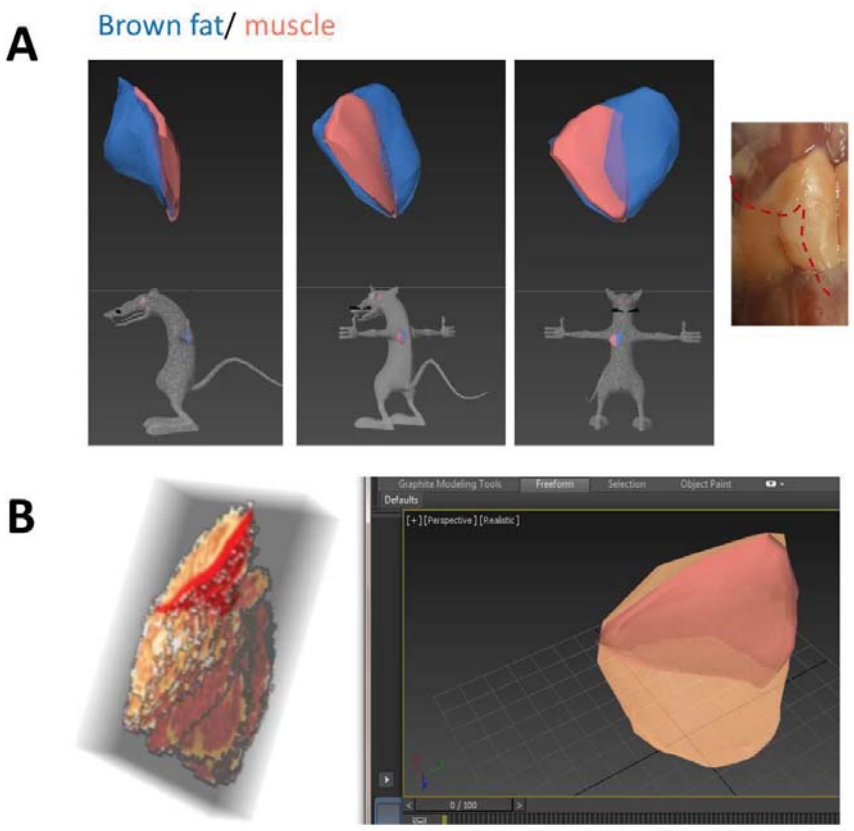

Figure 41: Relative location of muscle inserted in isBAT

(A) 3D reconstructed isBAT with muscle and their relative position in mouse viewed from 3 different angles. (B) Location of muscle (red) in isBAT confirmed by two 3D reconstruction methods.

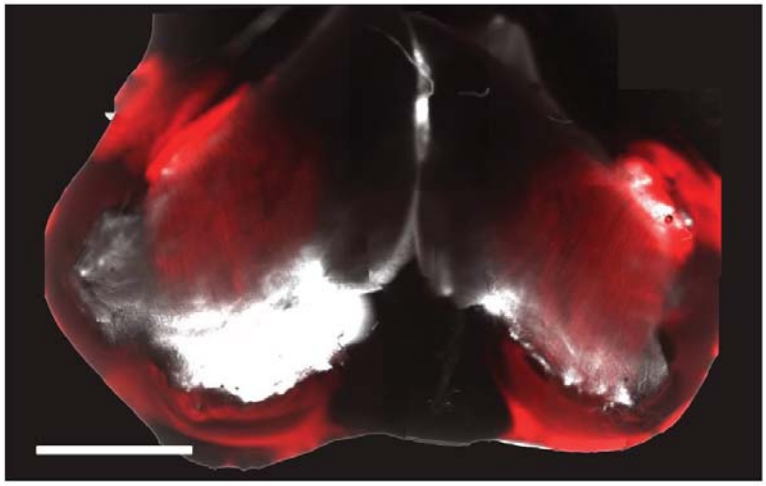

Figure 42: Location of muscle in isBAT visualized by SeeDB clarification method

Myod$^{cre/+}$/Rosa$^{iDTR/+}$/Rosa$^{td/+}$ mice isBAT. Red fluorescence from td-Tomato in red. Sale bar= 2.5mm.

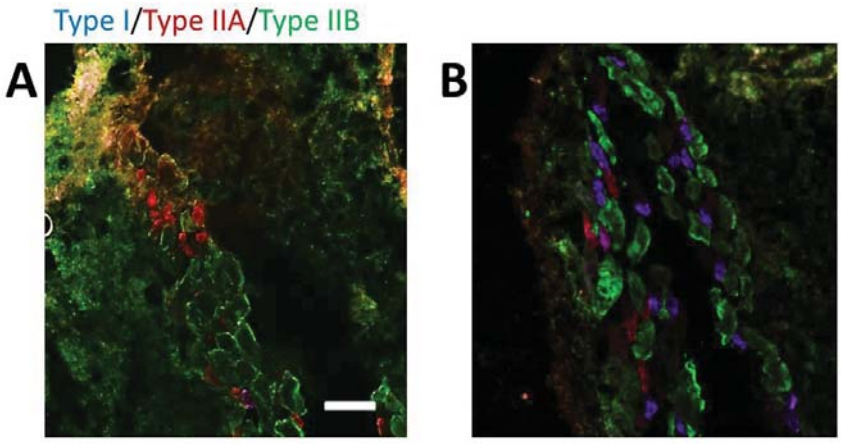

Figure 43: Fiber type of muscle in isBAT

(A) Region of muscle inserted into isBAT (B) Region of muscle beside isBAT. Scale bar 10μm.

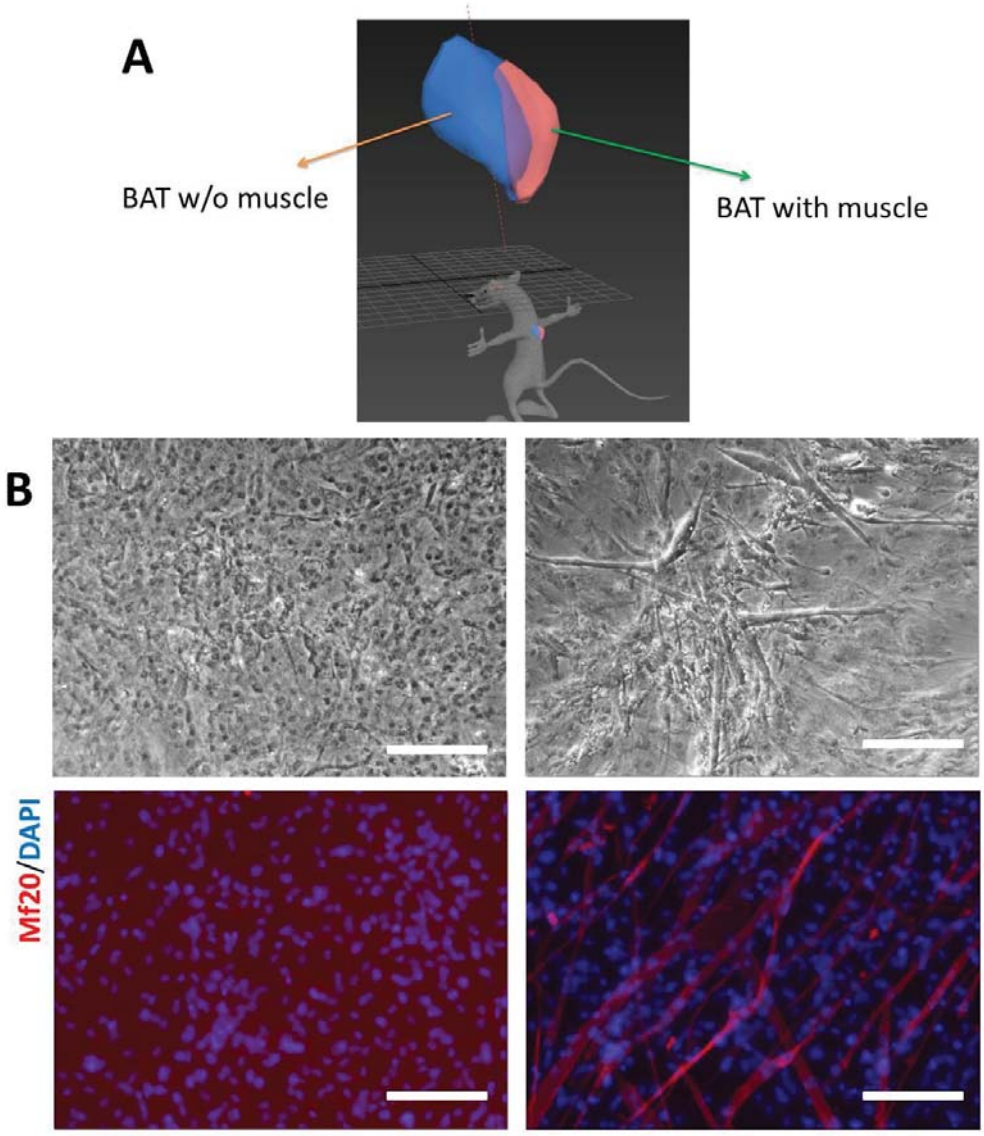

Figure 44: SVF culture of isBAT with muscle and without (w/o) muscle parts

(A) Partition of isBAT into with and w/o muscle parts. (B) isBAT SVF under myogenic differentiation 4 days. Left panels represent isBAT w/o muscle culture, right panels represent isBAT with muscle culture. Scale bar 10µm.

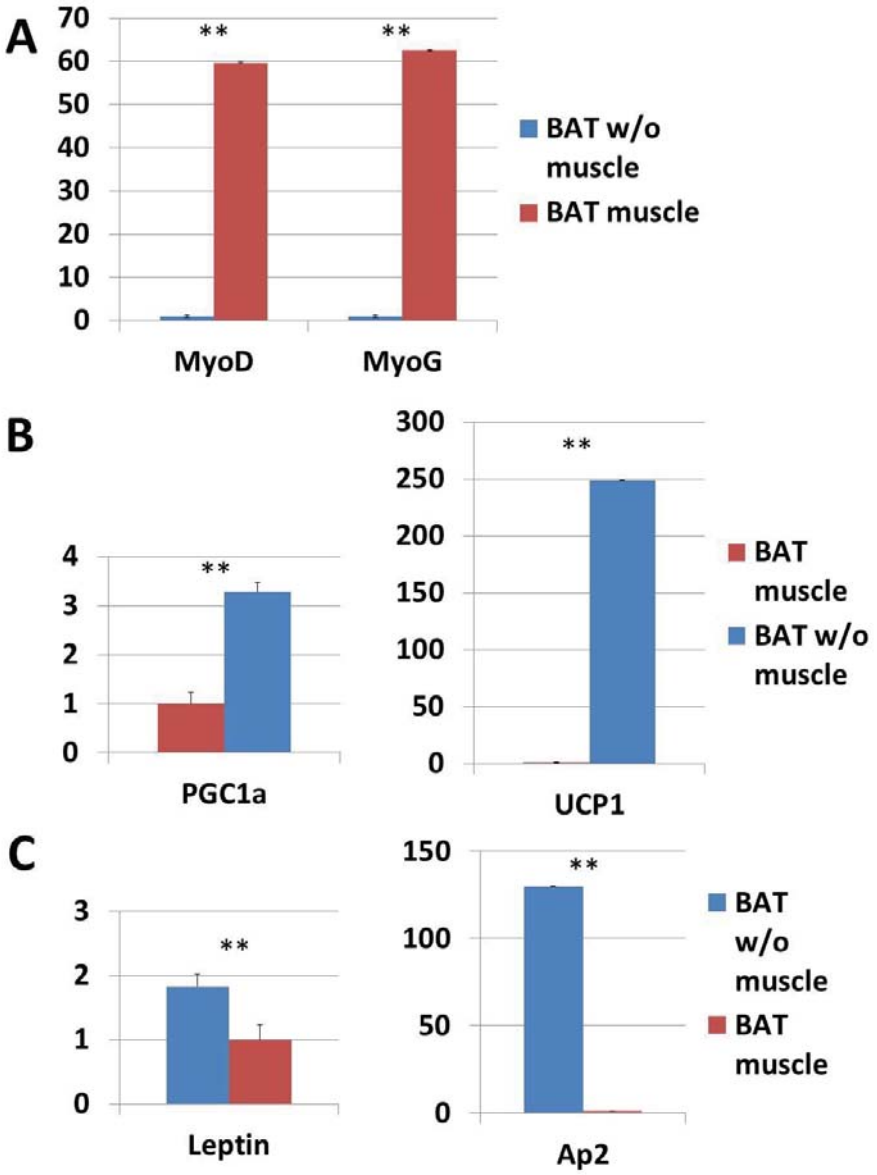

Figure 45: Gene expression profile of isBAT with and w/o muscle SVF

(A) Muscle related genes. (B) BAT related genes. (C) WAT related genes. Error bar represents SEM, *p<0.05, **p<0.01, N=3.

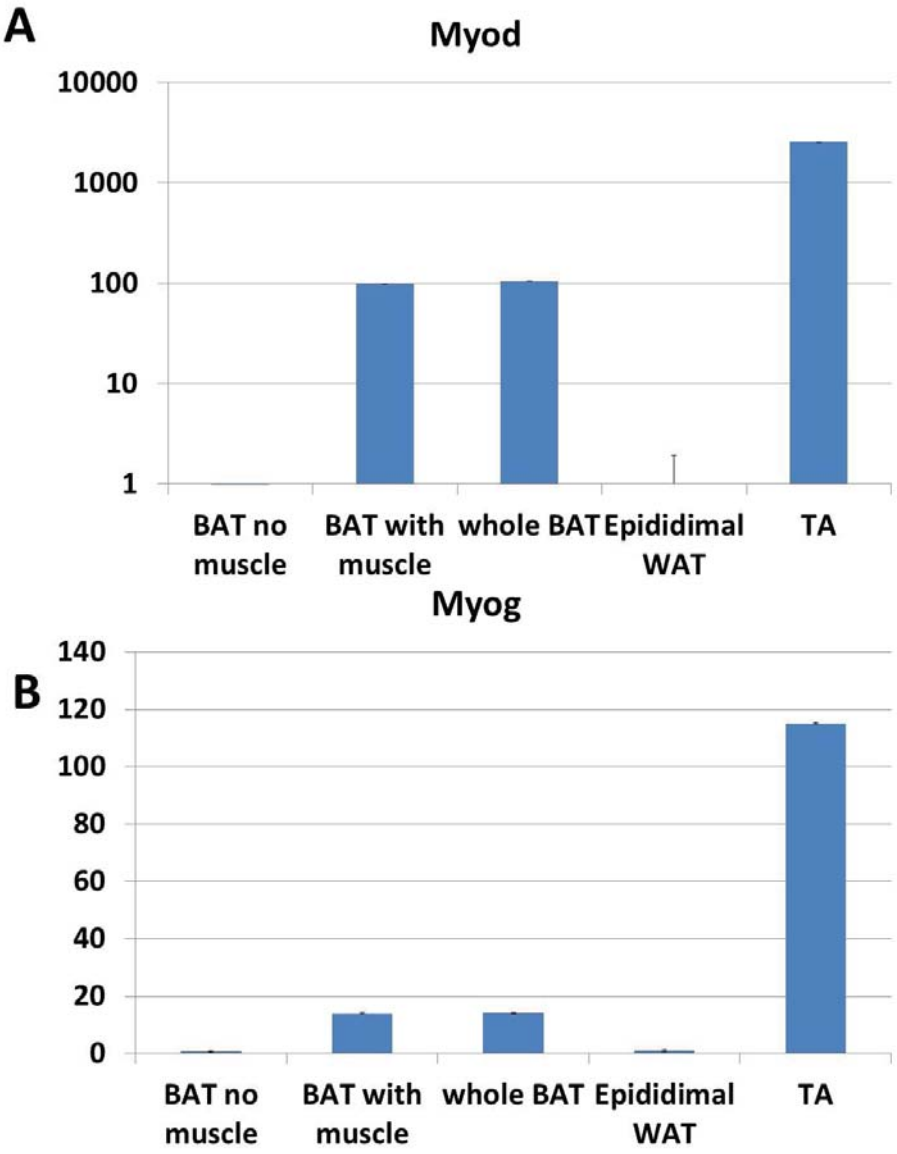

Figure 46: *Myod* and *Myog* expression levels in partitioned BAT, whole BAT, eWAT and TA muscle

(A) *Myod* expression. (B) *Myog* expression. Error bar represent SEM, N=3.

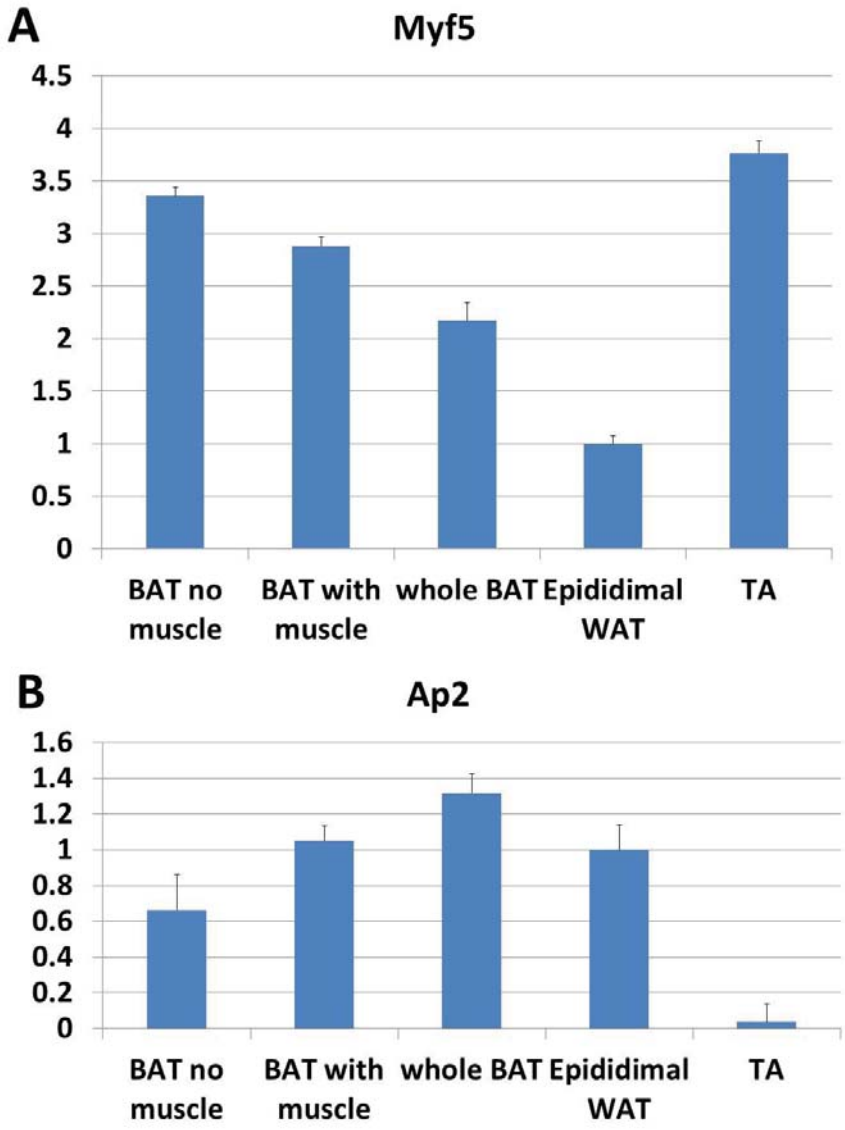

Figure 47: *Myf5* and *aP2* expression levels in partitioned BAT, whole BAT, eWAT and TA muscle

(A) *Myf5* expression. (B) *aP2* expression. Error bar represent SEM, N=3.

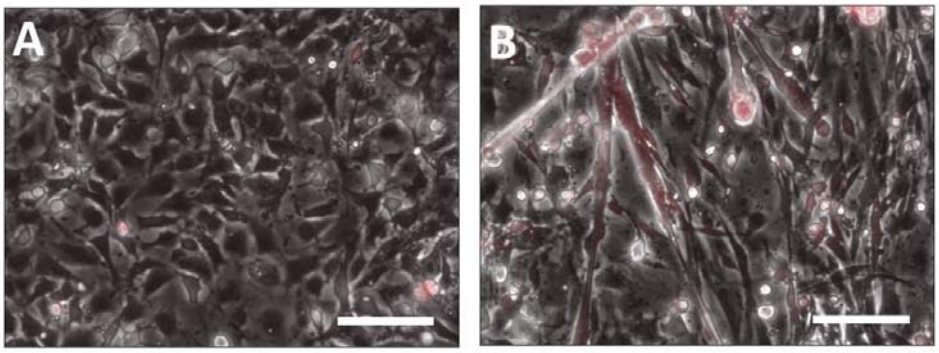

Figure 48: Elimination of myogenic cells in isBAT SVF culture

(A) isBAT SVF from Myod$^{cre/+}$/Rosa$^{iDTR/+}$/Rosa$^{td/+}$ mouse under 2 days of myogenic differentiation with in vivo DT. (B) isBAT SVF from Myod$^{cre/+}$/Rosa$^{iDTR/+}$/Rosa$^{td/+}$mouse under 2 days of myogenic differentiation with in vivo DMSO control. Scale bar 10µm.

References

Berry, R., & Rodeheffer, M. S. (2013). Characterization of the adipocyte cellular lineage in vivo. *Nat Cell Biol, 15*(3), 302-308. doi: 10.1038/ncb2696

Borensztein, M., Viengchareun, S., Montarras, D., Journot, L., Binart, N., Lombes, M., & Dandolo, L. (2012). Double Myod and Igf2 inactivation promotes brown adipose tissue development by increasing Prdm16 expression. *FASEB J, 26*(11), 4584-4591. doi: 10.1096/fj.12-208496

Bostrom, P., Wu, J., Jedrychowski, M. P., Korde, A., Ye, L., Lo, J. C., . . . Spiegelman, B. M. (2012). A PGC1-alpha-dependent myokine that drives brown-fat-like development of white fat and thermogenesis. *Nature, 481*(7382), 463-468. doi: 10.1038/nature10777

Bukowiecki, L., Collet, A. J., Follea, N., Guay, G., & Jahjah, L. (1982). Brown adipose tissue hyperplasia: a fundamental mechanism of adaptation to cold and hyperphagia. *Am J Physiol, 242*(6), E353-359.

Bukowiecki, L. J., Geloen, A., & Collet, A. J. (1986). Proliferation and differentiation of brown adipocytes from interstitial cells during cold acclimation. *Am J Physiol, 250*(6 Pt 1), C880-887.

Cai, X., Lin, Y., Hauschka, P. V., & Grottkau, B. E. (2011). Adipose stem cells originate from perivascular cells. *Biol Cell, 103*(9), 435-447. doi: 10.1042/BC20110033

Cannon, B., & Nedergaard, J. (2001). Cultures of adipose precursor cells from brown adipose tissue and of clonal brown-adipocyte-like cell lines. *Methods Mol Biol, 155*, 213-224. doi: 10.1385/1-59259-231-7:213

Cinti, S., & Morroni, M. (1995). Brown adipocyte precursor cells: a morphological study. *Ital J Anat Embryol, 100 Suppl 1*, 75-81.

Cohen, P., Levy, J. D., Zhang, Y., Frontini, A., Kolodin, D. P., Svensson, K. J., . . . Spiegelman, B. M. (2014). Ablation of PRDM16 and beige adipose causes metabolic dysfunction and a subcutaneous to visceral fat switch. *Cell, 156*(1-2), 304-316. doi: 10.1016/j.cell.2013.12.021

Gupta, R. K., Mepani, R. J., Kleiner, S., Lo, J. C., Khandekar, M. J., Cohen, P., . . . Spiegelman, B. M. (2012). Zfp423 expression identifies committed preadipocytes and localizes to adipose endothelial and perivascular cells. *Cell Metab, 15*(2), 230-239. doi: 10.1016/j.cmet.2012.01.010

Hoch, R. V., & Soriano, P. (2003). Roles of PDGF in animal development. *Development, 130*(20), 4769-4784. doi: 10.1242/dev.00721

Lee, Y. H., Petkova, A. P., Mottillo, E. P., & Granneman, J. G. (2012). In vivo identification of bipotential adipocyte progenitors recruited by beta3-adrenoceptor activation and high-fat feeding. *Cell Metab, 15*(4), 480-491. doi: 10.1016/j.cmet.2012.03.009

Macdougald, Ormond A. (2014). *Methods of Adipose Tissue Biology*: Academic Press.

Nagase, I., Sasaki, N., Tsukazaki, K., Yoshida, T., Morimatsu, M., & Saito, M. (1994). Hyperplasia of brown adipose tissue after chronic stimulation of beta 3-adrenergic receptor in rats. *Jpn J Vet Res, 42*(3-4), 137-145.

Nechad, M. (1983). Development of brown fat cells in monolayer culture. II. Ultrastructural characterization of precursors, differentiating adipocytes and their mitochondria. *Exp Cell Res, 149*(1), 119-127.

Pretheeban, T., Lemos, D. R., Paylor, B., Zhang, R. H., & Rossi, F. M. (2012). Role of stem/progenitor cells in reparative disorders. *Fibrogenesis Tissue Repair, 5*(1), 20. doi: 10.1186/1755-1536-5-20

Rodeheffer, M. S., Birsoy, K., & Friedman, J. M. (2008). Identification of white adipocyte progenitor cells in vivo. *Cell, 135*(2), 240-249. doi: 10.1016/j.cell.2008.09.036

Rothwell, N. J., & Stock, M. J. (1989). Surgical removal of brown fat results in rapid and complete compensation by other depots. *Am J Physiol, 257*(2 Pt 2), R253-258.

Sanchez-Gurmaches, J., & Guertin, D. A. (2014). Adipocytes arise from multiple lineages that are heterogeneously and dynamically distributed. *Nat Commun, 5*, 4099. doi: 10.1038/ncomms5099

Seale, P., Bjork, B., Yang, W., Kajimura, S., Chin, S., Kuang, S., . . . Spiegelman, B. M. (2008). PRDM16 controls a brown fat/skeletal muscle switch. *Nature, 454*(7207), 961-967. doi: 10.1038/nature07182

Shan, T., Liu, W., & Kuang, S. (2013). Fatty acid binding protein 4 expression marks a population of adipocyte progenitors in white and brown adipose tissues. *FASEB J, 27*(1), 277-287. doi: 10.1096/fj.12-211516

Sharma, A., Huard, C., Vernochet, C., Ziemek, D., Knowlton, K. M., Tyminski, E., . . . Martinez, R. V. (2014). Brown fat determination and development from muscle precursor cells by novel action of bone morphogenetic protein 6. *PLoS One, 9*(3), e92608. doi: 10.1371/journal.pone.0092608

Timmons, J. A., Wennmalm, K., Larsson, O., Walden, T. B., Lassmann, T., Petrovic, N., . . . Cannon, B. (2007). Myogenic gene expression signature establishes that brown and white adipocytes originate from distinct cell lineages. *Proc Natl Acad Sci U S A, 104*(11), 4401-4406. doi: 10.1073/pnas.0610615104

Tran, K. V., Gealekman, O., Frontini, A., Zingaretti, M. C., Morroni, M., Giordano, A., . . . Cinti, S. (2012). The vascular endothelium of the adipose tissue gives rise to both white and brown fat cells. *Cell Metab, 15*(2), 222-229. doi: 10.1016/j.cmet.2012.01.008

Uezumi, A., Fukada, S., Yamamoto, N., Ikemoto-Uezumi, M., Nakatani, M., Morita, M., . . . Tsuchida, K. (2014). Identification and characterization of PDGFRalpha+ mesenchymal progenitors in human skeletal muscle. *Cell Death Dis, 5*, e1186. doi: 10.1038/cddis.2014.161

Uezumi, A., Fukada, S., Yamamoto, N., Takeda, S., & Tsuchida, K. (2010). Mesenchymal progenitors distinct from satellite cells contribute to ectopic fat cell formation in skeletal muscle. *Nat Cell Biol, 12*(2), 143-152. doi: 10.1038/ncb2014

Zhang, J., Cao, R., Zhang, Y., Jia, T., Cao, Y., & Wahlberg, E. (2009). Differential roles of PDGFR-alpha and PDGFR-beta in angiogenesis and vessel stability. *FASEB J, 23*(1), 153-163. doi: 10.1096/fj.08-113860

CHAPTER 4. SUMMARY AND FUTURE DIRECTIONS

In conclusion, embryonic adipogenic stem cells in classic BAT differentiate from the adult BAT. Adult BAT is structurally connected to skeletal muscles, and the myogenic progenitor population in BAT and BAT culture is a result of skeletal muscle contamination. Detailed summaries have been included in Chapter 3 under "Conclusion and discussion" and will not be repeated here.

Current understanding of BAT progenitor cells is very limited. Molecular characteristics that distinguish BAT progenitors from WAT progenitors is currently lacking. The method to isolate pure BAT ASCs/progenitors has not been developed. The mechanism underlying the interaction between classic BAT and other tissues is not fully illustrated. We believe the future direction of studying BAT ASCs/progenitors can be categorized into, but not limited to, the following aspects:

4.1 Localization of developmental and adult BAT ASCs

To date, although multiple lines of evidence point to a vasculature localization of BAT and WAT progenitors, the exact niche of BAT stem cells is not known. A recent study in WAT identified the "crown-like structure" as the adipogenic niche during WAT remodeling (Lee, Petkova, & Granneman, 2013). The chemokine osteopoten is essential

for attracting the Pdgfrα+/CD44+ WAT progenitors to the crown like structure through activation of β3Adr. Whether similar mechanisms occur in BAT and during BAT regeneration is not known. A characteristic of BAT progenitor niche is particularly needed.

Study of embryonic development of classic BAT is also lacking. Lineage tracing experiments using different gene driven Cre with fluorescent reporter mice are useful. The $Myf5^{cre/+}$ reporter mice model is the only model employed for studying embryonic BAT development. This model is advantageous in showing the common origin of BAT cells with skeletal muscle cells, but cannot differentiate the subpopulations of BAT stem cells. Ucp1 Cre reporter mouse model shows that the maturation of BAT occurs around birth signified by Ucp1 expression and is therefore not suitable for embryonic study. $Myod^{cre/+}/Rosa^{LSLmTmG}$ reporter model shows that embryonic and adult BAT adipocytes are completely from non-*Myod* lineage. Lineage study of embryonic BAT is difficult because the gene specifically expressed in embryonic BAT stem cells has not been identified. In addition, the culture of embryonic BAT precursors is technically challenging.

In adult BAT, a main argument is that vascular associated cell type gives rise to ASCs (Cai, Lin, Hauschka, & Grottkau, 2011). Murine vasculature consists of endothelial cells and mural cells. Mural cells include muscular smooth muscle cells and pericytes (Armulik, Abramsson, & Betsholtz, 2005). Cdh5 and Tie2 are two endothelial cell markers, and it was shown that BAT is not originated from Cdh5 or Tie2 lineage cells (Berry & Rodeheffer, 2013). This indicates adult ASCs in BAT are not from endothelial cells from the vasculature. Two studies independently show that BAT ASCs may be a

population of pericytic cells marked by Zfp423 and VE-Cadherin expression (Gupta et al., 2012; Tran et al., 2012). This suggests that pericytes contain the adult BAT ASCs. However, Zfp423 negative or VE-Cadherin negative populations still exhibit a certain degree of adipogenic ability *in vitro*. This may be a result of the efficiency of FASC gating or a subpopulation of ASCs in the negative population. Whether the *Pdgfra*$^{+}$ BAT progenitors belong to the pericytic BAT stem cell population can be examined in the future by immunohistochemistry and gene profiling.

Other cells within and close to the adipose tissue vasculature have not yet been examined for adipogenic potential. Possible sources of adult BAT ASCs can be MSCs, skeletal muscle cells and cells that circulate in the blood. To our knowledge, no clear criteria have been set up to distinguish MSCs with ASCs. Many studies regard ASCs as a different population from MSCs based on place of origin (ASCs in adipose and MSCs from bone marrow and other mesenchymal tissues). This classification is not stringent since MSCs may circulate or migrate into adipose tissue (Augello, Kurth, & De Bari, 2010). In addition, MSCs in adipose tissue also possess a perivascular location (Corselli et al., 2013). Therefore we suspect that a subpopulation of MSCs overlaps with subpopulation of ASCs. Whether the *Pdgfra*$^{+}$ cells are MSCs remains to be examined.

4.2 Understanding of BAT ASC contribution to dynamic and species differences

Contribution of BAT ASCs to BAT dynamic is largely unknown. As indicated in the literature review, BAT in many mammals exhibit seasonal dynamics. Photoperiod and temperature are the two key environmental regulators of BAT dynamic (Heldmaier,

Steinlechner, Rafael, & Vsiansky, 1981). Early studies showed BAT weight, BAT adipocyte size and lipid accumulation commonly vary monthly in many species (Didow & Hayward, 1969; Heldmaier, 1974; Mcdevitt & Andrews, 1997; Rafael, Vsiansky, & Heldmaier, 1985). For example, BAT weight of Pygmy shrews peaks in winter while the BAT cell size is smallest around this time (Rafael et al., 1985). Multiple authors argue that this dynamic is due to the increased utilization of lipid content during winter for thermogenesis. However, no research directly reported an increase in brown adipocyte numbers among these cases. This is possibly due to the difficulties in determination of cell number when tissue size and cell size are both changing, especially when cell sizes are heterogeneous from site to site. There are only two reports from the same group marked that rat brown adipocytes proliferate in cold by radio labeling, however their result is contradictory to our data that we obtained in mice. Humans also have seasonal variations of BAT amounts, with the highest peak detected in winter (Au-Yong, Thorn, Ganatra, Perkins, & Symonds, 2009). The same study showed that the photoperiod, however, exhibits a greater correlation with BAT amount than ambient temperature. No records were reported concerning ASC action during this process. Whether adult progenitor cells contribute through proliferation and differentiation and to what degree these cells contribute to BAT dynamics may be a future direction for understanding the mechanism of BAT behavior under stimuli.

The species differences of BAT behavior raise the question whether characteristics of BAT stem cells diverge from species to species. It is reasonable to inference that mice possess an active pool of adult BAT ASCs for maintaining the

existence of BAT mass throughout their lifetime, while humans may lose classic BAT progenitor populations after birth. Whether this is the case is completely unknown. Furthermore, human classic BAT ASCs are not yet identified. It would be metabolically beneficial if one can sustain or continuously activate BAT ASCs in humans to maintain functional classic BAT throughout the life. Lastly, molecular events that activate BAT function has been extensively studied, however, the mechanism that activates BAT ASC proliferation remains elusive. Since the proliferation of BAT ASCs is not yet evident and may exhibit species specificity, the mechanism of BAT ASC activation would be a new area of research. These would be interesting points when characterizing classic BAT ASCs.

4.3 Comparison study of molecular characteristics of BAT ASCs with WAT ASCs and beige ASCs

Molecular characteristics of BAT ASCs are important for isolation and study of classic BAT cells. Currently, molecular markers identified for fat progenitor cells such as Zfp423, VE-cad, and Pdgfra cannot distinguish BAT ASCs from WAT or beige ASCs. Brown adipose specific markers such as Ucp1 cannot be utilized as BAT ASC markers since the expression is only detectable after differentiation. Therefore, establishment of molecular characteristics of BAT ASCs is necessary, which will help to establish stringent selection criteria of BAT ASCs by FACS. Comparison studies such as chip assay, RNA sequencing or mitogen screening of BAT and WAT $Lin^-/Pdgfr\alpha^+/Sca1^+$ cells can be an immediate future direction for this study.

Pdgfra^{+} cells give rise to beige and white adipocytes (Lee, Petkova, Mottillo, & Granneman, 2012). Our study suggests that adult BAT stem cells are also from the *Pdgfra*$^{+}$ lineage. Whether the progenitors in classic BAT are distinct from beige adipocyte progenitors is not known. Furthermore, whether the adult BAT progenitors give rise to WAT and beige adipocytes is not known. With this respect, practical future study would be single clone assay of the Pdgfrα+/Sca1+ adult BAT SVF cells. After adipogenic differentiation, mature adipocytes from each clone will be subjected to gene profiling on BAT, beige and WAT signature genes.

4.4 Study of mechanisms mediating BAT-muscle and BAT-WAT interconversion

Myogenic cells possess a certain ability to switch to BAT progenitors. C2C12 cells overexpressed with retroviral Prdm16 become adipogenic *in vitro* after adipogenic induction (Seale et al., 2008). Satellite cells within the musculature have the ability to form adipocytes expressing Ucp1, suggesting a possibility of muscle stem cells becoming BAT progenitor cells (Asakura, Komaki, & Rudnicki, 2001). This notion is also partially supported by the similar lineage origin of muscle and BAT cells (Timmons et al., 2007). The inter-conversion likely occurs between the progenitors since direct and complete conversion of mature myotubes to mature adipocytes has not yet been reported.

Extensive reports have been filed about BAT and WAT inter-conversion. A naturally occurring example is that aged brown adipocytes acquire white adipocyte characteristics (McDonald & Horwitz, 1999; Rogers, 2014). Whether the conversion is reversible has not been examined. One may also think that BAT and WAT are essentially the same tissues with different degrees of maturation. This is partially proven untrue by

the distinct lineage origin of these two tissues (Timmons et al., 2007). With the discovery of beige adipocytes (Wu et al., 2012), it is now widely accepted that there is a population of beige progenitors within WAT (Lee et al., 2012). Upon stimulation such as cold, these progenitors undergo *de novo* differentiation into brown adipocytes and regain white adipocyte signatures when temperature rises (Rosenwald, Perdikari, Rulicke, & Wolfrum, 2013). This in part supports the possibility of BAT and WAT inter-conversion by showing that one adipocyte is able to possess both WAT and BAT characteristics. Mechanism of the inter-conversion can be utilized to convert excessive WAT into BAT. This will be greatly valuable in treating obesity.

4.5 Distinguishing embryonic and adult adipose progenitors

Our discovery that embryonic and adult BAT ASCs are distinct populations gives rise to the question whether the same case exists in other adipose tissues. FACS sorting have shown that CD24+ and CD24- population of WAT progenitors both give rise to adipocytes *in vitro*, but only the CD24+ population are adipogenic *in vivo* (Rodeheffer, Birsoy, & Friedman, 2008). This infers that there is heterogeneity within the WAT stem cell population. It is possible that these two populations are different hierarchies of multipotency. It is also possible that the CD24+ population represent a truly functional population of adipose progenitor that contributes to embryonic adipogenesis as well. The study of WAT embryonic and adult stem cells will help with the understanding of WAT plasticity.

The majority of adult *Pdgfra*$^+$ BAT stem cells may represent a population corresponding to the CD24- progenitors in WAT, which probably do not contribute to *in vivo* adipogenesis. Gene profiling of embryonic and adult BAT stem cells will give a clue about the difference between these two populations. By quantification of *Pdgfra*$^+$ expression in these two kinds of cells, one can verify if *Pdgfra*$^+$ cells truly represent adult BAT stem cells.

4.6 Characterization of *Pdgfra*$^+$ cells during tissue regeneration

As we observed in BAT regeneration model, *Pdgfra*$^+$ lineage cells increase during tissue damage and the early stage of regeneration. This is also evident in muscle regeneration. *Pdgfra*$^+$ cells are believed to represent a population of fibroblastic cells that are adipogenic and facilitated with the muscle regeneration process (Uezumi et al., 2014). Studies should be conducted to test if the *Pdgfra*$^+$ population contributes to BAT regeneration through as ASCs or interstitial cells. It could be possible that a subpopulation of *Pdgfra*$^+$ cells in BAT are fibroblast, which may facilitate the process of repair and scaring through signaling or paracrine effects. The decline of *Pdgfra*$^+$ lineage population upon regeneration completion makes us wonder whether they undergo cell death after serving their purpose. The mechanism controlling *Pdgfra*$^+$ cell involvement in tissue repair may be interesting.

References

Armulik, A., Abramsson, A., & Betsholtz, C. (2005). Endothelial/pericyte interactions. *Circ Res, 97*(6), 512-523. doi: 10.1161/01.RES.0000182903.16652.d7

Asakura, A., Komaki, M., & Rudnicki, M. (2001). Muscle satellite cells are multipotential stem cells that exhibit myogenic, osteogenic, and adipogenic differentiation. *Differentiation, 68*(4-5), 245-253.

Au-Yong, I. T., Thorn, N., Ganatra, R., Perkins, A. C., & Symonds, M. E. (2009). Brown adipose tissue and seasonal variation in humans. *Diabetes, 58*(11), 2583-2587. doi: 10.2337/db09-0833

Augello, A., Kurth, T. B., & De Bari, C. (2010). Mesenchymal stem cells: a perspective from in vitro cultures to in vivo migration and niches. *Eur Cell Mater, 20*, 121-133.

Berry, R., & Rodeheffer, M. S. (2013). Characterization of the adipocyte cellular lineage in vivo. *Nat Cell Biol, 15*(3), 302-308. doi: 10.1038/ncb2696

Cai, X., Lin, Y., Hauschka, P. V., & Grottkau, B. E. (2011). Adipose stem cells originate from perivascular cells. *Biol Cell, 103*(9), 435-447. doi: 10.1042/BC20110033

Corselli, M., Crisan, M., Murray, I. R., West, C. C., Scholes, J., Codrea, F., . . . Peault, B. (2013). Identification of perivascular mesenchymal stromal/stem cells by flow cytometry. *Cytometry A, 83*(8), 714-720. doi: 10.1002/cyto.a.22313

Didow, Larry Alvin, & Hayward, JS. (1969). Seasonal variations in the mass and composition of brown adipose tissue in the meadow vole, Microtus pennsylvanicus. *Canadian Journal of Zoology, 47*(4), 547-555.

Gupta, R. K., Mepani, R. J., Kleiner, S., Lo, J. C., Khandekar, M. J., Cohen, P., . . . Spiegelman, B. M. (2012). Zfp423 expression identifies committed preadipocytes and localizes to adipose endothelial and perivascular cells. *Cell Metab, 15*(2), 230-239. doi: 10.1016/j.cmet.2012.01.010

Heldmaier, Gerhard. (1974). Temperature adaptation and brown adipose tissue in hairless and albino mice. *Journal of comparative physiology, 92*(3), 281-292.

Heldmaier, Gerhard, Steinlechner, Stephan, Rafael, Johannes, & Vsiansky, Pavel. (1981). Photoperiodic control and effects of melatonin on nonshivering thermogenesis and brown adipose tissue. *Science, 212*(4497), 917-919.

Lee, Y. H., Petkova, A. P., & Granneman, J. G. (2013). Identification of an adipogenic niche for adipose tissue remodeling and restoration. *Cell Metab, 18*(3), 355-367. doi: 10.1016/j.cmet.2013.08.003

Lee, Y. H., Petkova, A. P., Mottillo, E. P., & Granneman, J. G. (2012). In vivo identification of bipotential adipocyte progenitors recruited by beta3-adrenoceptor activation and high-fat feeding. *Cell Metab, 15*(4), 480-491. doi: 10.1016/j.cmet.2012.03.009

Mcdevitt, Regina M, & Andrews, JF. (1997). Seasonal variation in brown adipose tissue mass and lipid droplet size of< i> Sorex minutus</i>, the pygmy shrew; The relationship between morphology and metabolic rate. *Journal of thermal biology, 22*(2), 127-135.

McDonald, R. B., & Horwitz, B. A. (1999). Brown adipose tissue thermogenesis during aging and senescence. *J Bioenerg Biomembr, 31*(5), 507-516.

Rafael, Johannes, Vsiansky, Pavel, & Heldmaier, Gerhard. (1985). Seasonal adaptation of brown adipose tissue in the Djungarian hamster. *Journal of Comparative Physiology B, 155*(4), 521-528.

Rodeheffer, M. S., Birsoy, K., & Friedman, J. M. (2008). Identification of white adipocyte progenitor cells in vivo. *Cell, 135*(2), 240-249. doi: 10.1016/j.cell.2008.09.036

Rogers, N. H. (2014). Brown adipose tissue during puberty and with aging. *Ann Med*, 1-8. doi: 10.3109/07853890.2014.914807

Rosenwald, M., Perdikari, A., Rulicke, T., & Wolfrum, C. (2013). Bi-directional interconversion of brite and white adipocytes. *Nat Cell Biol, 15*(6), 659-667. doi: 10.1038/ncb2740

Seale, P., Bjork, B., Yang, W., Kajimura, S., Chin, S., Kuang, S., . . . Spiegelman, B. M. (2008). PRDM16 controls a brown fat/skeletal muscle switch. *Nature, 454*(7207), 961-967. doi: 10.1038/nature07182

Timmons, J. A., Wennmalm, K., Larsson, O., Walden, T. B., Lassmann, T., Petrovic, N., . . . Cannon, B. (2007). Myogenic gene expression signature establishes that brown and white adipocytes originate from distinct cell lineages. *Proc Natl Acad Sci U S A, 104*(11), 4401-4406. doi: 10.1073/pnas.0610615104

Tran, K. V., Gealekman, O., Frontini, A., Zingaretti, M. C., Morroni, M., Giordano, A., . . . Cinti, S. (2012). The vascular endothelium of the adipose tissue gives rise to both white and brown fat cells. *Cell Metab, 15*(2), 222-229. doi: 10.1016/j.cmet.2012.01.008

Uezumi, A., Fukada, S., Yamamoto, N., Ikemoto-Uezumi, M., Nakatani, M., Morita, M., . . . Tsuchida, K. (2014). Identification and characterization of PDGFRalpha+ mesenchymal progenitors in human skeletal muscle. *Cell Death Dis, 5*, e1186. doi: 10.1038/cddis.2014.161

Wu, J., Bostrom, P., Sparks, L. M., Ye, L., Choi, J. H., Giang, A. H., . . . Spiegelman, B. M. (2012). Beige adipocytes are a distinct type of thermogenic fat cell in mouse and human. *Cell, 150*(2), 366-376. doi: 10.1016/j.cell.2012.05.016

VITA

VITA

Xin (Cindy) Yang is the child of Yasheng Yang and Yan Huang. She was born in 1989 at Fuzhou, Fujian, PRC. Xin graduated from the Fuzhou No.1 High School in 2008 and obtained a Bachelor of Agronomy from China Agricultural University (CAU) and a Bachelor of Science from Purdue University in 2012 through the “2+2 transfer program” between CAU and Purdue. Xin then continued in searches of muscle and adipose stem cells as a M.S. student under the supervision of Dr. Shihuan Kuang in the department of Animal Sciences at Purdue and graduated in 2014. Xin strive to be a highly motivated and rigorous individual with a broad interest in computation, economics and leadership. It is her hope to utilize the knowledge of biotechnology obtained to benefit the agricultural or medical community.

PUBLICATIONS

PUBLICATIONS

Liu W, Bi P, Shan T, **Yang X**, Yin H, Wang YX, Liu N, Rudnicki MA, Kuang S. 2013. miR-133a regulates adipocyte browning in vivo. Plos Genet. 9(7): e1003626.

Liu W, Shan T, **Yang X**, Liu Y, Liang X, Zhang P, Liu X, Kuang S. 2013. A heterogeneous lineage origin underlies phenotypic and molecular differences of white and beige adipocytes. J Cell Sci. 126(16):3527-32.

Bi, P., Shan, T., Liu, W., Yue, F., **Yang, X.**, Liang, X. R., . . . Kuang, S. (2014). Inhibition of Notch signaling promotes browning of white adipose tissue and ameliorates obesity. *Nat Med*. doi: 10.1038/nm.3615

Yang X, Bi P, Kuang S. 2014. Fighting Obesity: When muscle meets fat. Adipocyte. (In press)